Analysis of sequence-selective guanine oxidation by biological agents

by

Yelena Margolin

B.S. in Chemistry, Massachusetts Institute of Technology, 1999

B.S. in Biology, Massachusetts Institute of Technology, 1999

Submitted to the Department of Biological Engineering in Partial Fulfillment of the requirements for the degree of

Ph.D. in Toxicology

at the

MASSACHUSETTS INSTITUTE OF TECHNOLOGY

[February 2008]
October 2007

Signature of Author: _____
Department of Biological Engineering
October, 2007

Certified by: _____
Peter C. Dedon
Professor of Toxicology and Biological Engineering
Thesis supervisor

Accepted by: _____
Alan Grodzinsky
Professor of Biological Engineering
Chairman, Committee for Graduate Students

This doctoral thesis has been examined by a committee of the Department of Biological Engineering as follows:

Associate Professor Bevin P. Engelward _____
Chairperson

Professor Peter C. Dedon _____
Supervisor

Professor John M. Essigmann _____

Professor Steven R. Tannenbaum _____

Analysis of sequence-selective guanine oxidation by biological agents

by

Yelena Margolin

Submitted to the Department of Biological Engineering on October 5, 2007 in partial fulfillment of the requirements for the degree of Doctor of Philosophy in Toxicology

ABSTRACT

Oxidatively damaged DNA has been strongly associated with cancer, chronic degenerative diseases and aging. Guanine is the most frequently oxidized base in the DNA, and generation of a guanine radical cation ($G^{\bullet+}$) as an intermediate in the oxidation reaction leads to migration of a resulting cationic hole through the DNA π-stack until it is trapped at the lowest-energy sites. These sites reside at runs of guanines, such as 5'-GG-3' sequences, and are characterized by the lowest sequence-specific ionization potentials (IPs). The charge transfer mechanism suggests that hotspots of oxidative DNA damage induced by electron transfer reagents can be predicted based on the primary DNA sequence. However, preliminary data indicated that nitrosoperoxycarbonate ($ONOOCO_2^-$), a mediator of chronic inflammation and a one-electron oxidant, displayed unusual guanine oxidation properties that were the focus of present work.

As a first step in our study, we determined relative levels of guanine oxidation, induced by $ONOOCO_2^-$ in all possible three-base sequence contexts (XGY) within double-stranded oligonucleotides. These levels were compared to

the relative oxidation induced within the same guanines by photoactivated riboflavin, a one-electron reagent. We found that, in agreement with previous studies, photoactivated riboflavin was selective for guanines of lowest IPs located within 5'-GG-3' sequences. In contrast, $ONOOCO_2^-$ preferentially reacted with guanines located within 5'-GC-3' sequences characterized by the highest IPs. This demonstrated that that sequence-specific IP was not a determinant of guanine reactivity with $ONOOCO_2^-$. Sequence selectivities for both reagents were double-strand specific. Selectivity of $ONOOCO_2^-$ for 5'-GC-3' sites was also observed in human genomic DNA after ligation-mediated PCR analysis. Relative yields of different guanine lesions produced by both $ONOOCO_2^-$ and riboflavin varied 4- to 5-fold across all sequence contexts.

To assess the role of solvent exposure in mediating guanine oxidation by $ONOOCO_2^-$, relative reactivities of mismatched guanines with $ONOOCO_2^-$ were measured. The majority of the mismatches displayed an increased reactivity with $ONOOCO_2^-$ as compared to the fully matched G-C base-pairs. The extent of reactivity enhancement was sequence context-dependent, and the greatest levels of enhancement were observed for the conformationally flexible guanine-guanine (G-G) mismatches and for guanines located across from a synthetic abasic site.

To test the hypothesis that the negative charge of an oxidant influences its reactivity with guanines in DNA, sequence-selective guanine oxidation by a negatively charged reagent, Fe^{+2}-EDTA, was assessed and compared to guanine oxidation produced by a neutral oxidant, γ-radiation. Because both of these agents cause high levels of deoxyribose oxidation, a general method to quantify sequence-specific nucleobase oxidation in the presence of direct strand breaks was developed. This method exploited activity of exonuclease III (Exo III), a 3' to 5' exonuclease, and utilized phosphorothioate-modified synthetic oligonucleotides that were resistant to Exo III activity. This method was employed to determine sequence-selective guanine oxidation by Fe^{+2}-EDTA complex and γ-radiation and to show that both agents produced identical guanine oxidation patterns and were equally reactive with all guanines, irrespective of their sequence-specific IPs or sequence context. This showed that negative charge was not a determinant of Fe^{+2}-EDTA-mediated guanine oxidation.

Finally, the role of oxidant binding on nucleobase damage was assessed by studying sequence-selective oxidation produced by DNA-bound Fe^{+2} ions in the presence of H_2O_2. We found that the major oxidation targets were thymines located within 5'-TGG-3' motifs, demonstrating that while guanines were a required element for coordination of Fe^{+2} to DNA, they were not oxidized.

Our results suggest that factors other than sequence-specific IPs can act as major determinants of sequence-selective guanine oxidation, and that current models of guanine oxidation and charge transfer in DNA cannot be used to adequately predict the location and identity of mutagenic lesions in the genome.

Acknowledgements

I am very grateful to my thesis advisor, Prof. Peter C. Dedon, for all of his support, generosity and encouragement, especially through the difficult times when things did not work out as expected. I have learned a great deal from him and have enjoyed interacting with him both on a professional and personal level. I feel that I am very lucky to have had an opportunity to work in his lab.

I am indebted to all the past and present members of the Dedon lab both for their friendship and for their willingness to share their scientific knowledge and expertise with me. I would particularly like to acknowledge the help of Dr. Michael Demott, Dr. Min Dong, Dr. Christianne Collins, and Dr. Marita Barth. Debra Dederich, Jose McFaline, Bahar Edrissi, and Dr. Erin Prestwich proofread parts of this thesis. Olga Parkin, Christine Marzilli, Dawn Erickson and Jackie Goodluck-Griffith have made my everyday life in the lab easy and organized, and I will be forever thankful for their help.

I am very grateful to the members of my thesis committee Prof. Bevin P. Engelward, Prof. John M. Essigmann and Prof. Steven R. Tannenbaum for their continuing encouragement and advice, as well as their enthusiasm for science and sense of humor. I very much appreciate the time and the knowledge they shared with me.

I would like to acknowledge our collaborators in the Geacintov laboratory at the NYU Department of Chemistry Prof. Nicholas E. Geacintov, Prof. Vladimir

Shafirovich, Dr. Young-Ae Lee and Dr. Fabian A. Rodriguez, who have contributed much to our understanding of the mechanisms of guanine oxidation by the carbonate radical anion.

I would like to thank the members my family – my father Yulis, my mother Raisa, my sisters Irene and Masha, my cousin Iva, and my husband Mark for their love and support.

During my undergraduate years at MIT, I was extremely fortunate to have had an opportunity to work in the laboratory of Prof. Vernon M. Ingram, who was not only an outstanding scientist, but also a very kind and gracious human being. I would like to dedicate this thesis to his memory.

Table of Contents

Abbreviations

$^1O_2$	singlet oxygen
8-oxoG	8-oxo-7,8-dihydroguanine
$^{\bullet}OH$	hydroxyl radical
$CO_3^{\bullet-}$	carbonate radical anion
ddH_2O	distilled and deionized water
DGh	dehydroguanidinohydantoin
DNA	deoxyribonucleic acid
E. coli	*Escherichia coli*
EDTA	ethylenediaminetetraacetic acid
Exo III	exonuclease III
FapyG	2,6-diamino-4-hydroxy-5-formamidopyrimidine
Fpg	formamidopyrimidine-DNA glycosylase
$G^{\bullet}$	neutral guanine radical
$G^{\bullet+}$	guanine radical cation
Gh	guanidinohydantoin
γ-^{32}P-ATP	adenosine 5'-triphosphate, [γ-^{32}P]
H_2O_2	hydrogen peroxide
hr	hour
Im	imidazolone
LMPCR	ligation-mediated polymerase chain reaction
min	minute
NHE	normal hydrogen electrode
NMR	nuclear magnetic resonance
$NO^{\bullet}$	nitric oxide
$NO_2^{\bullet}$	nitrogen dioxide radical
$O_2^{\bullet-}$	superoxide
Oa	oxaluric acid
$ONOO^-$	peroxynitrite
$ONOOCO_2^-$	nitrosoperoxycarbonate
PNK	polynucleotide kinase
RNS	reactive nitrogen species
ROS	reactive oxygen species
Sp	spiroiminohydantoin
Tris	2-amino-2-(hydroxymethyl)-1,3-propanediol

List of Figures

List of Tables

Chapter 1

Introduction

ABSTRACT

DNA damage resulting from oxidative stress has been strongly associated with cancer, chronic degenerative diseases and aging. Both the nucleobase and deoxyribose moieties of the DNA are targets for oxidative damage. Guanine is the most frequently oxidized base because of its low ionization potential, and it can be converted into a variety of primary and secondary oxidation products. Generation of a guanine radical cation ($G^{\bullet+}$) as an intermediate in the oxidation reaction leads to migration of the resulting cationic hole through the DNA π-stack until it is trapped at runs of guanines which are characterized by the lowest sequence-specific ionization potentials. This charge transfer mechanism suggests that hotspots of oxidative DNA damage induced by electron transfer reagents can be predicted based on the primary DNA sequence. However, preliminary data indicates that guanine oxidation mediated by nitrosoperoxycarbonate ($ONOOCO_2^-$), a mediator of chronic inflammation, may not conform to the rules of oxidative charge transfer.

BIOLOGICAL IMPORTANCE OF GUANINE OXIDATION

Cellular DNA is being constantly subjected to attack by a variety of oxidizing agents, including environmental pollutants, ionizing radiation, and endogenous reactive intermediates. The latter are responsible for the majority of oxidative damage sustained by nuclear and mitochondrial DNA in aerobic cells, and are overproduced during conditions of chronic inflammation and oxidative stress (1-3). These reactive oxygen and nitrogen species (ROS and RNS, respectively) include hydrogen peroxide (H_2O_2), superoxide ($O_2^{\bullet-}$), nitric oxide ($NO^{\bullet}$), peroxynitrite ($ONOO^-$), nitrosoperoxycarbonate ($ONOOCO_2^-$) and the hydroxyl radical ($^{\bullet}OH$) (4).

A variety of deleterious conditions, including chronic neurodegenerative diseases, artherosclerosis, and carcinogenesis are associated with oxidative stress and chronic inflammation (4-8). For example, recent estimations link approximately 20% of all cancers to chronic inflammatory conditions, such as pancreatitis, inflammatory bowel disease, hepatitis, and inflammation of the prostate that lead to the increased risk of malignancies in the affected organs, while chronic infection of gastric mucosa with *H. pylori* causes an increased risk of gastric cancer (9-11). Oxidative DNA damage is a strong component of the pathologies associated with such diseases, and has been suggested to contribute to disease progression (5). For example, the mechanism of carcinogenesis associated with chronic inflammation is thought to involve chromosomal instability arising from DNA damage by ROS and RNS produced

by activated macrophages and neutrophils in inflamed tissues (5, 12) (Figure 1-1).

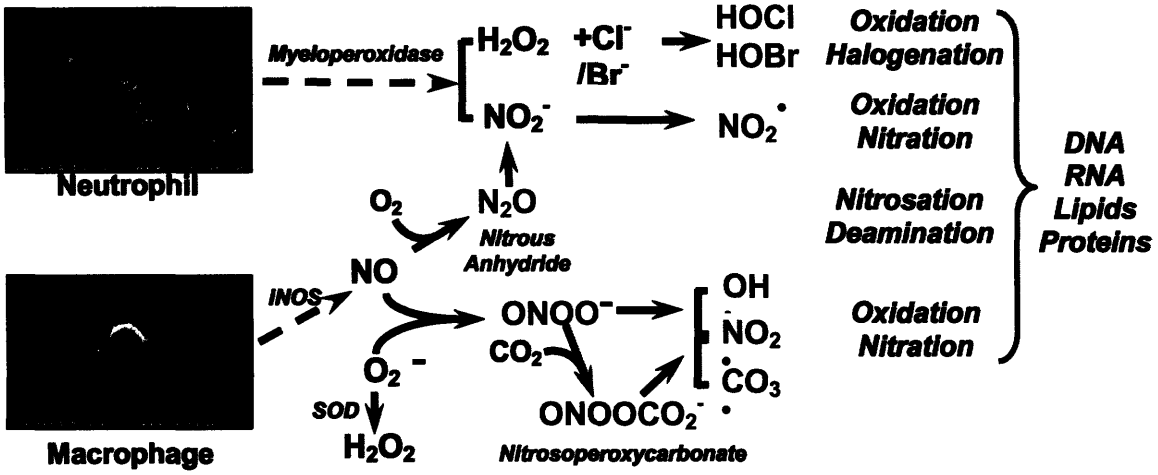

Figure 1-1. ROS and RNS (shown in red) produced by the activated macrophages and neutrophils during chronic inflammation.

While both deoxyribose and nucleobase oxidation constitute the spectrum of DNA damage chemistries, guanine stands out as the major oxidation target due to its low ionization potential and high reactivity with a variety of oxidizing agents (13, 14). A study by Polyak *et al.* found that the majority of mutational hotspots identified within mitochondrial DNA from human colorectal cancer cell lines resided at guanine residues, thus providing direct evidence for the dominating nature and biological importance of oxidative guanine damage mediated by ROS (15). In fact, 8-oxoguanine, the most abundant oxidative guanine lesion, has been commonly employed as a biomarker of conditions

associated with oxidative stress (16, 17). The following sections will briefly discuss the chemistry of guanine oxidation and the determinants of hotspots of oxidative guanine damage in double-stranded DNA.

CHEMISTRY OF GUANINE OXIDATION

Guanine is characterized by the lowest ionization potential of all canonical DNA bases (E^0 = 1.29 V vs normal hydrogen electrode, NHE) and is, therefore, the major target of oxidative damage in DNA (18). The mechanism of guanine oxidation is highly dependent on the nature of the oxidizing species and may involve [4+2] cycloaddition of singlet oxygen ($^1O_2$), direct transfer of an electron from the guanine base, or addition of a hydroxyl radicals ($^{\bullet}OH$) onto the double bonds of a guanine heterocycle (19). Nevertheless, subsequent transformations of the reactive intermediates produced in each case result in their eventual conversion to the same final lesions (19). Mechanisms of generation of primary and secondary guanine oxidation products by a variety of damaging agents have recently been reviewed (19-21), and a brief summary will be presented here with the focus on guanine oxidation mediated by electron transfer reagents as the most relevant to the present discussion.

The initial step in oxidation of a guanine base by electron transfer involves abstraction of an electron from guanine and generation of a guanine radical cation ($G^{\bullet+}$) (Figure 1-2). The deprotonated form of this intermediate, a relatively long-lived neutral guanine radical ($G^{\bullet}$), can be experimentally observed by time-

resolved spectroscopic methods (22-24). Deprotonation of $G^{\bullet+}$ in the context of double-stranded DNA has been demonstrated to proceed in a two-phase process with the rate constants of 1.3×10^7 s^{-1} and 3×10^6 s^{-1} for the fast and slow processes, respectively (25). These phases correspond to deprotonation of the $G^{\bullet+}$ moiety in the G:C base-pair to generate $G^{\bullet}:(C+H)^+$, followed by the loss of a proton by cytosine to produce $G^{\bullet}$:C (25).

The rate of $G^{\bullet}$ recombination with other radical species is close to being diffusion-controlled, and was measured to be 4.7×10^8 s^{-1} and 4.3×10^8 s^{-1} for superoxide ($O_2^{\bullet-}$) and nitrogen dioxide radical ($NO_2^{\bullet}$), respectively (26, 27). A hydroperoxide intermediate results from recombination of $G^{\bullet}$ with $O_2^{\bullet-}$ and is a commonly accepted precursor of imidazolone (Figure 1-1), a major guanine oxidation product that forms in high yields in DNA oxidation reactions mediated by type I photosensitizers, such as benzophenone or riboflavin (19, 28-30).

Trapping of a $G^{\bullet+}$ by a water molecule is a commonly accepted route to formation of 8-oxo-7,8-dihydroguanine or 8-oxoguanine (8-oxoG), another major guanine oxidation product (19, 21). Addition of a water molecule to the C8 of guanine, followed by deprotonation, generates a reducing $G8^{\bullet}OH$ species (Figure 1-1) (19). Loss of a second electron by this intermediate leads to its eventual transformation to 8-oxoG, while presence of reductants in the reaction mixture results in formation of 2,6-diamino-4-hydroxy-5-formamidopyrimidine (FapyG), the reduced and ring-opened form of 8-oxoG (31). 8-oxoG is generally considered to be the most abundant product that forms in high yields upon oxidation of double-stranded DNA by a variety of oxidizing agents (29, 32-34).

The modified base 8-oxoG is highly prone to oxidation as its ionization potential (E^0 = 0.74 V vs NHE) is even lower than that of guanine (35). Therefore, once it forms, 8-oxoG becomes a target for oxidation and a precursor for a number of secondary oxidation lesions (19). The steps of 8-oxoG oxidation by electron transfer are analogous to those for guanine and involve electron transfer from 8-oxoG to an oxidant with subsequent generation of an 8-oxoG radical cation (8-oxoG$^{\bullet+}$) that can undergo deprotonation or hydration (19-21, 36). Final lesions arising from 8-oxoG oxidation are listed in Figure 1-3 and include spiroiminohydantoin (Sp), guanidinohydantoin (Gh), imidazolone (Im), and dehydroguanidinohydantoin (DGh), a precursor to oxaluric acid (Oa) and a major product of 8-oxoG oxidation by type I photosensitizers in double-stranded oligonucleotides (19-21).

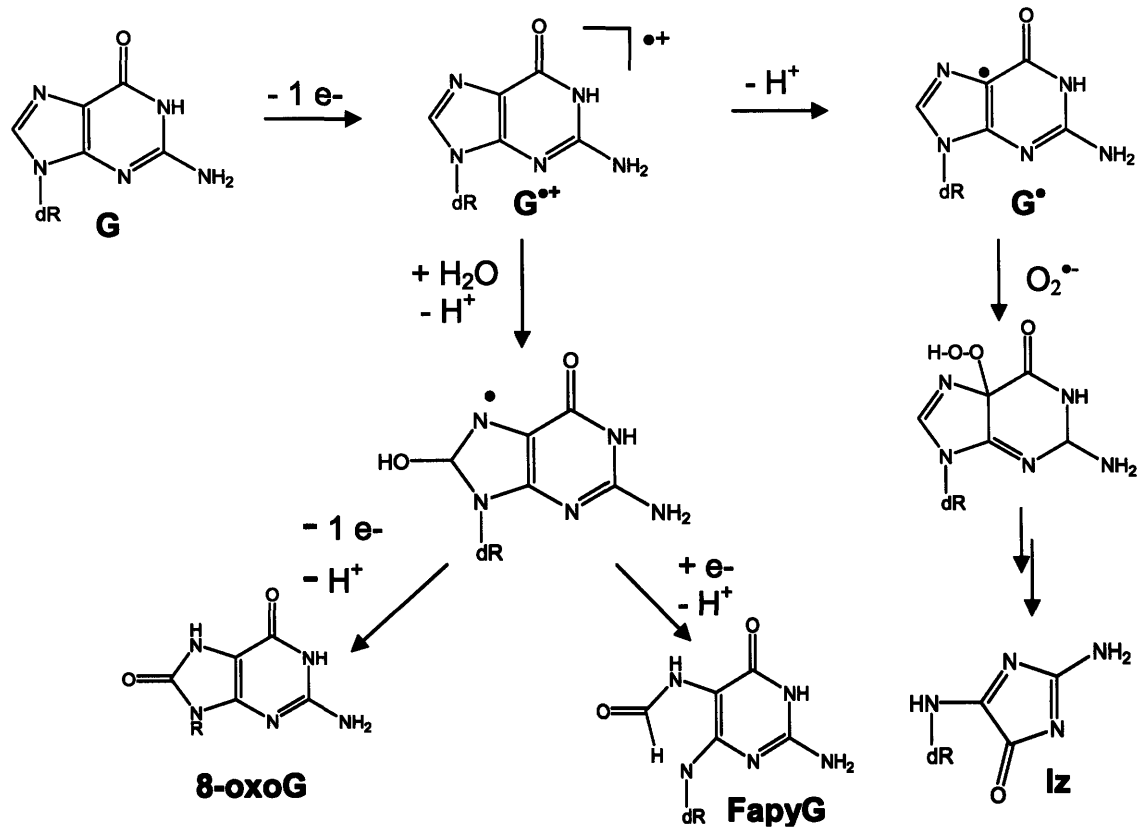

Figure 1-2. Oxidation of guanine by electron transfer. Abbreviations: G, guanine; $G^{\bullet+}$, guanine radical cation; $G^{\bullet}$, neutral guanine radical; 8-oxoG, 8-oxo-7,8-dihydroguanine; Iz, imidazolone; Fapy, 2,6-diamino-4-hydroxy-5-formamidopyrimidine.

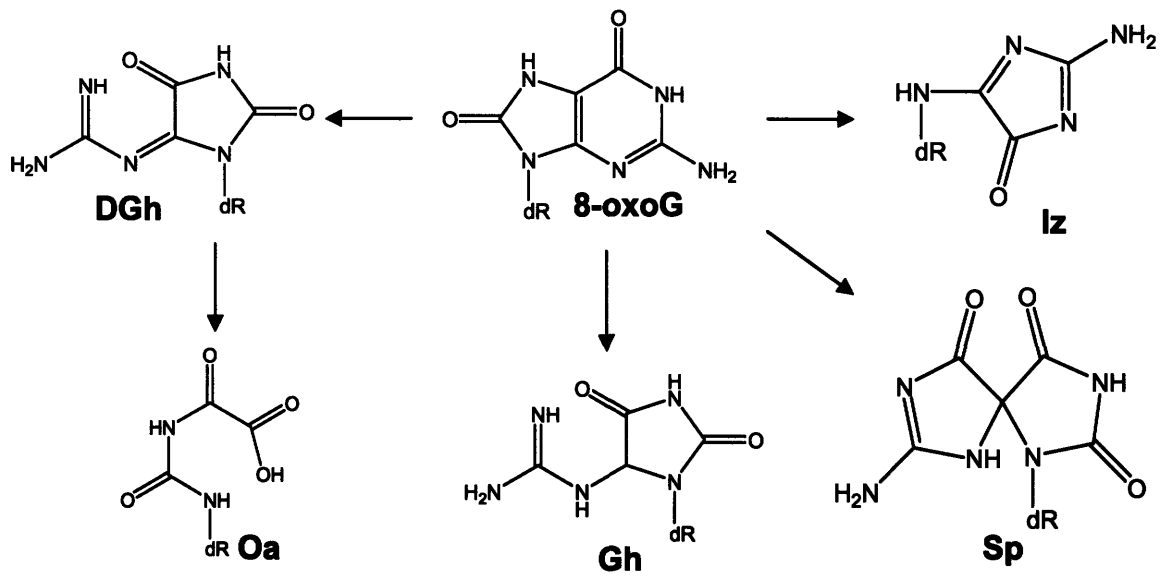

Figure 1-3. Products of 8-oxoguanine oxidation by electron transfer. Abbreviations: 8-oxoG, 8-oxo-7,8-dihydroguanine; Iz, imidazolone; Sp, spiroiminohydantoin, Gh, guanidinohydantoin; DGh, dehydroguanidinohydantoin; Oa, oxaluric acid.

DETERMINANTS OF GUANINE REACTIVITY IN DOUBLE-STRANDED DNA

Oxidative charge transfer. An initial transfer of an electron from guanine to the oxidizing agent produces a cationic hole within DNA π-stack that can migrate long distances though the helix until being irreversibly trapped (Figure 1-4) (37). Trapping involves deprotonation or hydration of $G^{\bullet+}$ and results in formation of oxidative guanine lesions (38). Long-range oxidative charge transfer has been directly observed within synthetic assemblies of double-stranded oligonucleotides covalently linked at their 5' ends to a photooxidizing agent, such

as a $[Rh(phi)_2bpy']^{3+}$ (phi = phenanthrenequinone diimine; bpy' = 4'-methylbipyridine-4-butyric acid) complex studied by the Barton group (37), or an anthraquinone studied by the Schuster group (39). A cationic hole initially injected into the π-stack upon photoactivation of the tethered oxidant has been observed to cause oxidative damage at the sites located up to 200 Å away from the 5' end of such synthetic DNA assemblies (39, 40).

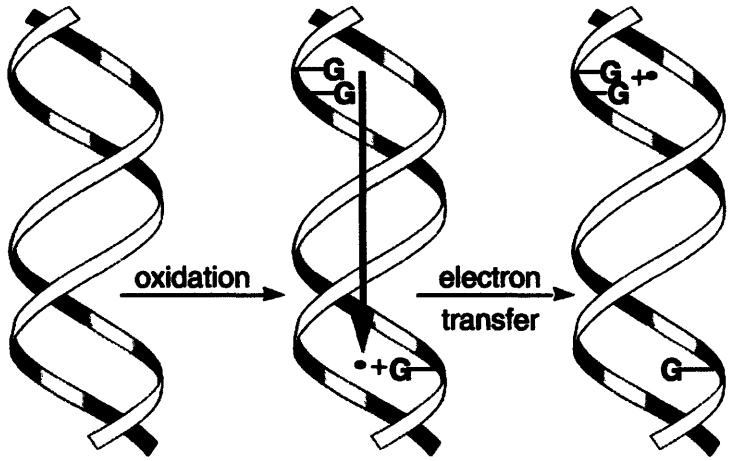

Figure 1-4. Oxidative electron transfer through DNA helix. Adapted from (38).

The mechanism of long-range electron hole migration through DNA has been a subject of intensive investigations and is currently believed to involve short-range fast superexchange combined with a longer-range hopping mechanism. In the fast superexchange process, a cationic hole tunnels over short distances through a DNA bridge between the electron donor and electron acceptor, whereas migration of charge over longer distances consists of distinct

"hops" between guanine bases (41). The Schuster group proposed that the latter involves thermally-assisted hopping of a "polaron", a structure consisting of a cationic hole delocalized in a sequence-dependent manner over several base-pairs in a DNA helix (42). Recently, Lewis *et al.* have directly observed a cross-over from superexchange to the hopping mechanism that occurred at the donor-acceptor distance of about 20 Å, or about 5 base-pairs (43). Short-range electron hole migration occurs on a very short time-scale of around 10^9-10^{12} s^{-1} (41), while the rate for a single hopping step from an isolated guanine to a guanine doublet has been measured to be $k_{hop} = 10^6 - 10^8$ s^{-1} (44). The rates for the long-range electron hole migration are comparable to the rates of $G^{\bullet+}$ trapping through deprotonation or hydration (25).

Guanine runs as the most efficient electron hole traps. It has been consistently noted that guanines located at the 5' positions within runs of guanines, such as 5'-GG-3' and 5'-GGG-3' motifs, acted as the most efficient electron hole traps during oxidative charge transfer. Indeed, the charge transfer mechanism has been evoked to explain preferential damage of guanine runs that has been observed for a variety of structurally diverse one-electron oxidants, including photoactivatable Rh(III) complexes (37), anthraquinones (39), riboflavin (45), pterins (46) and benzophenone (47); Ru(III) metallointercalators (48) and Ni(II) complexes in the presence of sulfite (49); as well as direct laser irradiation (50). Conversely, preferential damage at 5' positions of guanine runs has been a

widely accepted hallmark of oxidative charge migration induced by a DNA damaging agent acting through electron transfer.

Saito and co-workers have examined the properties of 5'-GG-3' and 5'-GGG-3' sequences that conferred to the 5' guanines the ability to act as the most efficient electron hole traps. They showed that stacking interactions of bases in these sequence contexts resulted in lowering guanine's sequence-specific ionization potentials (IPs) that, in turn, determined guanine's reactivity toward one-electron oxidation (51, 52). In a comprehensive study, they used short oligonucleotides containing guanines in all possible three-base sequence contexts (XGY) in a one-electron oxidation reaction mediated by photoactivated riboflavin, and quantified relative amounts of piperidine-sensitive lesions induced within each guanine using sequencing gel (45). These relative reactivity values for guanines were then compared to guanines' sequence-specific IPs, calculated by *ab initio* methods. A strong inverse correlation was observed between IPs and relative reactivities, and guanines located at the 5' position within 5'-GG-3' sequence contexts were characterized by the lowest sequence-specific IPs and highest reactivities toward one-electron oxidation (Figure 1-5). This experiment demonstrated that sequence-specific IPs were the major determinants of guanine's reactivity with electron transfer reagents in double-stranded DNA.

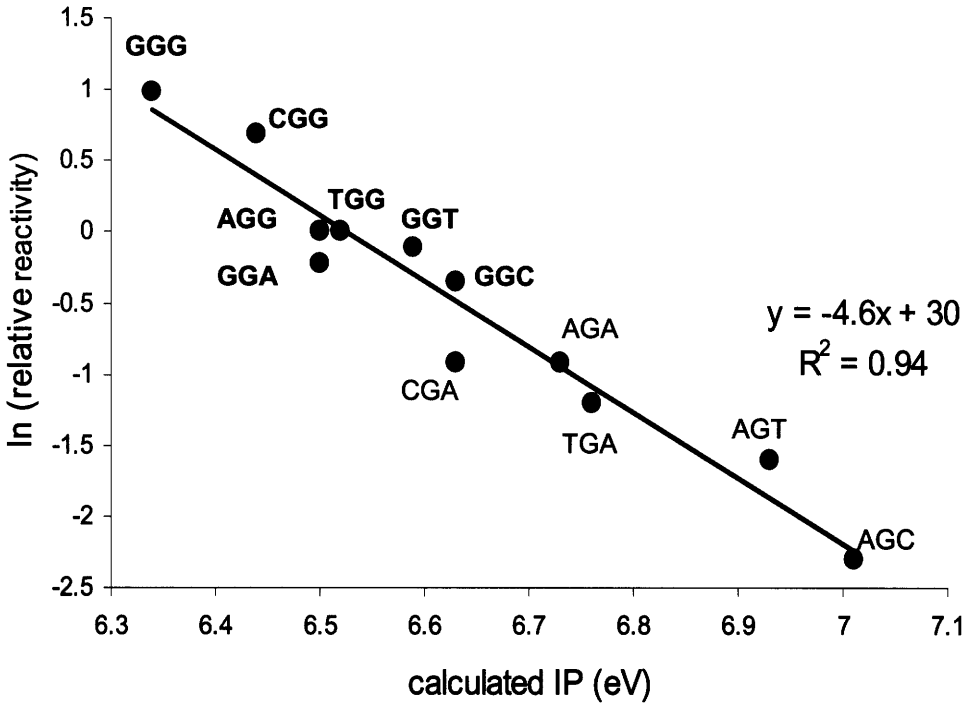

Figure 1-5. Relative numbers of hot piperidine-sensitive guanine lesions produced by photoactivated riboflavin in XGY sequence contexts versus their calculated sequence-specific ionization potentials (IPs). Data points corresponding to sequences containing runs of guanines are marked in bold. Adapted from (45).

UNUSUAL GUANINE OXIDATION BY NITROSOPEROXYCARBONATE

Chronic inflammatory conditions are characterized by overproduction of ROS and RNS that are secreted by activated macrophages and neutrophils to cause elimination of the infections agents (53). The same species can also cause substantial damage to the surrounding biomolecules, including lipid

peroxidation and oxidation and nitration of lipids and DNA (5, 54) (Figure 1-1). Peroxynitrite ($ONOO^-$), a powerful oxidant and DNA damaging agent, is produced by recombination of macrophage-derived nitric oxide ($NO^\bullet$) and superoxide ($O_2^{\bullet-}$) that occurs with a diffusion-controlled rate of 6.6-19 x 10^9 M^{-1} s^{-1} (55, 56). In physiological tissues, where carbon dioxide (CO_2) is present at an approximate concentration of 1 mM, decomposition of $ONOO^-$ proceeds via bimolecular recombination with CO_2 at the rate of 2.9 x 10^4 M^{-1} s^{-1}, resulting in the formation of nitrosoperoxycarbonate ($ONOOCO_2^-$) (57). Scission of the O-O bond in this very unstable intermediate produces carbonate anion ($CO_3^{\bullet-}$) and nitrogen dioxide ($NO_2^\bullet$) radicals that can escape the solvent cage in 30-35% of cases to react with surrounding biomolecules, causing damage (58, 59). Both $ONOOCO_2^-$ and independently generated $CO_3^{\bullet-}$ have been previously shown to cause selective oxidation of guanines in double-stranded DNA (60, 61). In the case of $CO_3^{\bullet-}$, guanine oxidation has been demonstrated to proceed through electron transfer with the generation of a $G^{\bullet+}$, a charge transfer intermediate, the deprotonated form of which has been detected in pulse radiolysis experiments involving guanine-containing oligonucleotides (22).

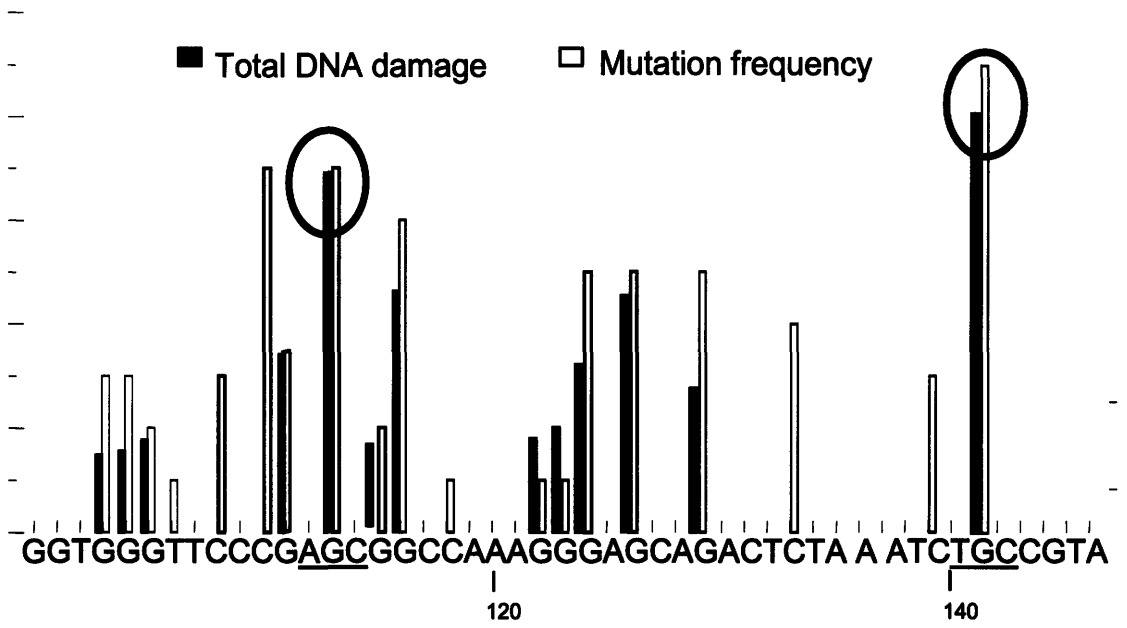

Figure 1-6. Normalized frequency of Fpg-sensitive DNA damage (% total damage) and mutation frequency (total number of mutations) after exposure to $ONOOCO_2^-$. Circled are the observed hotspots of total DNA damage, with their sequence contexts underlined. Adapted from (61).

Our interest in sequence-selective guanine oxidation by $ONOOCO_2^-$ derives from an initial observation of unusual damage patterns produced within a short DNA fragment upon treatment with $ONOOCO_2^-$. Specifically, an experiment was carried out by the Tannenbaum, Dedon and Wogan groups with the purpose of correlating the sites of DNA damage and mutational hotspots produced by $ONOOCO_2^-$ within a *supF* gene in *E. coli* cells (61). While a strong correlation between sites of guanine damage and mutations has indeed been observed, examination of oxidative damage hotspots induced within a 135 bp restriction fragment revealed that guanine runs, characterized by the lowest

sequence-specific ionization potentials, sustained only relatively low levels of oxidative damage (Figure 1-5). Moreover, it was found that 5'-AGC-3' and 5'-TGC-3' sites, characterized by the highest sequence-specific ionization potentials, were the hotspots of $ONOOCO_2^-$-induced damage (Figure 1-5). These preliminary observations contradicted the predictions of based on the oxidative charge transfer model and suggested that sequence-specific ionization potentials were not the predictors of oxidative damage hotspots produced by $ONOOCO_2^-$.

Building upon these observations, this work explores the basis of the unusual sequence selectivity of guanine oxidation by $ONOOCO_2^-$. It has been previously observed that guanines located within single-stranded oligonucleotides displayed a higher reactivity toward $ONOO^-$ and $ONOOCO_2^-$ than guanines located within duplex DNA (60, 62). This has led us to hypothesize than solvent exposure may play a more dominant role in selection of oxidation targets by $ONOOCO_2^-$ than sequence-specific ionization potentials. Solvent exposure is indeed a determining factor of the reactivity of DNA bases with chemical probes of DNA structure such as Ni(II) complexes (63), bromoacetaldehyde (64), diethylpyrocarbonate, and hydroxylamine (65). Additionally, we have also hypothesized that unfavorable electrostatic interactions between the negatively charged $ONOOCO_2^-$ and the DNA backbone precluded access of $ONOOCO_2^-$ to the bases stably stacked inside the DNA helix, limiting its reactivity to the sites with more solvent exposed guanines.

As an initial step in exploring the unusual guanine oxidation by $ONOOCO_2^-$, a comprehensive and a systematic study was undertaken to define relative reactivities of guanines in all possible three-base sequence contexts (XGY) with $ONOOCO_2^-$. The role of solvent exposure in determining guanine reactivity with $ONOOCO_2^-$ was explored by measuring oxidation of mismatched guanines in several sequence contexts. To test the hypothesis that the negative charge of $ONOOCO_2^-$ favors its selectivity for the more solvent-exposed bases, sequence-selective guanine oxidation by another negatively charged oxidant, the Fe^{+2}-EDTA compex, was studied and compared to guanine oxidation produced by γ-radiation, a neutral oxidant. Because both Fe^{+2}-EDTA and γ-radiation produce high level direct strand breaks that can interfere with nucleobase oxidation analysis (66), a method to remove the high strand break background has been developed. Finally, the role of oxidant binding in influencing sequence-selective nucleobase oxidation has been examined by analyzing damage produced by DNA-bound Fe^{+2} ions. Overall, our studies explored the factors that determine the location and identity of mutagenic oxidation lesions in the genome.

REFERENCES

1. Ames, B. N., Shigenaga, M. K., and Hagen, T. M. (1993) Oxidants, antioxidants, and the degenerative diseases of aging. *Proc Natl Acad Sci U S A* 90, 7915-7922
2. Jaruga, P., and Dizdaroglu, M. (1996) Repair of products of oxidative DNA base damage in human cells. *Nucleic Acids Res* 24, 1389-1394
3. Richter, C. (1995) Oxidative damage to mitochondrial DNA and its relationship to ageing. *Int J Biochem Cell Biol* 27, 647-653

4. Valko, M., Leibfritz, D., Moncol, J., Cronin, M. T., Mazur, M., and Telser, J. (2007) Free radicals and antioxidants in normal physiological functions and human disease. *Int J Biochem Cell Biol* 39, 44-84
5. Bartsch, H., and Nair, J. (2006) Chronic inflammation and oxidative stress in the genesis and perpetuation of cancer: role of lipid peroxidation, DNA damage, and repair. *Langenbecks Arch Surg* 391, 499-510
6. Hussain, S. P., Hofseth, L. J., and Harris, C. C. (2003) Radical causes of cancer. *Nat Rev Cancer* 3, 276-285
7. Mercer, J., Mahmoudi, M., and Bennett, M. (2007) DNA damage, p53, apoptosis and vascular disease. *Mutat Res* 621, 75-86
8. Reynolds, A., Laurie, C., Lee Mosley, R., and Gendelman, H. E. (2007) Oxidative stress and the pathogenesis of neurodegenerative disorders. *Int Rev Neurobiol* 82, 297-325
9. Coussens, L. M., and Werb, Z. (2002) Inflammation and cancer. *Nature* 420, 860-867
10. De Marzo, A. M., Platz, E. A., Sutcliffe, S., Xu, J., Gronberg, H., Drake, C. G., Nakai, Y., Isaacs, W. B., and Nelson, W. G. (2007) Inflammation in prostate carcinogenesis. *Nat Rev Cancer* 7, 256-269
11. Lochhead, P., and El-Omar, E. M. (2007) Helicobacter pylori infection and gastric cancer. *Best Pract Res Clin Gastroenterol* 21, 281-297
12. Ohshima, H., Tatemichi, M., and Sawa, T. (2003) Chemical basis of inflammation-induced carcinogenesis. *Arch Biochem Biophys* 417, 3-11
13. Steenken, S., Jovanovic, S.V. (1997) How easily oxidizable is DNA? One-electron reduction potentials of adenosine and guanosine radicals in aqueous solution. *J Am Chem Soc* 119, 617-618
14. Burrows, C. J., and Muller, J. G. (1998) Oxidative Nucleobase Modifications Leading to Strand Scission. *Chem Rev* 98, 1109-1152
15. Polyak, K., Li, Y., Zhu, H., Lengauer, C., Willson, J. K., Markowitz, S. D., Trush, M. A., Kinzler, K. W., and Vogelstein, B. (1998) Somatic mutations of the mitochondrial genome in human colorectal tumours. *Nat Genet* 20, 291-293
16. Loft, S., and Poulsen, H. E. (1996) Cancer risk and oxidative DNA damage in man. *J Mol Med* 74, 297-312
17. Loft, S., Fischer-Nielsen, A., Jeding, I. B., Vistisen, K., and Poulsen, H. E. (1993) 8-Hydroxydeoxyguanosine as a urinary biomarker of oxidative DNA damage. *J Toxicol Environ Health* 40, 391-404
18. Steenken, S., Jovanovic, S.V. (1997) How easily oxidized is DNA? One-electron reduction potentials of adenosine and guanosine radicals in aqueous solution. *J Am Chem Soc* 119, 617-618
19. Pratviel, G., and Meunier, B. (2006) Guanine oxidation: one- and two-electron reactions. *Chemistry* 12, 6018-6030
20. Neeley, W. L., and Essigmann, J. M. (2006) Mechanisms of formation, genotoxicity, and mutation of guanine oxidation products. *Chem Res Toxicol* 19, 491-505

21. Niles, J. C., Wishnok, J. S., and Tannenbaum, S. R. (2006) Peroxynitrite-induced oxidation and nitration products of guanine and 8-oxoguanine: structures and mechanisms of product formation. *Nitric Oxide* 14, 109-121
22. Shafirovich, V., Dourandin, A., Huang, W., and Geacintov, N. E. (2001) The carbonate radical is a site-selective oxidizing agent of guanine in double-stranded oligonucleotides. *J Biol Chem* 276, 24621-24626
23. Shafirovich, V., Dourandin, A., Huang, W. D., Luneva, N. P., and Geacintov, N. E. (1999) Oxidation of guanine at a distance in oligonucleotides induced by two-photon photoionization of 2-aminopurine. *Journal of Physical Chemistry B* 103, 10924-10933
24. Stemp, E. D. A., Arkin, M. R., Barton, J. K. (1997) Oxidation of guanine in DNA by $Ru(phen)_2(dppz)^{3+}$ using the flash-quench technique. *J Am Chem Soc* 119, 2921-2925
25. Kobayashi, K., Tagawa, S. (2003) Direct observation of guanine radical cation deprotonation in duplex DNA using pulse radiolysis. *J Am Chem Soc* 125, 10213-10218
26. Misiaszek, R., Crean, C., Joffe, A., Geacintov, N. E., and Shafirovich, V. (2004) Oxidative DNA damage associated with combination of guanine and superoxide radicals and repair mechanisms via radical trapping. *J Biol Chem* 279, 32106-32115
27. Misiaszek, R., Crean, C., Geacintov, N. E., and Shafirovich, V. (2005) Combination of nitrogen dioxide radicals with 8-oxo-7,8-dihydroguanine and guanine radicals in DNA: oxidation and nitration end-products. *J Am Chem Soc* 127, 2191-2200
28. Kupan, A., Sauliere, A., Broussy, S., Seguy, C., Pratviel, G., and Meunier, B. (2006) Guanine oxidation by electron transfer: one- versus two-electron oxidation mechanism. *Chembiochem* 7, 125-133
29. Douki, T., and Cadet, J. (1999) Modification of DNA bases by photosensitized one-electron oxidation. *Int J Radiat Biol* 75, 571-581
30. Kino, K., Saito, I. (1998) Product analysis of GG-specific photooxidation of DNA via electron transfer: 2-aminoimidazolone as a major guanine oxidation product. *J Am Chem Soc* 120, 7373-7374
31. Candeias, L. P., and Steenken, S. (2000) Reaction of HO* with guanine derivatives in aqueous solution: formation of two different redox-active OH-adduct radicals and their unimolecular transformation reactions. Properties of G(-H)*. *Chemistry* 6, 475-484
32. Yu, H., Venkatarangan, L., Wishnok, J. S., and Tannenbaum, S. R. (2005) Quantitation of four guanine oxidation products from reaction of DNA with varying doses of peroxynitrite. *Chem Res Toxicol* 18, 1849-1857
33. Cadet, J., Delatour, T., Douki, T., Gasparutto, D., Pouget, J. P., Ravanat, J. L., and Sauvaigo, S. (1999) Hydroxyl radicals and DNA base damage. *Mutat Res* 424, 9-21
34. Ravanat, J. L., and Cadet, J. (1995) Reaction of singlet oxygen with 2'-deoxyguanosine and DNA. Isolation and characterization of the main oxidation products. *Chem Res Toxicol* 8, 379-388

35. Steenken, S., Jovanovic, S.V., Bietti, M., Bernhard, K. (2000) The trap depth (in DNA) of 8-oxo-7,8-dihydro-2'deoxyguanosine as derived from electron-transfer equilibria in aqueous solution. *J Am Chem Soc* 122, 2373-2374
36. Shafirovich, V., Cadet, J., Gasparutto, D., Dourandin, A., Huang, W. D., and Geacintov, N. E. (2001) Direct spectroscopic observation of 8-oxo-7,8-dihydro-2 '-deoxyguanosine radicals in double-stranded DNA generated by one-electron oxidation at a distance by 2-aminopurine radicals. *Journal of Physical Chemistry B* 105, 586-592
37. Hall, D. B., Holmlin, R. E., and Barton, J. K. (1996) Oxidative DNA damage through long-range electron transfer. *Nature* 382, 731-735
38. Giese, B. (2002) Long-distance electron transfer through DNA. *Annu Rev Biochem* 71, 51-70
39. Ly, D., Sanii, L., Schuster, G. B. (1999) Mechanism of charge transport in DNA: internally-linked anthraquinone conjugates support phonon-assisted polaron hopping. *J Am Chem Soc* 121, 9400-9410
40. Nunez, M. E., Hall, D. B., and Barton, J. K. (1999) Long-range oxidative damage to DNA: effects of distance and sequence. *Chem Biol* 6, 85-97
41. Wagenknecht, H. A. (2006) Electron transfer processes in DNA: mechanisms, biological relevance and applications in DNA analytics. *Nat Prod Rep* 23, 973-1006
42. Henderson, P. T., Jones, D., Hampikian, G., Kan, Y., and Schuster, G. B. (1999) Long-distance charge transport in duplex DNA: the phonon-assisted polaron-like hopping mechanism. *Proc Natl Acad Sci U S A* 96, 8353-8358
43. Lewis, F. D., Zhu, H., Daublain, P., Fiebig, T., Raytchev, M., Wang, Q., and Shafirovich, V. (2006) Crossover from superexchange to hopping as the mechanism for photoinduced charge transfer in DNA hairpin conjugates. *J Am Chem Soc* 128, 791-800
44. Lewis, F. D., Liu, X., Liu, J., Miller, S. E., Hayes, R. T., and Wasielewski, M. R. (2000) Direct measurement of hole transport dynamics in DNA. *Nature* 406, 51-53
45. Saito, I., Nakamura T., Nakatani K., Yoshioka Y., Yamaguchi K., Sugiyama H. (1998) Mapping of the hot spots for DNA damage by one-electron oxidation: Efficacy of GG doublets and GGG triplets as a trap in long-range hole migration. *J Am Chem Soc* 120, 12686-12687
46. Ito, K., and Kawanishi, S. (1997) Photoinduced hydroxylation of deoxyguanosine in DNA by pterins: sequence specificity and mechanism. *Biochemistry* 36, 1774-1781
47. Nakatani, K., Dohno, C., Nakamura, T., Saito, I. (1998) p-Cyano substituted benzophenone as an excellent photophore for one-electron oxidation of DNA. *Tetrahedron Lett* 39, 2779-2782
48. Arkin, M. R., Stemp, E. D., Pulver, S. C., and Barton, J. K. (1997) Long-range oxidation of guanine by Ru(III) in duplex DNA. *Chem Biol* 4, 389-400

49. Muller, J. G., Hickerson, R. P., Perez, R. J., Burrows, C. J. (1997) DNA damage from sulfite autoxidation catalyzed by a nickel(II) peptide. *J Am Chem Soc* 119, 1501-1506
50. Spassky, A., and Angelov, D. (1997) Influence of the local helical conformation on the guanine modifications generated from one-electron DNA oxidation. *Biochemistry* 36, 6571-6576
51. Saito, I., Takayama, M., Sugiyama, H., Nakatani, K., Tsuchida, A., Yamamoto, M. (1995) Photoinduced DNA cleavage via electron transfer: demonstration that guanine residues located 5' guanine are the most electron-donating sites. *J Am Chem Soc* 117, 6406-6407
52. Sugiyama, H., Saito, I. (1996) Theoretical studies of GG-specific photocleavage of DNA via electron transfer: significant lowering of ionization potential and 5'-localization of HOMO of stacked GG bases in B-form DNA. *J Am Chem Soc* 118, 7063-7068
53. Nathan, C., and Shiloh, M. U. (2000) Reactive oxygen and nitrogen intermediates in the relationship between mammalian hosts and microbial pathogens. *Proc Natl Acad Sci U S A* 97, 8841-8848
54. Dedon, P. C., and Tannenbaum, S. R. (2004) Reactive nitrogen species in the chemical biology of inflammation. *Arch Biochem Biophys* 423, 12-22
55. Huie, R. E., and Padmaja, S. (1993) The reaction of no with superoxide. *Free Radic Res Commun* 18, 195-199
56. Kissner, R., Nauser, T., Bugnon, P., Lye, P. G., and Koppenol, W. H. (1997) Formation and properties of peroxynitrite as studied by laser flash photolysis, high-pressure stopped-flow technique, and pulse radiolysis. *Chem Res Toxicol* 10, 1285-1292
57. Lymar, S. V., Hurst, J.K. (1995) Rapid reaction between peroxynitrite ion and carbon dioxide: implications for biological activity. *J Am Chem Soc* 117, 8867-8868
58. Squadrito, G. L., Pryor, W. A. (2002) Mapping the reaction of peroxynitrite with CO_2: energetics, reactive species and biological implications. *Chem Res Toxicol* 15, 885-895
59. Lymar, S. V., Jiang, Q., and Hurst, J. K. (1996) Mechanism of carbon dioxide-catalyzed oxidation of tyrosine by peroxynitrite. *Biochemistry* 35, 7855-7861
60. Burney, S., Niles, J. C., Dedon, P. C., and Tannenbaum, S. R. (1999) DNA damage in deoxynucleosides and oligonucleotides treated with peroxynitrite. *Chem Res Toxicol* 12, 513-520
61. Tretyakova, N. Y., Burney, S., Pamir, B., Wishnok, J. S., Dedon, P. C., Wogan, G. N., and Tannenbaum, S. R. (2000) Peroxynitrite-induced DNA damage in the supF gene: correlation with the mutational spectrum. *Mutat Res* 447, 287-303
62. Gu, F., Stillwell, W. G., Wishnok, J. S., Shallop, A. J., Jones, R. A., and Tannenbaum, S. R. (2002) Peroxynitrite-induced reactions of synthetic oligo 2'-deoxynucleotides and DNA containing guanine: formation and stability of a 5-guanidino-4-nitroimidazole lesion. *Biochemistry* 41, 7508-7518

63. Chen, X., Burrows, C. J., and Rokita, S. E. (1992) Conformation-specific detection of guanine in DNA: ends, mismatches, bulges, and loops. *J Am Chem Soc* 114, 322-325
64. Kohwi-Shigematsu, T., Gelinas, R., and Weintraub, H. (1983) Detection of an altered DNA conformation at specific sites in chromatin and supercoiled DNA. *Proc Natl Acad Sci U S A* 80, 4389-4393
65. Ross, M. K., Said, B., Shank, R. C. (2000) DNA-damaging effects of genotoxins in mixture: modulation of covalent binding to DNA. *Toxicol Sci* 53, 224-236
66. Kennedy, L. J., Moore, K., Jr., Caulfield, J. L., Tannenbaum, S. R., and Dedon, P. C. (1997) Quantitation of 8-oxoguanine and strand breaks produced by four oxidizing agents. *Chem Res Toxicol* 10, 386-392

Chapter 2

Paradoxical hotspots for guanine oxidation by a chemical mediator of inflammation

ABSTRACT

Peroxynitrite ($ONOO^-$) is produced during chronic inflammation and may contribute to carcinogenesis through oxidative DNA damage. Its decomposition in the presence of carbon dioxide leads to formation of nitrosoperoxycarbonate ($ONOOCO_2^-$), an unstable intermediate that produces carbonate anion ($CO_3^{\bullet-}$) and nitrogen dioxide ($NO_2^{\bullet}$) radicals through disproportionation. When added to the buffer containing bicarbonate, $ONOO^-$ leads to selective oxidation of guanines in the DNA, as does independently generated $CO_3^{\bullet-}$, through a mechanism involving electron transfer from guanine and generation of a guanine radical cation ($G^{\bullet+}$) as an intermediate. Previous studies of $ONOOCO_2^-$-mediated DNA damage have indicated that, unlike other classical, one-electron oxidants that are selective for guanines of lowest ionization potentials (IPs) located within guanine runs, $ONOOCO_2^-$ causes preferential damage at guanines located within 5'-AGC-3' and 5'-TGC-3' sequences characterized by the highest IPs. In a methodical study of sequence-selective guanine oxidation by $ONOOCO_2^-$, we

have determined relative reactivities of guanines within all possible three-base sequence contexts in double-stranded oligonucleotides, and have compared them to the relative reactivities of the same guanines toward photooxidized riboflavin, a classical, one-electron oxidant. In agreement with previous studies, we have determined that photooxidized riboflavin was selective for guanines of lowest IPs, located within guanine runs. In contrast, $ONOOCO_2^-$ preferentially reacted with guanines located within 5'-GC-3' motifs, characterized by the highest IPs. Sequence selectivities for both reagents were double-strand specific. $ONOOCO_2^-$-mediated oxidation of human genomic DNA exhibited a similar selectivity for 5'-GC-3' motifs, as was determined by ligation-mediated PCR analysis. We have also demonstrated sequence-dependent variation in the guanine oxidation chemistry, as relative yields of different guanine oxidation products, produced by both $ONOOCO_2^-$ and photooxidized riboflavin, varied as a function of sequence. Our results demonstrate that factors other than sequence-specific ionization potentials have a role in the selection of targets by $ONOOCO_2^-$, and this complicates efforts to predict the location and chemistry of mutagenic DNA oxidation in the genome.

INTRODUCTION

The association between chronic inflammation and an elevated cancer risk is now well established. A recent estimation links approximately 20% of all cancers to chronic inflammatory conditions, such as pancreatitis, inflammatory

bowel disease, hepatitis, and inflammation of the prostate that lead to the increased risk of malignancies in the affected organs, while chronic infection of gastric mucosa with *H. pylori* causes an increased risk of gastric cancer (1-3). The mechanism of carcinogenesis associated with chronic inflammation is thought to involve chromosomal instability arising from DNA damage by reactive oxygen and nitrogen species (ROS and RNS) produced by the activated macrophages and neutrophils in the inflamed tissues (4, 5) (Figure 1-1).

Peroxynitrite ($ONOO^-$), a powerful oxidant and a DNA damaging agent, is a major example of such a species, produced by a reaction of macrophage-derived nitric oxide ($NO^\bullet$) with superoxide ($O_2^{\bullet-}$) that occurs with a diffusion-controlled rate of 6.6-19 x 10^9 M^{-1} s^{-1} (6, 7). The rate of $O_2^{\bullet-}$ dismutation by superoxide dismutase (SOD) is about 3-8 times lower (k = 2.5 x 10^9 M^{-1} s^{-1}), allowing for initial accumulation of $ONOO^-$ in tissues (8). Indeed, microelectrode-based measurements have established that a single activated RAW264.7 macrophage produces ~9 fmol of $ONOO^-$ in approximately 50 seconds, from estimated ~30 fmol of $NO^\bullet$ and 24 fmol of $O_2^{\bullet-}$ generated by the same cell per oxidative burst (9). It has been further suggested that because $ONOO^-$ is released into a microenvironment of only a few femtoliters, local $ONOO^-$ concentrations may reach into tens of millimolar (9).

Decomposition of peroxynitrite proceeds very rapidly in an aqueous solution at physiological pH, and is dependent on the presence of carbon dioxide (CO_2) in the reaction buffer. In the absence of CO_2, $ONOO^-$ decomposes with a half-life of about 1 second and involves partial protonation to form peroxynitrous

acid (10, 11). This species can undergo homolytic bond scission to produce nitrogen dioxide radical ($NO_2^{\bullet}$) and a hydroxyl radical ($OH^{\bullet}$) in a solvent cage, approximately 70% of which degrades into NO_3^- and H^+, while the remaining 30% escapes the solvent cage and can diffuse across biological membranes to react with surrounding biomolecules (Scheme 2-1) (10, 12). Indeed, peroxynitrite has been shown to oxidize proteins, cause lipid peroxydation and induce both deoxyribose and nucleobase oxidation and nitration in the DNA (13). In physiological tissues, where carbon dioxide (CO_2) is present at an approximate concentration of 1 mM, decomposition of peroxynitrite proceeds via bimolecular recombination of $ONOO^-$ and CO_2 at the rate of $2.9 \times 10^4\ M^{-1}\ s^{-1}$, resulting in the formation of nitrosoperoxycarbonate ($ONOOCO_2^-$) (14). Analogous to decomposition of peroxynitrous acid, scission of the O-O bond in this very unstable intermediate produces carbonate anion ($CO_3^{\bullet-}$) and nitrogen dioxide ($NO_2^{\bullet}$) radicals that can escape solvent cage in 30-35% of the cases to react with surrounding biomolecules, causing damage (Scheme 2-1) (11, 15). Consistent with formation of $OH^{\bullet}$ in the absence, and of $CO_3^{\bullet-}$ in the presence of CO_2 during $ONOO^-$ decomposition, a change in $ONOO^-$-mediated DNA damage chemistry has been observed, with the spectrum of lesions shifting from deoxyribose oxidation leading to strand breaks toward predominant nucleobase oxidation (16, 17). Guanine (G) is the most frequently oxidized nucleobase in the DNA because of its low ionization potential (1.29 V vs. NHE), and its selective damage has indeed been observed within oligonucleotides reacted with $ONOO^-$ in the presence of 25 mM bicarbonate (17, 18).

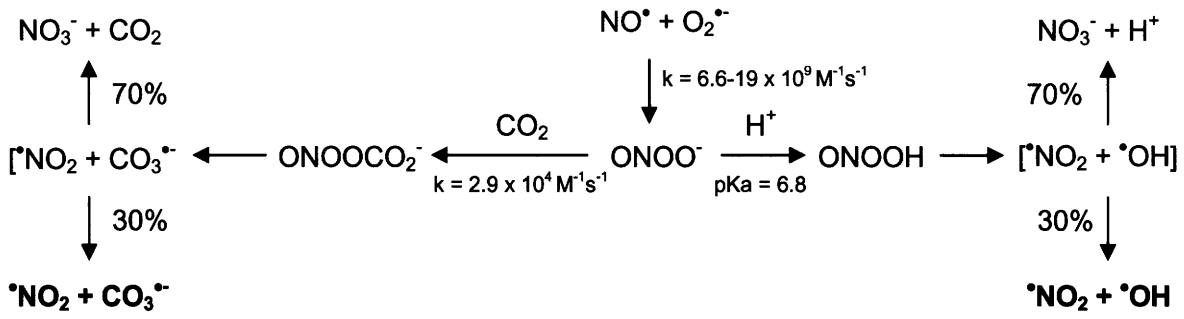

Figure 2-1. Decomposition of peroxynitrite in the absence and presence of CO_2.

The chemistry of guanine oxidation by $ONOO^-$ has been extensively investigated and has recently been reviewed (19). The spectrum of lesions arising from $ONOO^-$-induced guanine damage at physiological pH of 7.4 in the phosphate buffer includes both primary and secondary oxidation, as well as nitration products (Figure 2-2). Secondary oxidation products arise from oxidation of 8-oxoguanine (8-oxoG), the most studied guanine lesion that is inherently more prone to oxidation than G due to its low ionization potential (E^0 = 0.74 V vs. E^0 = 1.29 V vs. NHE, respectively) (20). The nitration products of guanine characterized to date include a stable nitroimidazole (NI) lesion and 8-nitroguanine (8-nitroG); the latter depurinates within several hours to produce abasic sites (17). Primary oxidation products include 8-oxoG and imidazolone (Iz) with its hydrolysis product, oxazolone (Oz) (Figure 2-1) (17, 19, 21-23). Once formed, 8-oxoG is further oxidized to yield spiroiminodihydantoin (Sp), guanidinohydantoin (Gh), HICA, oxaluric acid (OA), and cyanuric acid (CA) as final products that can be detected by liquid chromatography and mass

spectrometry (LC/MS) (19, 24-26). In addition, Iz and Oz can also be formed from oxidation of 8-oxoG (19, 27). The concentration of $ONOO^-$ and its mode of addition to the reaction mixture greatly influence relative efficiencies of formation of various secondary products. If a very high local concentration of $ONOO^-$ is instantaneously achieved by bolus addition, the secondary oxidative lesion spectrum will be dominated by cyanuric acid, oxaluric acid, and oxazolone (19, 23, 26). When $ONOO^-$ is slowly infused into a reaction mixture over time, HICA, Sp and Gh will be primarily observed (19, 25).

Guanine oxidation by independently generated products of $ONOOCO_2^-$ decomposition, $CO_3^{\bullet-}$ and $NO_2^{\bullet}$, has also been investigated. Specifically, it was demonstrated that $CO_3^{\bullet-}$, but not $NO_2^{\bullet}$, is capable of selectively oxidizing guanine through electron transfer to produce the guanine radical cation ($G^{\bullet+}$) (28, 29). The deprotonated form of this intermediate, the neutral guanine radical ($G^{\bullet}$), has been detected in pulse radiolysis experiments involving guanine-containing oligonucleotides (28). The reaction of $G^{\bullet}$ with $O_2^{\bullet-}$ leads to formation of Im as a major product, while its reaction with $NO_2^{\bullet}$ leads to production of NI (30-32). Recent work has also shown that final products of guanine oxidation by $CO_3^{\bullet-}$ in the absence of $NO_2^{\bullet}$ are Sp and Gh, produced through the intermediacy of 8-oxoG (25, 33, 34). Unlike $CO_3^{\bullet-}$, $NO_2^{\bullet}$ does not oxidize guanine, but its oxidation of 8-oxoG leads to the same final products (29, 32).

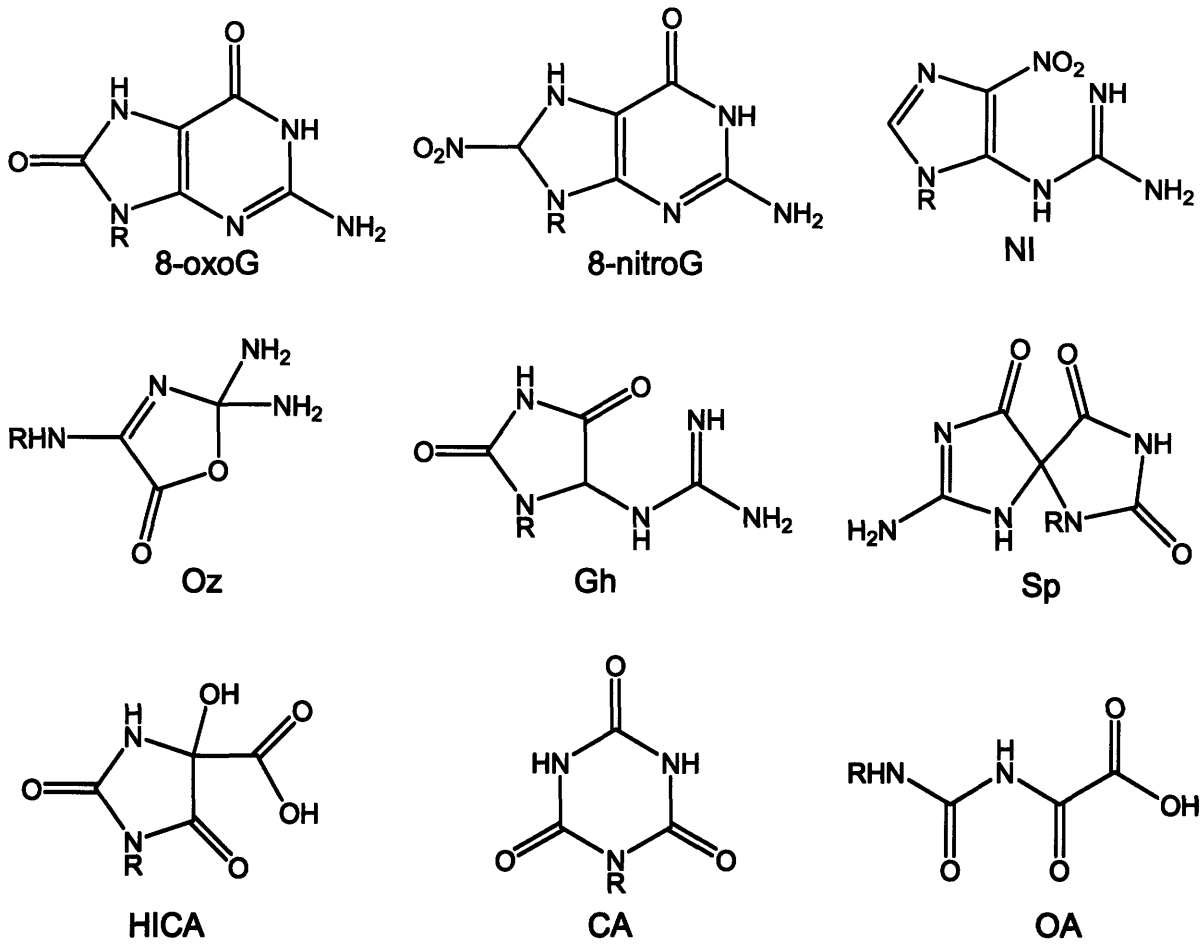

Figure 2-2. Guanine lesions observed at high and low $ONOO^-$ fluxes in phosphate buffer at physiological pH.

As has been reviewed in Chapter 1, oxidizing agents that act by electron transfer and generate $G^{\bullet+}$ cause selective oxidation of runs of guanines within double-stranded DNA, a result of migration of the electron hole through the π-stack to the sites of lowest ionization potentials (35, 36). Surprisingly, guanine runs did not emerge as oxidative damage hotspots in the studies that probed sequence-specific guanine damage induced within a restriction fragment by

$ONOOCO_2^-$ (17). Instead, guanines at positions 113 and 141 in the *supF* gene, located within 5'-AGC-3' and 5'-TGC-3' sequences contexts, respectively, sustained the highest levels of damage (17). These contexts are characterized by the highest sequence-specific guanine ionization potentials, as has been previously calculated using *ab initio* methods by Saito and co-workers (36). We have pursued this curious observation by systematically defining sequence-specific reactivity of $ONOOCO_2^-$. This has been accomplished by determining relative levels of oxidative damage, sustained by guanines within all possible sixteen three-base sequence contexts located within short, single-stranded or duplex oligonucleotides. In addition, we have also utilized ligation-mediated PCR (LMPCR) to analyze sequence-specific guanine damage induced by $ONOOCO_2^-$ within genomic DNA isolated from human TK6 cells. We have compared these relative damage levels to the ones induced by photoactivated riboflavin, a classical one-electron oxidant that is selective for guanine runs. We have also indirectly probed the influence of the sequence context on the efficiencies of formation of various oxidative lesions in the DNA.

MATERIALS AND METHODS

Materials. Synthetic oligonucleotides were purchased from Integrated DNA Technologies (Coralville, IA). $ONOO^-$ was purchased from Cayman Chemical (Ann Arbor, MI). Riboflavin, piperidine and TEMED (N,N,N',N'-Tetramethylethylenediamine) were purchased from Sigma-Aldrich. Urea, boric

acid, tris base, ammonium persulfate and 40% solution of acrylamide:bis (19:1) were obtained from American Bioanalytical (Natick, MA). K_2HPO_4, KH_2PO_4, $NaHCO_3$ and EDTA (ethylenediaminetetraacetic acid, sodium salt) were purchased from Mallinckrodt Baker (Phillipsburg, NJ). All chemicals were used without further purification. Chelex-100 was purchased from Bio-Rad (Hercules, CA), and Sephadex G-25 mini-spin columns were purchased from Roche Diagnostics. *E. Coli* Fpg (formamidopyrimidine [fapy]-DNA glycosylase) was purchased from Trevigen (Gaithersburg, MD), and T4 PNK (polynucleotide kinase) was obtained from New England Biolabs (Ipswich, MA). [γ-^{32}P]-ATP with activity of 6000 Ci/mmol was purchased from Perkin Elmer (Waltham, MA). Distilled and deionized water (ddH_2O) was purified using a Milli-Q system from Millipore (Bedford, MA) and was used for all experiments.

Preparation of buffers. A buffer containing 150 mM potassium phosphate and 25 mM sodium bicarbonate at pH 7.4 was prepared and treated with Chelex-100 resin overnight at 4 ^{0}C to remove adventitious metals. Following treatment, the buffer was passed through a 0.2 micron filter and stored at 4 ^{0}C.

Design of oligonucleotides. The oligonucleotide sequences used for analyses were adapted from previous studies and were of the type 5' – CGTACTCTTTGGT**X_1GY$_1$TX_2GY$_2$**TTCTTCTAT – 3' (36). This sequence contains consensus portions on both 5' and 3' ends, an invariant TGG sequence at the same position in all oligonucleotides for normalizing damage (underlined),

and two variable guanine sequence contexts X_1GY_1 and X_2GX_2. For each oligonucleotide, counterparts with the relative positions of X_1GY_1 and X_2GX_2 reversed were also analyzed to account for longer-range sequence effects. Table 2-1 shows sequences of all oligonucleotides used in experiments.

Purification of synthetic oligonucleotides. To remove the background of oxidized bases, all oligonucleotides were treated with 1 M piperidine at 90^0 C for 30 minutes and lyophilized prior to gel purification. The oligonucleotides were re-dissolved in TE buffer, pH 8.0 with 20% glycerol, and loaded on a 20% acrylamide:bis, 8M urea preparative gel electrophoresis. The gel was run in 1x TBE at a constant power of 70 watts for 6 hours. Oligonucleotides were visualized by UV shadowing, cut out from the gel, eluted by overnight shaking in 0.5 M ammounium acetate and 10 mM magnesium acetate, filtered and ethanol precipitated. All oligonucleotides were desalted by Sephadex G-25 spin columns and transferred to 150 mM potassium phosphate, 25 mM sodium bicarbonate buffer before use.

Oligonucleotide name	Oligonucleotide sequence (5' to 3')
S1	CGTACTCTT***TGG***TTGATGGGTTCTTTCTAT
1S	CGTACTCTT***TGG***TGGGTTGATTCTTTCTAT
S2	CGTACTCTT***TGG***TCGGTTGCTTCTTTCTAT
2S	CGTACTCTT***TGG***TTGCTCGGTTCTTTCTAT
S3	CGTACTCTT***TGG***TAGTTGGATTCTTTCTAT
3S	CGTACTCTT***TGG***TGGATAGTTTCTTTCTAT
S4	CGTACTCTT***TGG***TAGGTTGTTTCTTTCTAT
4S	CGTACTCTT***TGG***TTGTTAGGTTCTTTCTAT
S5	CGTACTCTT***TGG***TCGCTCGATTCTTTCTAT
5S	CGTACTCTT***TGG***TCGATCGCTTCTTTCTAT
S6	CGTACTCTT***TGG***TAGCTAGATTCTTTCTAT
6S	CGTACTCTT***TGG***TAGATAGCTTCTTTCTAT
S8	CGTACTCTT***TGG***TGGCTCGTTTCTTTCTAT
8S	CGTACTCTT***TGG***TCGTTGGCTTCTTTCTAT
S9	CGTACTCTT***TGG***TAGCTGGTTTCTTTCTAT
9S	CGTACTCTT***TGG***TGGTTAGCTTCTTTCTAT

Table 2-1. Sequences of oligonucleotides used for the analysis of relative guanine damage induced by photoactivated riboflavin and $ONOOCO_2^-$. Relative reactivities of guanines shown in bold within underlined sequence contexts have been quantified, and the invariant TGG sequence used for normalizing damage is italicized.

Labelling and annealing of oligonucleotides. Oligonucleotides were 5'-end labeled with ^{32}P in a reaction containing approximately 100 pmol of 5' ends,

20 units of T4 polynucleotide kinase and 50 μCi of γ-^{32}P-ATP in 1x PNK buffer (New England Biolabs, Ipswich, MA) in a total volume of 50 μl. After incubation at 37 ^{0}C for 1 hr, unreacted γ-^{32}P-ATP was removed by a G-25 Sephadex column that has been washed with 150 mM potassium phosphate, 25 mM sodium bicarbonate buffer. For annealing, approximately 200 pmol of unlabeled complement was added to the labeled oligonucleotide, the mixture was incubated at 95 ^{0}C for five min and then was allowed to cool down to room temperature over a course of approximately 90 min.

Damage of labeled oligonucleotides with riboflavin. Duplex or single-stranded 30-mer oligonucleotides (30 μM nt) were treated at 0 ^{0}C with 30 μM riboflavin/366 nm irradiation for 20 min as described by Saito *et al.* except for buffer conditions (150 mM potassium phosphate, 25 mM sodium bicarbonate, pH 7.4) (36). Following treatment, the oligonucleotides were de-salted by Sephadex G-25 columns. Control reactions contained 150 mM potassium phosphate, 25 mM sodium bicarbonate buffer instead of riboflavin. Three independent damage and control reactions were carried out for all oligonucleotides, and each independent reaction was carried out in triplicates.

Damage of labeled oligonucleotides with $ONOOCO_2^-$. Concentration of $ONOO^-$ stock solution was measured in 0.3 N NaOH using an absorption coefficient of ε_{302} = 1670 M^{-1} cm^{-1} (37). The stock solution in 0.3 N NaOH was stored at -80 ^{0}C and was kept on ice at all times during use. For damage

reaction, $ONOO^-$ stock solution or an equal volume of 0.3 N NaOH was added to the duplex or single-stranded labeled oligonucleotides in 150 mM potassium phosphate, 25 mM sodium bicarbonate buffer in a bolus manner for a final $ONOO^-$ concentration of 2 mM. The reactions were typically left on a benchtop for 1 hr before they were de-salted using Sephadex G-25 columns.

Piperidine and Fpg treatments of damaged oligonucleotides. Damaged and de-salted oligonucleotides were treated with 1 M piperidine at 90 ^{0}C for 20 min or with Fpg glycosylase at 37 ^{0}C for 1 hour in the supplied buffer (Trevigen, Gaithersburg, MD) under the conditions of enzyme excess (3 units/reaction; 1 unit is defined as the amount of enzyme required to cleave 1 pmole of a ^{32}P-labeled oligonucleotide probe containing 8-oxoguanine within an oligonucleotide duplex in 1 hr at 37 ^{0}C). Following lyophilization (or ethanol precipitation in the case of Fpg treatment), the DNA fragments were dissolved in a total of 5 µl of formamide gel-loading buffer.

Gel electrophoresis and damage quantification. The DNA was resolved on a 20% polyacrylamide gel (8M urea) that was run in 1xTBE at the constant power of 70 watts for 3 hrs. The gels were subjected to phosphorimager analysis (ImageQuant, Molecular Dynamics). Phosphorimager data for guanine cleavage were normalized to total radioactivity in the gel lane, with $ONOOCO_2^-$- or riboflavin-treated values corrected for background, and relative reactivity determined in relation to the 5'-TGG-3' sequence in each

oligonucleotide. Total damage in each oligonucleotide ranged over the following values: 6-17% for riboflavin in double-stranded DNA; 10-20% for riboflavin in single-stranded DNA; 1-2% for $ONOOCO_2^-$ in double-stranded DNA; 7-17% for $ONOOCO_2^-$ in single-stranded DNA.

Analysis of sequence-dependent guanine oxidation in genomic DNA by LMPCR (performed by Dr. Jean-Francois Cloutier). DNA was purified from human TK6 cell nuclei by a phenol extraction method in the presence of desferroxamine, as described in detail elsewhere (38). The purified genomic DNA was treated with 0-3 mM $ONOO^-$ in 150 mM potassium phosphate and 25 mM sodium bicarbonate buffer (pH 7.4, ambient temperature, 30 min). Oxidized bases were expressed as strand breaks by treatment with Fpg (oxidized purines) and Endo III (oxidizes pyrimidines; to rule out reactions at pyrimidine bases) and the strand breaks were mapped by LMPCR using primer sets developed for the hypoxanthine phosphoribosyltransferase gene (*HPRT*), as described in detail elsewhere (39).

RESULTS

Sequence-specific guanine oxidation by riboflavin and $ONOOCO_2^-$ in duplex oligonucleotides. 5'-^{32}P-end labeled duplex or single-stranded synthetic oligonucleotides containing guanines in all possible sixteen sequence contexts were damaged with either 30 μM riboflavin or 2 mM $ONOO^-$, treated with hot piperidine or Fpg glycosylase to convert oxidized guanines to strand breaks, and separated on a 20% sequencing gel. Damage induced within central guanine of each XGY sequence context was quantified relative to the damage at the central guanine within the invariant TGG normalization sequence. Figures 2-3A and 2-3B show representative gels used for damage quantification.

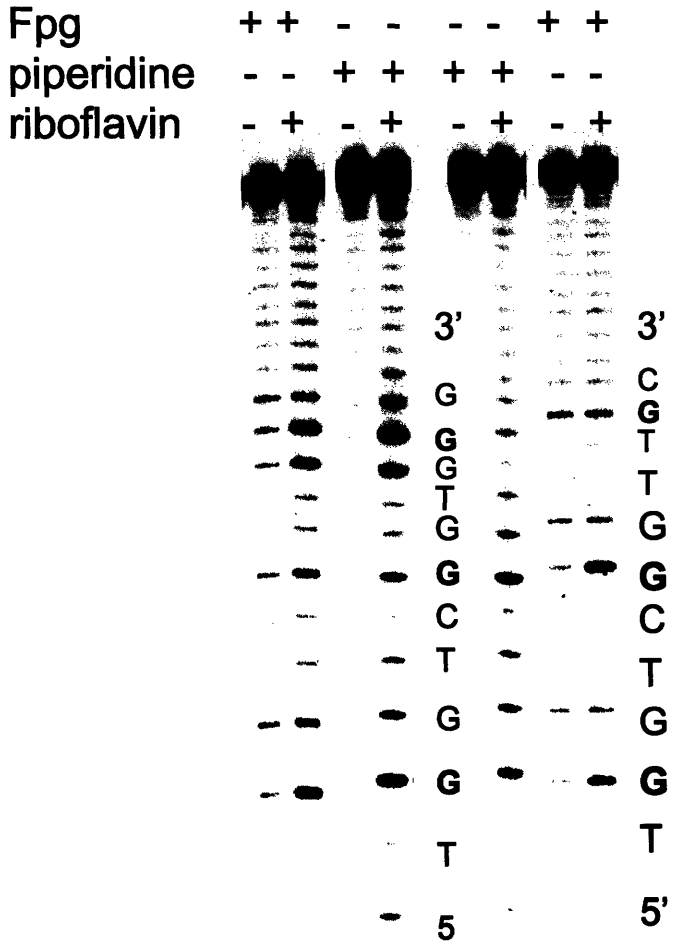

Figure 2-3A. A typical picture of a sequencing gel used for quantification of relative guanine damage induced by photoactivated riboflavin. 5'-^{32}P-end labeled, double-stranded oligonucleotides were reacted with 0 or 30 μM riboflavin/366 nm irradiation, then treated with 1M piperidine or Fpg, separated on a 20% acrylamide, 8M urea sequencing gel and visualized by autoradiography.

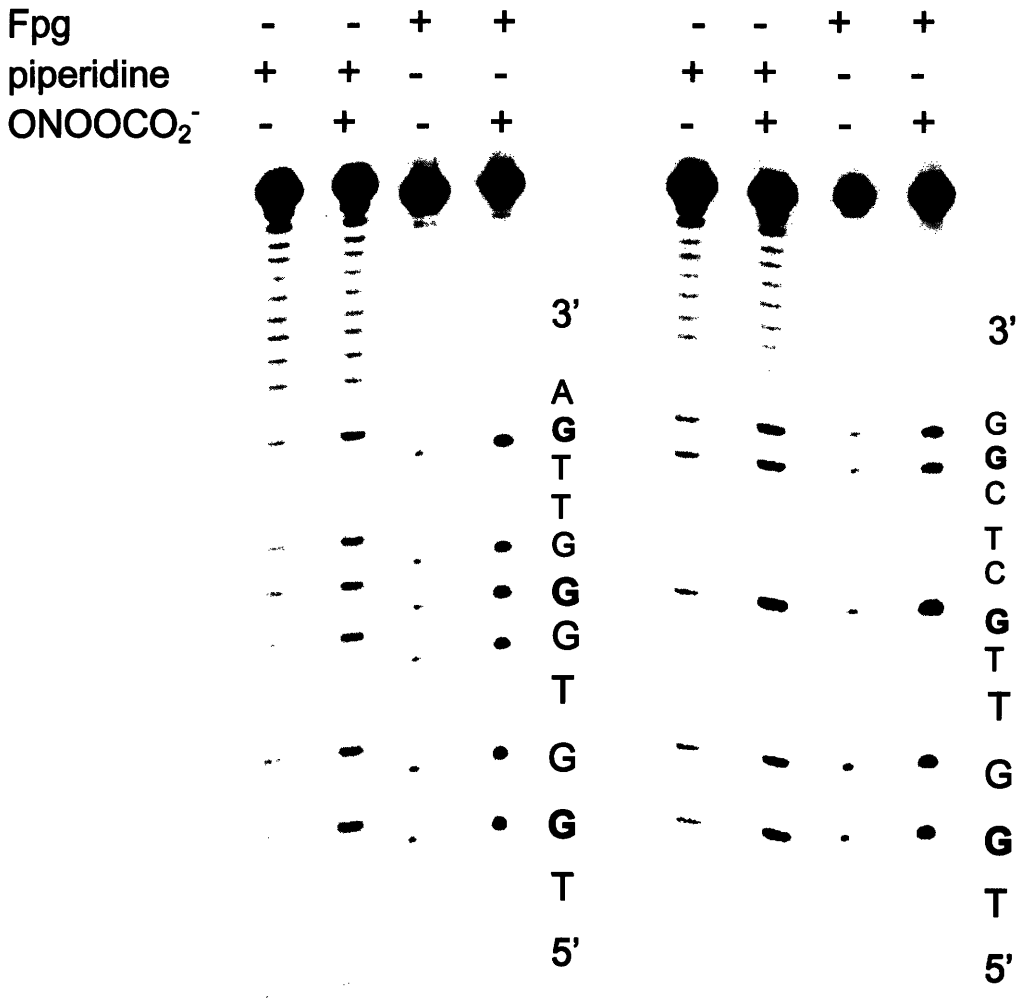

Figure 2-3B. A typical picture of a sequencing gel used for quantification of relative guanine damage induced by $ONOOCO_2^-$. 5'-^{32}P-end labeled, double-stranded oligonucleotides were reacted with 0 or 2 mM $ONOO^-$, then treated with 1M piperidine or Fpg, separated on a 20% acrylamide, 8M urea sequencing gel and visualized by autoradiography.

Figure 2-4 shows relative reactivities of guanines in all sequence contexts, expressed as relative amounts of hot piperidine-sensitive lesions, plotted as a function of their calculated sequence-specific ionization potentials (36). A plot of guanine damage frequency in different sequence contexts as a function of guanine IP reveals only a modest sequence dependence of guanine reactivity with $ONOOCO_2^-$, except at the highest IP values. This stands in sharp contrast to the inverse relationsip between IP and reactivity associated with the riboflavin-mediated photooxidation. The highest frequency of $ONOOCO_2^-$-induced damage occurred in AGC and TGC sequences, which also conferred the highest guanine IP (whereas GGG was characterized by the lowest reactivity and the lowest IP). With the notable exception of GGC, guanine oxidation varied only modestly with increasing IP up to 6.96 eV (TGT), after which there was a sharp increase in reactivity (CGC, AGC and TGC). GGC was unique in having both the highest IP of all GG-containing sequences and high relative reactivity with $ONOOCO_2^-$ in spite of the relatively low reactivity of other GG-containing sequences. With respect to riboflavin-mediated photooxidation, we have found the same linear relationship between relative reactivity and IP as reported in previously published work by Saito *et al.* (omitting data for TGT, CGT, CGC and TGC, as in ref. 36), even though we used different buffers (36). Sequence selectivity patterns obtained by plotting relative amounts of Fpg-sensitive lesions, produced very similar results for both oxidants. These patterns, however, are specific to the duplex DNA, and break down when single-stranded oligonucleotides are used for damage experiments, as is demonstrated in Figure 2-5.

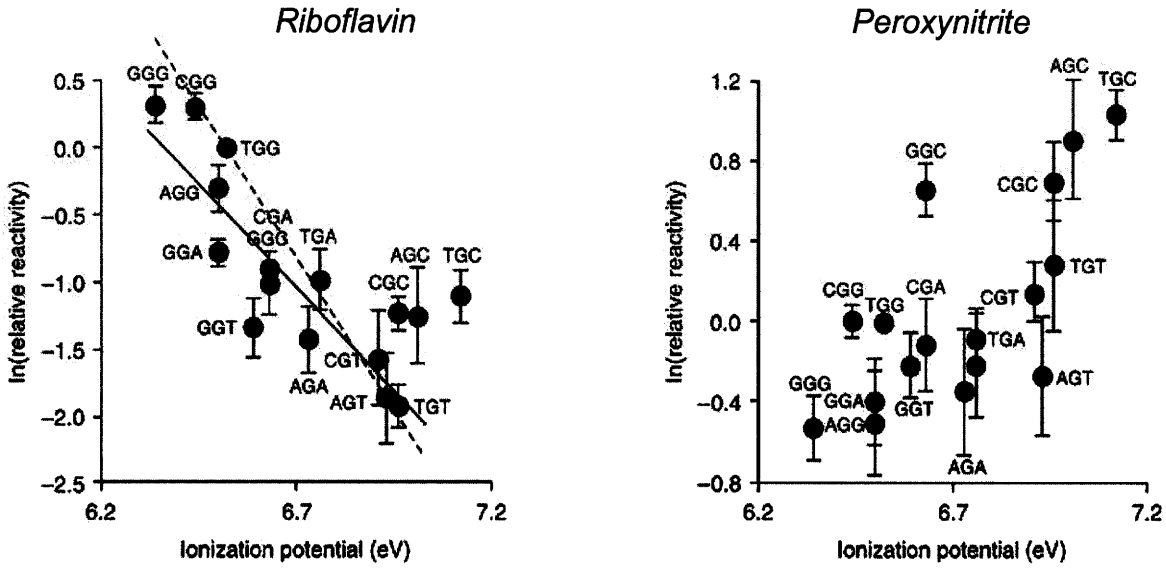

Figure 2-4. Sequence-selective guanine oxidation in duplex DNA by $ONOOCO_2^-$ and riboflavin-mediated photooxidation. Relative reactivity data, expressed as relative amounts of piperidine-sensitive lesions induced by $ONOOCO_2^-$ and riboflavin photooxidation in XGY motifs in oligodeoxynucleotides are plotted against guanine sequence-specific ionization potentials (IP), obtained from ref 36. Lines in the riboflavin graph represent linear regression fits of riboflavin-mediated photooxidation data from our studies (solid line; y = 18.5 – 2.90x; data for TGT, CGT, CGC and TGC omitted) and from other published work (dashed line; y = 30.2 – 4.62x). Data represent mean ± s.d. for three independent experiments.

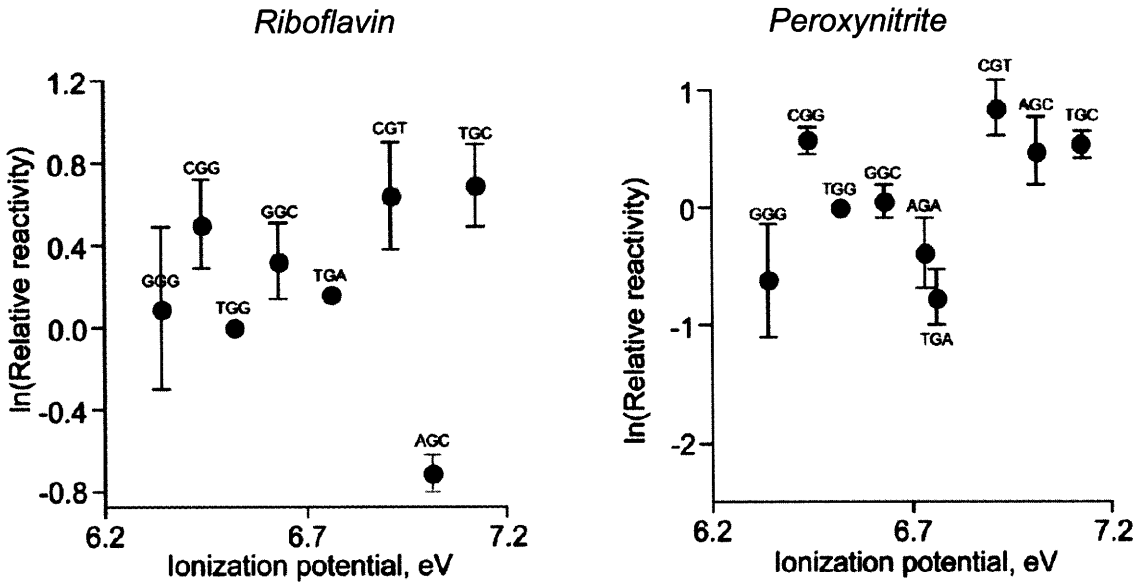

Figure 2-5. Sequence-selective guanine oxidation in single-stranded DNA by $ONOOCO_2^-$ and riboflavin-mediated photooxidation. Relative amounts of hot piperidine-labile guanine lesions induced by photooxidized riboflavin and $ONOOCO_2^-$ in single-stranded oligonucleotides in different sequence contexts were graphed vs. guanine's sequence-specific ionization potentials. Data represent mean ± s.d. for three independent experiments.

Sequence-selective guanine oxidation by $ONOOCO_2^-$ in human genomic DNA (performed by Dr. Jean-Francois Cloutier). Oxidative base damage hotspots induced by $ONOOCO_2^-$ in the *HPRT* gene of human lymphoblastoid TK6 cell genomic DNA were mapped by ligation-mediated PCR. Figure 2-6 displays representative gel traces of control and $ONOOCO_2^-$-treated lanes. Damage hotspots occurred almost exclusively at AGC and TGC sites, again consistent with the observed selectivity of $ONOOCO_2^-$ for guanines with the highest IP.

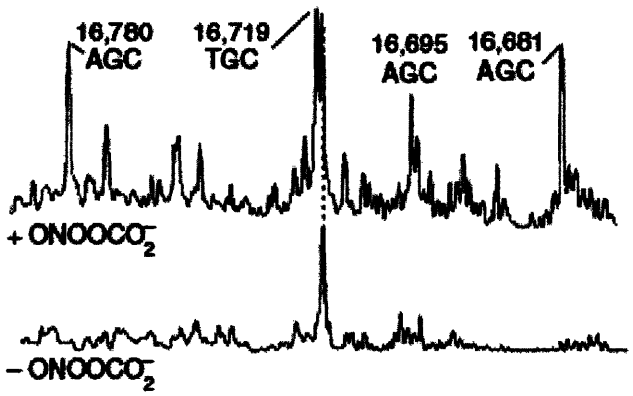

Figure 2-6. Sequence-selective guanine oxidation by $ONOOCO_2^-$ in human genomic DNA. Frequency of guanine oxidation by $ONOOCO_2^-$ in the *HPRT* gene in human lymphoblastoid TK6 cell genomic DNA was mapped by ligation-mediated PCR (See Materials and Methods). Oxidized guanines noted above specific peaks in the line graphs are derived from phosphorimager analysis of an LMPCR sequencing gel (not shown).

Sequence-specific distribution of guanine lesions produced by $ONOOCO_2^-$ and riboflavin. Since guanine lesions induced by both $ONOOCO_2^-$ and riboflavin-mediated photooxidation are characterized by differential sensitivities toward hot piperidine and Fpg treatments, comparison of the relative amounts of Fpg- to piperidine-sensitive lesions across all sequence contexts provides a measure of sequence-specific guanine oxidation chemistry. The ratios of Fpg- to piperidine-sensitive damage products in different guanine sequence contexts is graphed in Figure 2-7 and varies by approximately 5.4-fold for $ONOOCO_2^-$-induced damage, and by about 3.4-fold for riboflavin-induced damage. For both oxidants, CGT, AGT and GGT motifs are characterized by the lowest Fpg/piperidine ratios ($ONOOCO_2^-$ induced undetectable levels of Fpg-sensitive damage within GGT motif).

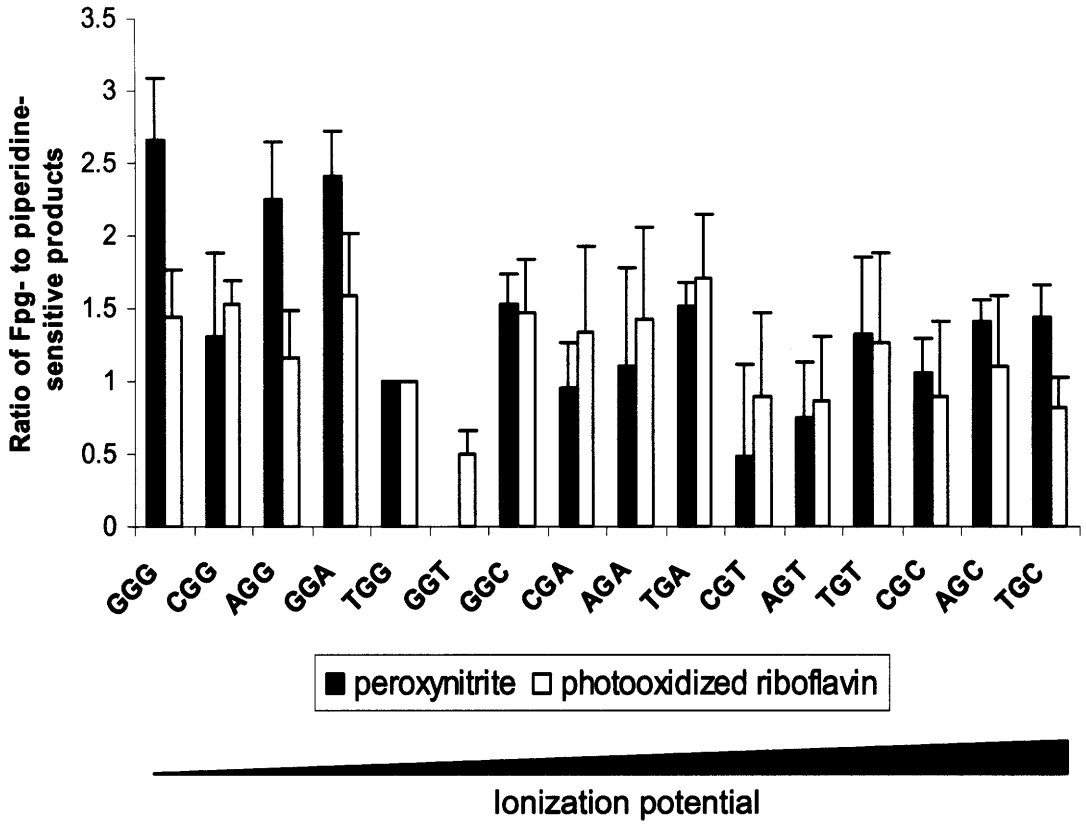

Figure 2-7. Sequence selectivity of photooxidized riboflavin- and $ONOOCO_2^-$-induced guanine oxidation chemistry. Duplex oligonucleotides were treated with photooxidized riboflavin or $ONOOCO_2^-$, and guanine lesions were expressed as strand breaks by either hot piperidine or Fpg treatments (See Materials and Methods). The ratio of Fpg- to piperidine-sensitive cleavage is plotted for each XGY motif, with IP increasing from left to right. Each bar graph represents mean ± propagated s.d. for three experiments.

DISCUSSION

Paradoxical sequence selectivity of guanine oxidation by $ONOOCO_2^-$. As has been reviewed in Chapter 1, selective oxidation of guanines located at the 5' positions within guanine runs is characteristic of the majority of DNA damaging agents that act through electron transfer. This sequence selectivity, shared by a variety of structurally diverse oxidants, can be explained by a generation of a common intermediate, guanine radical cation ($G^{\bullet+}$), and initiation of charge transfer through the DNA π stack to trap the electron hole at runs of guanines, with subsequent formation of oxidation products (35). Saito *et al.* have calculated ionization potentials (IP) of guanines located within all possible three-base sequence contexts, and have demonstrated that an inverse linear relationship exists between guanine's susceptibility to one-electron oxidation and its sequence-specific IP (36). Sequences containing guanine runs were found to be characterized by the lowest IP values and sustained the highest levels of damage by photooxidized riboflavin (36).

$CO_3^{\bullet-}$, formed during decomposition of $ONOOCO_2^-$, selectively oxidizes guanines through electron transfer to produce $G^{\bullet+}$, a charge transfer intermediate (28). Sequence-selective damage of double-stranded DNA, however, has revealed that oxidative damage hotspots, produced by $ONOOCO_2^-$, are located within AGC and TGC sites that are characterized by the highest ionization potentials, according to the Saito model (17, 36). We have confirmed these observations with our present data, demonstrating that AGC and TGC motifs

within double-stranded oligonucleotides are most frequently damaged by $ONOOCO_2^-$ in bicarbonate buffer. In addition, CGC and GGC motifs have also emerged as the most frequently damaged sites, making a 5'-GC-3' sequence context a major determinant of $ONOOCO_2^-$-mediated guanine oxidation. This unusual sequence selectivity is also confirmed within genomic DNA of TK6 cells. In contrast, we were able to reproduce published data of sequence-selectivite guanine oxidation by photoactivated riboflavin, and have found the same linear relationship between relative reactivity and IP values (omitting data for TGT, CGT, CGC and TGC, as in ref 36). These results indicate that the unusual sequence dependence of $ONOOCO_2^-$-induced guanine oxidation is not an experimental artifact, as we have observed no sequence dependence for damage frequency in single-stranded oligodeoxynucleotides with riboflavin or $ONOO^-$.

In support of our conclusion that 5'-GC-3' motif is a major determinant of $ONOOCO_2^-$-mediated guanine damage are the results of mutagenesis studies carried out in *E. coli* MBL50 cells using a *supF* shuttle vector pSP189 (40). Of the total of four guanine-centered mutational hotspots, identified between 100 and 180 nucleotide positions within the *supF* gene, three are located within 5'-GC-3' motifs (AGC, GGC and TGC) (40). Out of a total of three cytosine-centered hotspots, two are located within 5'-TCC-3' motifs, corresponding to the 5'-GGC-3' motifs on the complementary strand (40). In addition, earlier studies have found a good correlation between the levels of damage induced within the

same *supF* fragment by $ONOOCO_2^-$, and numbers of mutations produced after its replication in MBL50 bacterial cells (17).

Clearly, factors other than sequence-specific guanine IP have a role in selection of targets by $ONOOCO_2^-$ or its decomposition products during DNA oxidation. Our results showing that selectivity of $ONOOCO_2^-$ for 5'-GC-3' sites disappears in single-stranded oligonucleotides confirm that secondary structure of the DNA may be one such factor. Solvent exposure is another possible determining factor in sequence-selective guanine oxidation by $ONOOCO_2^-$, as single-stranded oligonucleotides are, on average, about 5- to 9-times more reactive than duplex DNA (See Materials and Methods), consistent with previous results (21). In contrast, no difference in total reactivity between single- and double-stranded oligonucleotides was evident in the case of riboflavin-mediated photooxidation (See Materials and Methods). It is possible that repulsion of the negative charge of $ONOO^-$, $ONOOCO_2^-$ or $CO_3^{\bullet-}$ by the negatively charged DNA backbone limits their accessibility to guanines within the double helix and drives their reactions with transiently solvent-exposed bases. In support of this model, Ingold and co-workers have observed major differences in the levels of deoxyribose and nucleobase oxidation, induced by positively charged, neutral and negatively charged peroxyl radicals in supercoiled DNA substrates, underscoring a possible role of electrostatic interactions in DNA oxidation (41, 42).

The rates of initial electron removal by $CO_3^{\bullet-}$ have been measured for isolated guanines and guanines located within guanine runs in duplex

oligonucleotides (43). No significant variations in the electron transfer rates have been found, in contrast to oxidation of the same oligonucleotides by an ionized pyrene derivative 7,8,9,10-tetrahydroxytetrahydrobenzo[*a*]pyrene (BPT), a classical one-electron oxidant, where a 40-fold higher electron transfer rate has been observed for guanine runs (43). Therefore, minimal variations in the electron transfer rates during $ONOOCO_2^-$-induced guanine oxidation may partially explain the unusual sequence selectivity of $ONOOCO_2^-$. Further studies, however, will be needed to identify factors responsible for preference of $ONOOCO_2^-$ for 5'-GC-3' sites. Interestingly, $ONOOCO_2^-$ may not be the only DNA oxidant that displays this unusual sequence selectivity. Rodriguez *et al.* have conducted LMPCR analysis of sequence-specific DNA oxidation in human fibroblast DNA by [2,2'-azobis(amidinopropane)hydrochloride] (AAPH), a source of positively charged peroxyl radicals, and have determined that a 5'-GC-3' sequence context was a major predictor of guanine damage (44).

Variations in sequence-specific distribution of guanine lesions produced by $ONOOCO_2^-$ and riboflavin. At our reaction conditions of high $ONOO^-$ fluxes, guanine oxidation is expected to yield six major products: 8-oxo-G, 8-nitro-G, nitroimidazole, oxazolone, cyanuric acid and oxaluric acid (19, 21, 23, 26, 45). Of these lesions, nitroimidazole and cyanuric acid are not cleaved by hot piperidine or Fpg to an appreciable extent (21, 45); oxazolone and oxaluric acid will be cleaved by both treatments to a similar extent (45); 8-nitro-G will be resistant to Fpg treatment, but will depurinate rapidly at 90 ^{0}C during hot

piperidine treatment, creating an abasic site that can be converted into a strand break (17). 8-oxo-G, on the other hand, is hot piperidine-resistant and is a substrate for Fpg (46, 47). Therefore, approximate 5.4-fold variations in the ratios of Fpg- to piperidine-sensitive lesions produced by $ONOOCO_2^-$ in our studies likely arise from differential distribution of 8-oxoG and 8-nitroG along the oligonucleotide sequence. Since all of $ONOOCO_2^-$-induced guanine lesions arise from a common guanine radical cation ($G^{\bullet+}$) intermediate, these observations are indicative of the effect that sequence context plays in influencing the chemical fate of $G^{\bullet+}$ by affecting the reactions that lead to final products. We observe a similar, albeit smaller, effect in the case of riboflavin-mediated photooxidation. Previous analyses of guanine lesions produced by photosensitized riboflavin within synthetic oligonucleotide of the sequence 5'-TTGGTA-3', at conditions similar to ours, have identified imidazolone and its hydrolysis product, oxazolone, as major lesions, with only minor amounts of 8-oxoG formed (48, 49). In contrast, Douki and Cadet have reported comparable amounts of 8-oxoG and oxazolone formed in calf thymus DNA upon its irradiation in the presence of riboflavin with continuous air bubbling (50). Our observations of approximate 3.4-fold variations in the ratios of Fpg- to piperidine-sensitive products across all three-base contexts suggest a role for the sequence context in modulating relative amounts of 8-oxoG, relative to oxazolone, and may provide an explanation for the discrepancies in the amounts of 8-oxoG measured in different studies (48-50). Interestingly, the smallest ratios of Fpg- to piperidine-labile lesions are consistently produced by both $ONOOCO_2^-$ and photooxidized

riboflavin within 5'-CGT-3', 5'-GGT-3' and 5'-AGT-3' motifs. This result indicates that a 5'-GT-3' sequence motif may create a less favorable environment for the hydration of a common intermediate $G^{\bullet+}$, a process that leads to 8-oxoG formation (27). Instead, 5'-GT-3' may promote deprotonation of $G^{\bullet+}$, leading to oxazolone. Our results of sequence-specific variations of Fpg- to piperidine-sensitive products induced by riboflavin-mediated photooxidation are closely paralleled by the results of Spassky and Angelov, who have investigated DNA damage induced by exposure to high-intensity UV laser pulses (51). In these experiments, the ratios of Fpg- to piperidine-sensitive damage varied approximately 4- to 5-fold across different sequence contexts, and guanines within 5'-GT-3' motifs were characterized by the lowest Fpg- to piperidine ratios (51).

The unusual sequence selectivity of $ONOOCO_2^-$ and the sequence dependence of the product spectra suggest that current models of guanine oxidation and charge transfer in DNA could follow paradigms other than those proposed in earlier reports that argue for a direct relationship between IP and the efficiency of guanine oxidation. This complicates efforts to predict the location and chemistry of mutagenic DNA oxidation in the genome.

REFERENCES

1. Coussens, L. M., and Werb, Z. (2002) Inflammation and cancer. *Nature* 420, 860-867
2. De Marzo, A. M., Platz, E. A., Sutcliffe, S., Xu, J., Gronberg, H., Drake, C. G., Nakai, Y., Isaacs, W. B., and Nelson, W. G. (2007) Inflammation in prostate carcinogenesis. *Nat Rev Cancer* 7, 256-269
3. Lochhead, P., and El-Omar, E. M. (2007) Helicobacter pylori infection and gastric cancer. *Best Pract Res Clin Gastroenterol* 21, 281-297
4. Bartsch, H., and Nair, J. (2006) Chronic inflammation and oxidative stress in the genesis and perpetuation of cancer: role of lipid peroxidation, DNA damage, and repair. *Langenbecks Arch Surg* 391, 499-510
5. Ohshima, H., Tatemichi, M., and Sawa, T. (2003) Chemical basis of inflammation-induced carcinogenesis. *Arch Biochem Biophys* 417, 3-11
6. Huie, R. E., and Padmaja, S. (1993) The reaction of no with superoxide. *Free Radic Res Commun* 18, 195-199
7. Kissner, R., Nauser, T., Bugnon, P., Lye, P. G., and Koppenol, W. H. (1997) Formation and properties of peroxynitrite as studied by laser flash photolysis, high-pressure stopped-flow technique, and pulse radiolysis. *Chem Res Toxicol* 10, 1285-1292
8. Fielden, E. M., Roberts, P. B., Bray, R. C., Lowe, D. J., Mautner, G. N., Rotilio, G., and Calabrese, L. (1974) Mechanism of action of superoxide dismutase from pulse radiolysis and electron paramagnetic resonance. Evidence that only half the active sites function in catalysis. *Biochem J* 139, 49-60
9. Amatore, C., Arbault, S., Bouton, C., Coffi, K., Drapier, J. C., Ghandour, H., and Tong, Y. H. (2006) Monitoring in real time with a microelectrode the release of reactive oxygen and nitrogen species by a single macrophage stimulated by its membrane mechanical depolarization. *Chembiochem* 7, 653-661
10. Pryor, W. A., and Squadrito, G. L. (1995) The chemistry of peroxynitrite: a product from the reaction of nitric oxide with superoxide. *Am J Physiol* 268, L699-722
11. Squadrito, G. L., Pryor, W. A. (2002) Mapping the reaction of peroxynitrite with CO_2: energetics, reactive species and biological implications. *Chem Res Toxicol* 15, 885-895
12. Gerasimov, O. V., Lymar, S. V. (1999) The yield of hydroxyl radical from decomposition of peroxynitrous acid. *Inorg Chem* 38, 4317-4321
13. Dedon, P. C., and Tannenbaum, S. R. (2004) Reactive nitrogen species in the chemical biology of inflammation. *Arch Biochem Biophys* 423, 12-22
14. Lymar, S. V., Hurst, J.K. (1995) Rapid reaction between peroxynitrite ion and carbon dioxide: implications for biological activity. *J Am Chem Soc* 117, 8867-8868

15. Lymar, S. V., Jiang, Q., and Hurst, J. K. (1996) Mechanism of carbon dioxide-catalyzed oxidation of tyrosine by peroxynitrite. *Biochemistry* 35, 7855-7861
16. Yermilov, V., Yoshie, Y., Rubio, J., and Ohshima, H. (1996) Effects of carbon dioxide/bicarbonate on induction of DNA single-strand breaks and formation of 8-nitroguanine, 8-oxoguanine and base-propenal mediated by peroxynitrite. *FEBS Lett* 399, 67-70
17. Tretyakova, N. Y., Burney, S., Pamir, B., Wishnok, J. S., Dedon, P. C., Wogan, G. N., and Tannenbaum, S. R. (2000) Peroxynitrite-induced DNA damage in the supF gene: correlation with the mutational spectrum. *Mutat Res* 447, 287-303
18. Steenken, S., Jovanovic, S.V. (1997) How easily oxidized is DNA? One-electron reduction potentials of adenosine and guanosine radicals in aqueous solution. *J Am Chem Soc* 119, 617-618
19. Niles, J. C., Wishnok, J. S., and Tannenbaum, S. R. (2006) Peroxynitrite-induced oxidation and nitration products of guanine and 8-oxoguanine: structures and mechanisms of product formation. *Nitric Oxide* 14, 109-121
20. Steenken, S., Jovanovic, S.V., Bietti, M., Bernhard, K. (2000) The trap depth (in DNA) of 8-oxo-7,8-dihydro-2'-deoxyguanosine as derived from electron-transfer equilibria in aqueous solution. *J Am Chem Soc* 122, 2373-2374
21. Gu, F., Stillwell, W. G., Wishnok, J. S., Shallop, A. J., Jones, R. A., and Tannenbaum, S. R. (2002) Peroxynitrite-induced reactions of synthetic oligo 2'-deoxynucleotides and DNA containing guanine: formation and stability of a 5-guanidino-4-nitroimidazole lesion. *Biochemistry* 41, 7508-7518
22. Niles, J. C., Wishnok, J. S., and Tannenbaum, S. R. (2001) A novel nitroimidazole compound formed during the reaction of peroxynitrite with 2',3',5'-tri-O-acetyl-guanosine. *J Am Chem Soc* 123, 12147-12151
23. Yu, H., Venkatarangan, L., Wishnok, J. S., and Tannenbaum, S. R. (2005) Quantitation of four guanine oxidation products from reaction of DNA with varying doses of peroxynitrite. *Chem Res Toxicol* 18, 1849-1857
24. Niles, J. C., Wishnok, J. S., and Tannenbaum, S. R. (2001) Spiroiminodihydantoin is the major product of the 8-oxo-7,8-dihydroguanosine reaction with peroxynitrite in the presence of thiols and guanosine photooxidation by methylene blue. *Org Lett* 3, 963-966
25. Niles, J. C., Wishnok, J. S., and Tannenbaum, S. R. (2004) Spiroiminodihydantoin and guanidinohydantoin are the dominant products of 8-oxoguanosine oxidation at low fluxes of peroxynitrite: mechanistic studies with 18O. *Chem Res Toxicol* 17, 1510-1519
26. Tretyakova, N. Y., Niles, J. C., Burney, S., Wishnok, J. S., and Tannenbaum, S. R. (1999) Peroxynitrite-induced reactions of synthetic oligonucleotides containing 8-oxoguanine. *Chem Res Toxicol* 12, 459-466
27. Pratviel, G., and Meunier, B. (2006) Guanine oxidation: one- and two-electron reactions. *Chemistry* 12, 6018-6030

28. Shafirovich, V., Dourandin, A., Huang, W., and Geacintov, N. E. (2001) The carbonate radical is a site-selective oxidizing agent of guanine in double-stranded oligonucleotides. *J Biol Chem* 276, 24621-24626
29. Shafirovich, V., Cadet, J., Gasparutto, D., Dourandin, A., and Geacintov, N. E. (2001) Nitrogen dioxide as an oxidizing agent of 8-oxo-7,8-dihydro-2'-deoxyguanosine but not of 2'-deoxyguanosine. *Chem Res Toxicol* 14, 233-241
30. Misiaszek, R., Crean, C., Joffe, A., Geacintov, N. E., and Shafirovich, V. (2004) Oxidative DNA damage associated with combination of guanine and superoxide radicals and repair mechanisms via radical trapping. *J Biol Chem* 279, 32106-32115
31. Joffe, A., Mock, S., Yun, B. H., Kolbanovskiy, A., Geacintov, N. E., and Shafirovich, V. (2003) Oxidative generation of guanine radicals by carbonate radicals and their reactions with nitrogen dioxide to form site specific 5-guanidino-4-nitroimidazole lesions in oligodeoxynucleotides. *Chem Res Toxicol* 16, 966-973
32. Misiaszek, R., Crean, C., Geacintov, N. E., and Shafirovich, V. (2005) Combination of nitrogen dioxide radicals with 8-oxo-7,8-dihydroguanine and guanine radicals in DNA: oxidation and nitration end-products. *J Am Chem Soc* 127, 2191-2200
33. Joffe, A., Geacintov, N. E., and Shafirovich, V. (2003) DNA lesions derived from the site selective oxidation of Guanine by carbonate radical anions. *Chem Res Toxicol* 16, 1528-1538
34. Crean, C., Geacintov, N. E., and Shafirovich, V. (2005) Oxidation of guanine and 8-oxo-7,8-dihydroguanine by carbonate radical anions: insight from oxygen-18 labeling experiments. *Angew Chem Int Ed Engl* 44, 5057-5060
35. Hall, D. B., Holmlin, R. E., and Barton, J. K. (1996) Oxidative DNA damage through long-range electron transfer. *Nature* 382, 731-735
36. Saito, I., Nakamura T., Nakatani K., Yoshioka Y., Yamaguchi K., Sugiyama H. (1998) Mapping of the hot spots for DNA damage by one-electron oxidation: Efficacy of GG doublets and GGG triplets as a trap in long-range hole migration. *J Am Chem Soc* 120, 12686-12687
37. Pryor, W. A., Cueto, R., Jin, X., Koppenol, W. H., Ngu-Schwemlein, M., Squadrito, G. L., Uppu, P. L., and Uppu, R. M. (1995) A practical method for preparing peroxynitrite solutions of low ionic strength and free of hydrogen peroxide. *Free Radic Biol Med* 18, 75-83
38. Dong, M., and Dedon, P. C. (2006) Relatively small increases in the steady-state levels of nucleobase deamination products in DNA from human TK6 cells exposed to toxic levels of nitric oxide. *Chem Res Toxicol* 19, 50-57
39. Drouin, R., Therrien, J.-P., Angers, M., Ouellet, S. (2001) In vivo DNA analysis. In *DNA-protein interactions: Principles and protocols* (Moss, T., ed) pp. 175-219, Humana Press, Totowa, NJ

40. Pamir, B., and Wogan, G. N. (2003) Carbon dioxide modulation of peroxynitrite-induced mutagenesis of the supF gene in pSP189. *Chem Res Toxicol* 16, 487-492
41. Paul, T., Young, M. J., Hill, I. E., and Ingold, K. U. (2000) Strand cleavage of supercoiled DNA by water-soluble peroxyl radicals. The overlooked importance of peroxyl radical charge. *Biochemistry* 39, 4129-4135
42. Sanchez, C., Shane, R. A., Paul, T., and Ingold, K. U. (2003) Oxidative damage to a supercoiled DNA by water soluble peroxyl radicals characterized with DNA repair enzymes. *Chem Res Toxicol* 16, 1118-1123
43. Lee, Y. A., Yun, B. H., Kim, S. K., Margolin, Y., Dedon, P. C., Geacintov, N. E., and Shafirovich, V. (2007) Mechanisms of oxidation of guanine in DNA by carbonate radical anion, a decomposition product of nitrosoperoxycarbonate. *Chemistry* 13, 4571-4581
44. Rodriguez, H., Valentine, M. R., Holmquist, G. P., Akman, S. A., and Termini, J. (1999) Mapping of peroxyl radical induced damage on genomic DNA. *Biochemistry* 38, 16578-16588
45. Tretyakova, N. Y., Wishnok, J. S., and Tannenbaum, S. R. (2000) Peroxynitrite-induced secondary oxidative lesions at guanine nucleobases: chemical stability and recognition by the Fpg DNA repair enzyme. *Chem Res Toxicol* 13, 658-664
46. Gasparutto, D., Ravanat, J.-L., Gerot, O., Cadet, J. (1998) Characterization and Chemical Stability of Photooxidized Oligonucleotides that Contain 2,2-Diamino-4-[(2-deoxy--D-erythro-pentofuranosyl)amino]-5(2H)-oxazolone. *J Am Chem Soc* 120, 10283-10286
47. Tchou, J., Kasai, H., Shibutani, S., Chung, M. H., Laval, J., Grollman, A. P., and Nishimura, S. (1991) 8-oxoguanine (8-hydroxyguanine) DNA glycosylase and its substrate specificity. *Proc Natl Acad Sci U S A* 88, 4690-4694
48. Kino, K., Saito, I. (1998) Product analysis of GG-specific photooxidation of DNA via electron transfer: 2-aminoimidazolone as a major guanine oxidation product. *J Am Chem Soc* 120, 7373-7374
49. Kupan, A., Sauliere, A., Broussy, S., Seguy, C., Pratviel, G., and Meunier, B. (2006) Guanine oxidation by electron transfer: one- versus two-electron oxidation mechanism. *Chembiochem* 7, 125-133
50. Douki, T., and Cadet, J. (1999) Modification of DNA bases by photosensitized one-electron oxidation. *Int J Radiat Biol* 75, 571-581
51. Spassky, A., and Angelov, D. (1997) Influence of the local helical conformation on the guanine modifications generated from one-electron DNA oxidation. *Biochemistry* 36, 6571-6576

Chapter 3

Solvent exposure as a determinant of sequence-selective guanine oxidation by nitrosoperoxycarbonate

ABSTRACT

Paradoxical selectivity of $ONOOCO_2^-$-mediated guanine oxidation demonstrated in earlier studies pointed to factors other than guanine's sequence specific ionization potential (IP) in influencing selection of targets by $ONOOCO_2^-$. To explore a role of solvent exposure in mediating guanine oxidation by $ONOOCO_2^-$, we analyzed the reactivities of mismatched guanines with $ONOOCO_2^-$ in four representative sequence contexts. We demonstrated that the majority of the mismatched guanines displayed an increased reactivity with $ONOOCO_2^-$, with the extent of the reactivity increase varying in a sequence context-dependent manner. The greatest levels of reactivity enhancement were observed for the guanines located within conformationally flexible guanine-guanine (G-G) mismatches or across from a synthetic abasic site. Our results

support the model that greater levels of solvent exposure cause increased oxidation of guanines by $ONOOCO_2^-$.

INTRODUCTION

Oxidatively damaged DNA is a hallmark of many pathological conditions, and is thought to contribute to the increased cancer risk associated with chronic inflammation (1-3). Guanine is the major oxidation target in the DNA owing to its low ionization potential (IP) (4), with the generation of a variety of toxic and mutagenic properties (5). An initial electron removal step during guanine oxidation results in formation of a guanine radical cation ($G^{\bullet+}$) and produces an electron hole in the DNA duplex that can travel through the π-stack to become trapped at the sites of lowest ionization potentials (IPs) (6, 7). These sites are located within guanine runs that have, indeed, been identified as oxidative damage hotspots in reactions mediated by a variety of one-electron transfer reagents such as anthraquinones (8), rhodium complexes (6) and photooxidized riboflavin (7).

We have previously explored sequence-selective guanine oxidation mediated by peroxynitrite ($ONOOCO_2^-$), a strong oxidant that forms in chronically inflamed tissues from macrophage-derived nitric oxide ($NO^{\bullet}$) and superoxide ($O_2^{\bullet-}$) (9, 10). Decomposition of $ONOO^-$ in the presence of carbon dioxide (CO_2) proceeds through formation of nitrosoperoxycarbonate ($ONOOCO_2^-$), an unstable intermediate that rapidly disproportionates to produce nitrogen dioxide ($NO_2^{\bullet}$)

and carbonate anion ($CO_3^{\bullet-}$) radicals (11-13). The latter species has been previously demonstrated to cause selective oxidation of guanines in the DNA through electron transfer and production of $G^{\bullet+}$ that becomes a neutral guanine radical ($G^{\bullet}$) after facile deprotonation (14). We have observed that, unlike other one-electron oxidants, $ONOOCO_2^-$ in bicarbonate buffer displayed a marked selectivity for guanines located within 5'-GC-3' motifs that were characterized by the highest ionization potentials (15). This result demonstrated that charge transfer failed to affect the final distribution of oxidative damage in the case of $ONOOCO_2^-$, and factors other than the sequence-specific ionization potential of guanine influenced selection of targets by this oxidizing agent.

To explain our observations, we have hypothesized that solvent accessibility may play a role in affecting guanine oxidation by $ONOOCO_2^-$. Previous studies have shown that solvent-exposed guanines within single-stranded oligonucleotides sustained, on average, 5- to 9-times more damage by $ONOOCO_2^-$ than guanines located within duplex DNA (15, 16). Additionally, guanines positioned close to a 5' or 3' end of an oligonucleotide duplex displayed higher reactivity with $CO_3^{\bullet-}$, probably due to greater solvent exposure through strand-fraying (14, 17). It is well known that transient breaking and re-forming of hydrogen bonds within base-pairs occur as a result of dynamic "breathing" of a double-stranded DNA molecule that can cause exposure of the nucleobases to the bulk solvent. Base-pair lifetime is a quantity that can be measured by monitoring rates of imino proton exchange in hydrogen-bonded nucleobases using NMR, and reflects an average length of time that a base-pair spends in a

fully hydrogen-bonded state (18). Experiments from a number of laboratories have shown that measured base-pair lifetimes displayed high degree of variability that depended on sequence composition, nature of the base-pair, or neighboring bases (19-22). We have hypothesized that guanines located within 5'-GC-3' motifs were characterized by shorter base-pair lifetimes and, as a result, greater levels of solvent exposure, as compared to guanines in other sequence contexts, such as stably stacked 5'-GG-3' motifs, and were, as a result, more reactive with $ONOOCO_2^-$.

As a starting point in defining the role of solvent exposure in sequence-selective guanine oxidation by $ONOOCO_2^-$, we have focused our attention on the mismatched guanines as a model of solvent-exposed bases. A number of previous studies have provided evidence for the increased solvent accessibility of the mispaired bases as compared to the normal Watson-Crick base-pairs. For example, Pardi *et al.* and Bhattacharya *et al.* have used NMR-based measurements of imino proton exchange to demonstrate a dramatic decrease in the lifetimes of the mismatched G-T and G-G base-pairs, as compared to the fully matched G-C pair (19, 21). Additionally, Johnston and co-workers have shown that greater rates of oxidation of the mismatched guanines by $Ru(bpy)_3^{2+}$ complexes correlated with their increased solvent accessibility, as compared to the G-C base-pairs (23). In the current studies, we determined relative reactivities of guanine-adenine (G-A), guanine-guanine (G-G), guanine-thymine (G-T) and guanine-synthetic abasic site (G-ab) mismatches with $ONOOCO_2^-$ in four different sequence contexts. We used sequencing gel-based approach

combined with hot piperidine treatment to detect oxidized guanines within oligonucleotides, and showed that mismatches resulted in greater yields of oxidative guanine lesion formation in a sequence context-dependent manner.

MATERIALS AND METHODS

Materials. All synthetic oligonucleotides, including the ones that contained an abasic site modification, were obtained from Integrated DNA Technologies (Coralville, IA) and purified according to the procedure previously described (See Chapter 2). $ONOO^-$ was purchased from Cayman Chemical (Ann Arbor, MI). Piperidine and TEMED (N,N,N',N'-Tetramethylethylenediamine) were purchased from Sigma-Aldrich. Urea, boric acid, tris base, ammonium persulfate and 40% solution of acrylamide:bis (19:1) were obtained from American Bioanalytical (Natick, MA). K_2HPO_4, KH_2PO_4, $NaHCO_3$ and EDTA (ethylenediaminetetraacetic acid, sodium salt) were purchased from Mallinckrodt Baker (Phillipsburg, NJ). All chemicals were used without further purification. Chelex-100 was purchased from Bio-Rad (Hercules, CA), and Sephadex G-25 mini-spin columns were purchased from Roche Diagnostics. [γ-^{32}P]-ATP with activity of 6000 Ci/mmol was purchased from Perkin Elmer (Waltham, MA). Distilled and deionized water (ddH_2O) was purified using a Milli-Q system from Millipore (Bedford, MA) and was used for all experiments. All melting temperature measurements were conducted on a Cary UV/Vis spectrometer with a separate temperature module.

Preparation of buffers. A buffer containing 150 mM potassium phosphate and 25 mM sodium bicarbonate at pH 7.4 was prepared and treated with Chelex-100 resin overnight at 4 ^{0}C to remove adventitious metals. Following treatment, the buffer was passed through a 0.2 micron filter and stored at 4 ^{0}C.

Design of oligonucleotides used for $ONOOCO_2^-$ damage studies. The mismatch studies utilized previously described oligonucleotides 1S, 3S and S6 (See Table 2-1, Chapter 2). These oligonucleotides had a general sequence 5'–CGTACTCTTTGGT**X_1GY$_1$TX_2GY$_2$**TTCTTCTAT–3' that included consensus portions on both 5' and 3' ends, an invariant TGG sequence at the same position in all oligonucleotides for normalizing damage (underlined), and two variable guanine sequence contexts X_1GY_1 and X_2GX_2. Complements for all oligonucleotides, in addition to perfect matches, contained appropriate sequences to create G-A, G-G, G-T and G-ab (abasic site) mismatches across from central guanines in 5'-GGG-3', 5'-TGA-3', 5'-GGA-3' and 5'-AGC-3' sequence contexts. Complete sequences of all oligonucleotides and their complements are listed in the Table 3-1.

Oligonucleotide name	Oligonucleotide sequence
1S	5'-CGTACTCTT*TGG*TGGGTTGATTCTTTCTAT-3'
Complements to 1S	3'-GCATGAGAAACCACCCAACTAAGAAAGATA-5'
	3'-GCATGAGAAACCACACAACTAAGAAAGATA-5'
	3'-GCATGAGAAACCACGCAACTAAGAAAGATA-5'
	3'-GCATGAGAAACCACTCAACTAAGAAAGATA-5'
	3'-GCATGAGAAACCACabCAACTAAGAAAGATA-5'
	3'-GCATGAGAAACCACCCAACTAAGAAAGATA-5'
	3'-GCATGAGAAACCACCCAACTAAGAAAGATA-5'
	3'-GCATGAGAAACCACCCAAATAAGAAAGATA-5'
	3'-GCATGAGAAACCACCCAAGTAAGAAAGATA-5'
	3'-GCATGAGAAACCACCCAATTAAGAAAGATA-5'
	3'-GCATGAGAAACCACCCAAabTAAGAAAGATA-5'
3S	5'-CGTACTCTT*TGG*TGGATAGTTTCTTTCTAT-3'
Complements to 3S	3'-GCATGAGAAACCACCTATCAAAGAAAGATA-5'
	3'-GCATGAGAAACCACATATCAAAGAAAGATA-5'
	3'-GCATGAGAAACCACGTATCAAAGAAAGATA-5'
	3'-GCATGAGAAACCACTTATCAAAGAAAGATA-5'
	3'-GCATGAGAAACCACabTATCAAAGAAAGATA-5'
S6	5'-CGTACTCTT*TGG*TAGCTAGATTCTTTCTAT-3'
Complements to S6	3'-GCATGAGAAACCATCGATCTAAGAAAGATA-5'
	3'-GCATGAGAAACCATAGATCTAAGAAAGATA-5'
	3'-GCATGAGAAACCATGGATCTAAGAAAGATA-5'
	3'-GCATGAGAAACCATTGATCTAAGAAAGATA-5'
	3'-GCATGAGAAACCATabGATCTAAGAAAGATA-5'

Table 3-1. Sequences of oligonucleotides used for mismatch damage analysis. Complement sequences are shown in a 3' to 5' direction for easy sequence comparison.

Oligonucleotide name	Oligonucleotide sequence
1S-GGG	5'-TT*TGG*TGGGTTGATT-3'
Complements to 1S-GGG	3'-AAACCACCCAACTAA-5'
	3'-AAACCACACAACTAA-5'
	3'-AAACCACGCAACTAA-5'
	3'-AAACCACTCAACTAA-5'
	3'-AAACCACabCAACTT-5'
1S-TGA	5'-*G*TGGGTTGATTCTTT-3'
Complements to 1S-TGA	3'-CACCCAACTAAGAAA-5'
	3'-CACCCAACTAAGAAA-5'
	3'-CACCCAAATAAGAAA-5'
	3'-CACCCAAGTAAGAAA-5'
	3'-CACCCAATTAAGAAA-5'
	3'-CACCCAAabTAAGAAA-5'
3S-GGA	5'-TT*TGG*TGGATAGTTT-3'
Complements to 3S-GGA	3'-AAACCACCTATCAAA-5'
	3'-AAACCACATATCAAA-5'
	3'-AAACCACGTATCAAA-5'
	3'-AAACCACTTATCAAA-5'
	3'-AAACCACabTATCAAA-5'
S6-AGC	5'-TT*TGG*TAGCTAGATT-3'
Complements to S6-AGC	3'-AAACCATCGATCTAA-5'
	3'-AAACCATAGATCTAA-5'
	3'-AAACCATGGATCTAA-5'
	3'-AAACCATTGATCTAA-5'
	3'-AAACCATabGATCTAA-5'

Table 3-2. Sequences of oligonucleotides used for T_m measurements. Complement sequences are shown in a 3' to 5' direction for easy sequence comparison.

Design of oligonucleotides used for melting temperature studies. Sequences of all oligonucleotides utilized for the melting temperature (T_m studies) are shown in Table 3-2 and represent the abridged sequences of oligonucleotides shown in Table 3-1.

Determination of relative damage induced in mismatched guanines by $ONOOCO_2^-$. Oligonucleotides 1S, 3S, and S6 were 5'-end labeled with ^{32}P in a reaction containing approximately 100 pmol of 5' ends, 20 units of T4 polynucleotide kinase and 50 μCi of γ-^{32}P-ATP in 1x PNK buffer (New England Biolabs, Ipswich, MA) in a total volume of 50 μl. After incubation at 37 ^{0}C for 1 hr, unreacted γ-^{32}P-ATP was removed by a G-25 Sephadex column that has been washed with 150 mM potassium phosphate, 25 mM sodium bicarbonate buffer. For annealing, approximately 200 pmol of appropriate, unlabeled complement was added to the labeled oligonucleotide, the mixture was incubated at 95 ^{0}C for five min and then was allowed to cool down to room temperature over a course of approximately 90 min.

Concentration of $ONOO^-$ stock solution was measured in 0.3 N NaOH using an absorption coefficient of $\varepsilon_{302} = 1670\ M^{-1}cm^{-1}$ (24). The stock solution in 0.3 N NaOH was stored at -80 ^{0}C and was kept on ice at all times during use. All damage and control reactions were performed three separate times, each time in triplicates. For the reactions, $ONOO^-$ stock solution or an equal volume of 0.3 N NaOH was added to the labeled duplex oligonucleotides in 150 mM potassium phosphate, 25 mM sodium bicarbonate buffer in a bolus manner for a final

$ONOO^-$ concentration of 2 mM. The reactions were typically left on a benchtop for 1 hr prior to de-salting by Sephadex G-25 columns.

Conversion of oxidized guanines to strand breaks was accomplished by incubating damaged oligonucleotides with 1M piperidine at 90 ^{0}C for 20 min in a total reaction volume of 60 µl. Followed by lyophilization, the resulting DNA fragments were dissolved in formamide gel loading buffer and resolved on a 20% polyacrylamide gel (8M urea) that was run in 1xTBE at the constant power of 70 watts for 3 hrs. The gels were subjected to phosphorimager analysis (ImageQuant, Molecular Dynamics). Phosphorimager data for the cleavage of mismatched guanines was normalized to total radioactivity in the gel lane, with $ONOOCO_2^-$-treated values corrected for background, and relative reactivity determined in relation to the 5'-TGG-3' sequence in each oligonucleotide.

Melting temperature T_m measurements. For each duplex, three separate T_m measurements were obtained. In a typical experiment, 2 nmol of each oligonucleotide 1S-GGG, 1S-TGA, 3S-GGA, and 6S-AGC were mixed with equimolar amount of the appropriate complement in a total of 1.3 ml of chelexed 150 mM potassium phosphate and 25 mM sodium bicarbonate buffer at pH 7.4. Absorbance at 260 nm was monitored as the temperature block containing oligonucleotide samples was allowed to cool from 95 ^{0}C to 10 ^{0}C at the rate of 1 ^{0}C/minute, prior to a 5 min incubation at 95 ^{0}C. All T_m values were calculated by a Cury Thermal program as a maximal derivative of the phase transition curve.

RESULTS

Melting temperatures of mismatched oligonucleotides. Disruptions of the helical structure of the DNA caused by base-pair mismatches translate into lower melting temperatures (T_m) for the oligonucleotides (25-29). To compare the effects of guanine mismatches in different sequence contexts on the global helix stability, we measured T_m values of the oligonucleotides containing G-A, G-G, G-T and G-ab mismatches within four representative sequence contexts, and compared them to the T_m values obtained for the perfectly matched sequences. For our studies, we chose to use shorter versions of oligonucleotides 1S, 3S, S6, because mismatched guanines caused minimal helical perturbations in the full-length oligonucleotide sequences that were impossible to measure with our instrument. Table 3-3 displays T_m values for oligonucleotides 1S-GGG, 1S-TGA, 2S-GGA and S6-AGC that contain matched and mismatched guanines within 5'-GGG-3', 5'-TGA-3', 5'-GGA-3' and 5'-AGC-3' sequence contexts.

As expected, all mismatches introduced instability into the DNA duplex and caused lowering of the T_m values. Of all mismatches, G-ab was the most destabilizing, because, unlike other bases, the furan ring does not afford the opportunity to the opposing guanine to form any additional base-pairs. All other mismatches (G-A, G-G, and G-T) caused comparable levels of helix destabilization in all sequence contexts studied.

Base-pair	G-C	G-A	G-G	G-T	G-ab
Sequence context					
GGG	**55.997**	**50.007**	**49.7**	**48.3**	38.987
	± 0.006	**± 0.006**	**± 0.6**	**± 0.6**	± 0.006
TGA	**55.6**	**43**	**43.3**	**45.98**	36.983
	± 0.6	**± 1**	**± 0.6**	**± 0.02**	± 0.006
GGA	**52.7**	**44.7**	**44.001**	**45.6**	34.99
	± 0.6	**± 0.6**	**± 0.006**	**± 0.6**	± 0.01
AGC	51.6	43.6	43.6	41.6	29.97
	± 0.6	± 0.6	± 0.6	± 0.6	± 0

Table 3-3. Melting temperatures of oligonucleotides (^{0}C) containing matched (G-C) and mismatched (G-A, G-G, G-T, and G-ab) guanines within four representative sequence contexts (GGG, TGA, GGA, and AGC).

Reactivities of the mismatched guanines with $ONOOCO_2^-$. To characterize the effect of increased solvent accessibility of guanine on its reactivity with $ONOOCO_2^-$, we measured relative numbers of oxidative lesions induced in matched and mismatched guanines by $ONOOCO_2^-$ in the presence of bicarbonate. For these measurements, ^{32}P-labeled duplex oligonucleotides containing guanines of interest in four representative sequence contexts were damaged with 2 mM $ONOO^-$ in the presence of bicarbonate, and converted to direct strand breaks by hot piperidine treatment. The resulting fragments were separated on a 20% sequencing gel, visualized by autoradiography, and oxidation induced within each matched or mismatched guanine was quantified

relative to the damage induced in the central guanine of the invariant 5'-TGG-3' normalization sequence. Figure 3-1 shows an example of a typical gel used for quantification of relative guanine damage for a 5'-GGA-3' sequence context. Graphed in Figure 3-2 are relative guanine reactivities, measured for all five base-pairs analyzed (G-C, G-A, G-G, G-T and G-ab) in four sequence contexts (5'-GGG-3', 5'-TGA-3', 5'-GGA-3' and 5'-AGC-3'). We observed that the mismatched guanines were at least as reactive with $ONOOCO_2^-$ as the G-C base-pairs, with the majority of the mismatches displaying marked increases in the reactivity. Generally, G-T mismatches caused little or no change in the extent of guanine oxidation as compared to the matched G-C base-pairs, with a single exception of a 5'-GGG-3' sequence context, where relative guanine reactivity was increased approximately two-fold. Guanines located across from adenines in G-A mismatches were characterized by the intermediate increases in the guanine reactivity compared to matched guanines, with the extent of the reactivity change displaying dependence on sequence context and varying from no change for the 5'-AGC-3' motif to an approximate 2.8-fold increase for 5'-GGG-3'. Both G-G and G-ab mismatches caused the largest, 3- to 10-fold increases in guanine reactivities with $ONOOCO_2^-$ that were sequence context-dependent. On average, the reactivity of the central guanine within a 5'-GGG-3' sequence context was the most perturbed by changes in base-pairing.

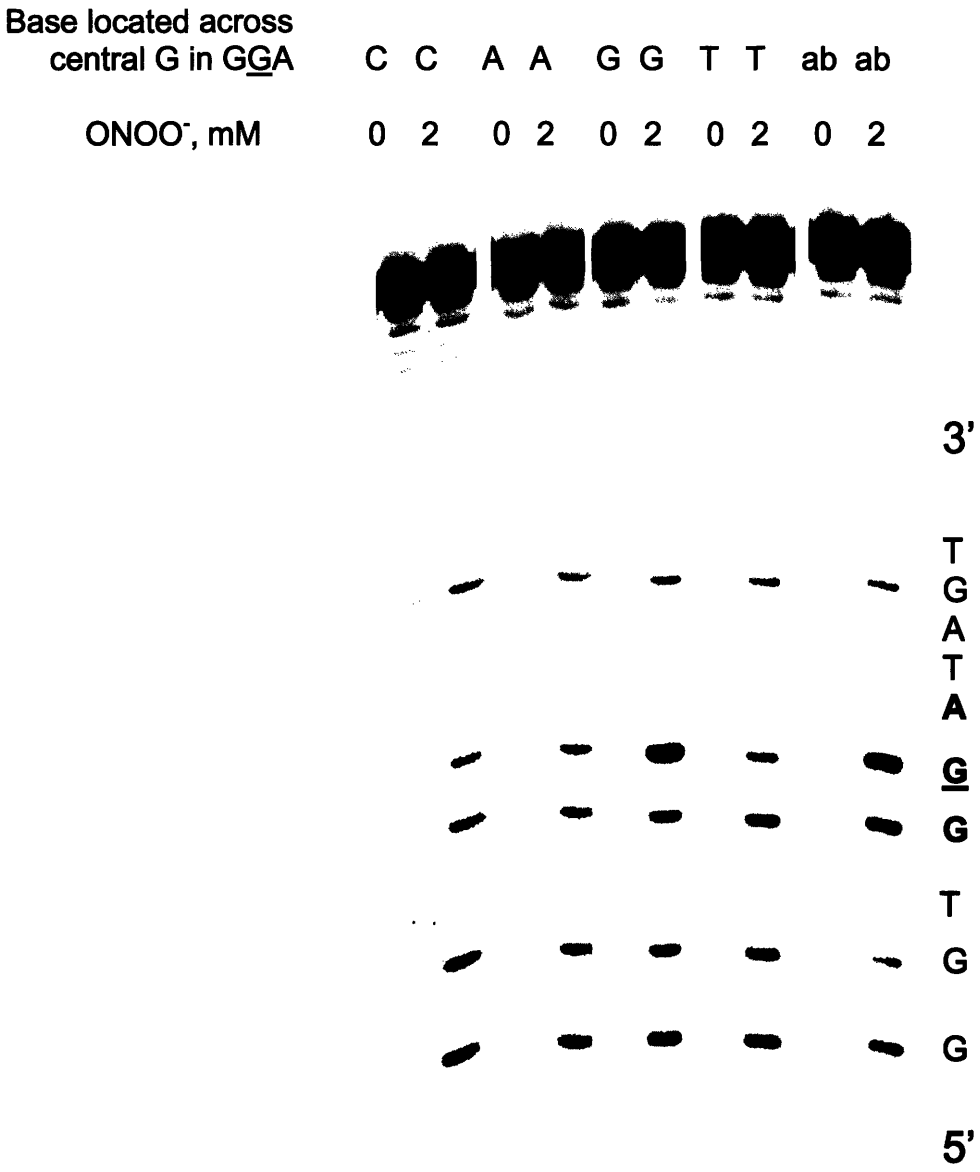

Figure 3-1. Representative gel picture used for quantification of relative damage induced within mismatched guanines by $ONOOCO_2^-$. ^{32}P-labeled oligonucleotide 3S was annealed with five different complements, creating a G-C match and G-A, G-G, G-T, and G-ab mismatches across from the central guanine in GGA motif. All oligonucleotides were subjected to oxidation by $ONOOCO_2^-$, hot

piperidine treatment, and gel electrophoresis, as described in Materials and Methods.

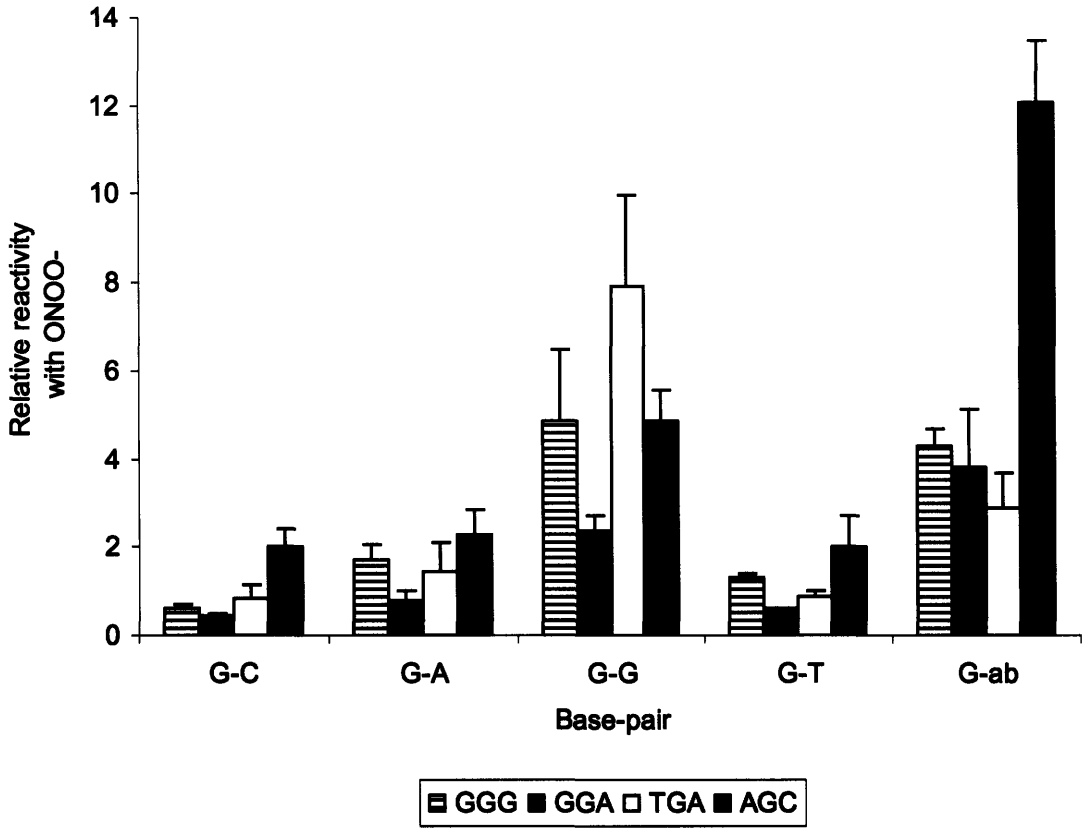

Figure 3-2. Relative reactivities of matched and mismatched guanines with $ONOOCO_2^-$. Amounts of piperidine-labile guanine lesions induced in the central positions of 5'-GGG-3', 5'-TGA-3', 5'-GGA-3', and 5'-AGC-3' sequence contexts and located across from cytosine, adenine, guanine, thymine, and the synthetic abasic site were quantified relative to the guanine damage induced in the central position of the invariant TGG motif by the ImageQuant program, as described in Materials and Methods.

DISCUSSION

To establish the role of solvent accessibility in modulating the reactivity of guanines in duplex DNA with $ONOOCO_2^-$, we determined yields of oxidative lesions produced by $ONOOCO_2^-$ within G-A, G-T, G-G, and G-ab mispairs in four representative sequence contexts. Numerous studies have found that guanines mispaired with adenines, thymines, or guanines caused limited structural perturbations of duplex DNA that did not extend beyond neighboring base-pairs (19, 30-33). Nevertheless, these mismatches produced thermodynamic destabilization of the helix in our studies, as was evidenced by a dramatic lowering of melting temperatures of mismatch-containing oligonucleotides. The greatest drop in T_m (17-21 ^{0}C, depending on sequence context) was caused by a G-ab mispair, reflecting the expected lack of hydrogen bond formation for guanine located opposite the furan ring.

The majority of mismatched guanines exhibited increased reactivity with $ONOOCO_2^-$, providing support to our hypothesis that increased solvent exposure played a role in modulating target selection by $ONOOCO_2^-$. This conclusion correlates with previous studies and with our own experiments that found enhanced reactivities of single-stranded oligonucleotides with $ONOOCO_2^-$, as compared to the duplex sequences (15, 16) (Chapter 2). G-ab mispairs, where guanine most capable of rotating about glycosidic bond in the absence of hydrogen bonding interactions, are characterized by the greatest (3.5- to 8-fold) enhancements in $ONOOCO_2^-$ reactivity, as compared to the fully matched bases.

The extent of the reactivity increase observed for G-A, G-G and G-T mismatches displays high levels of sequence context dependence and correlates well with a number of previous studies that have underscored the effect of flanking sequences on thermodynamic and structural properties of mismatch-containing oligonucleotides (25-29, 34).

Compared to the G-A and G-T mismatches, G-G base-pairs caused particularly high enhancements in guanine reactivity with $ONOOCO_2^-$ that were comparable to the enhancements measured for the G-ab mispairs, but could not be attributed to the greater levels of overall helix destabilization, as measured by T_m. A number of studies showed that the predominant conformation adapted by a G-A mispair in solution at physiological pH was a relatively stable and well-stacked G(*anti*)-A(*anti*) structure, although other, minor conformations were also possible in some sequence contexts (30, 35-38) (Figure 3-3). Similarly, a G-T mismatch was found to form a hydrogen-bonded wobble base-pair in different sequence motifs that was characterized by good stacking interactions (29, 31, 32) (Figure 3-3). In contrast to these results, several workers demonstrated that a G-G mismatch did not adapt a single conformational structure; rather, both guanines within the mispair slowly interconverted between G(*syn*) and G(*anti*) conformations by rotating about glycosydic bonds (33, 39-42) (Figure 3-3). This dynamic nature of a G-G mismatch necessitates transient elimination of hydrogen bonding, disruption of stacking interactions, and bulging of the base-pairs out of the DNA helix that have indeed all been observed in structural studies of G-G-containing oligonucleotides (33, 41). This conformational

flexibility is, in turn, likely to promote increased solvent exposure of the guanine bases, enhancing their reactivity with $ONOOCO_2^-$.

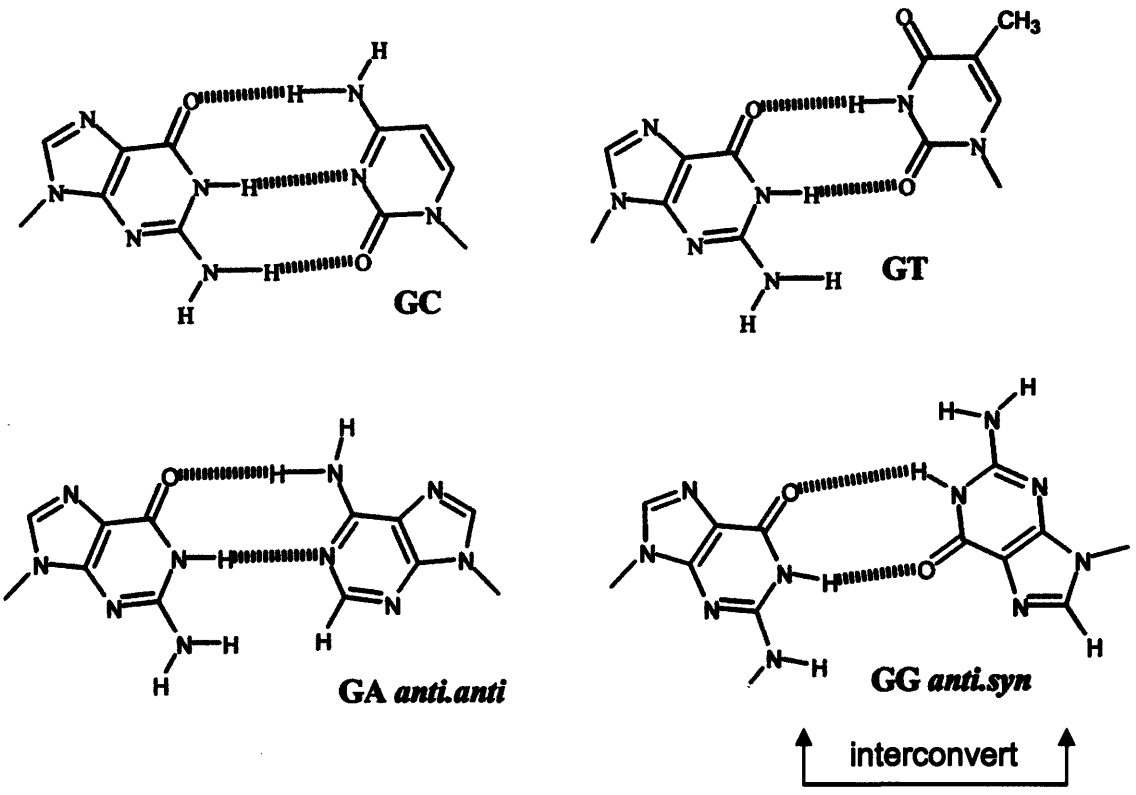

Figure 3-3. Predominant structures of G-C, G-T, G-A and G-G base-pairs in solution at pH 7.4. Adapted from (43)

The results of our present studies on oxidation of mispaired guanines by $ONOOCO_2^-$ are closely paralleled by the results of earlier experiments, in which oxidative cleavage induced by Ni^{II} complexes in the presence of $KHSO_5$ was investigated in mismatch-containing oligonucleotides (44). Guanine oxidation in

double-stranded DNA promoted by these complexes has been previously shown by Burrows and co-workers to be exquisitely sensitive to solvent accessibility of the guanine base, with enhanced reactivities displayed by bulges, loops, and mismatches in synthetic oligonucleotide duplexes (45, 46). In a systematic study, Wunderman *et al.* determined that guanines in G-G mismatches located within a 5'-GGG-3' sequence context were characterized by unusually high levels of reactivity with the Ni^{II} complex, contrasted with modest changes in the guanine oxidation seen for the G-A and G-T base-pairs, and similar to the patterns of guanine reactivity that we have observed for $ONOOCO_2^-$ (44). Inner-sphere electron transfer, a mechanism operative during Ni^{II}-mediated guanine oxidation has also been recently proposed for $CO_3^{\bullet-}$, a product of $ONOOCO_2^-$ disproportionation and a mediator of $ONOOCO_2^-$-induced guanine damage (17). This common mechanism of guanine oxidation for Ni^{II} complexes and $ONOO^-$ may explain the requirement for guanine solvent accessibility in both cases.

REFERENCES

1. Bartsch, H., and Nair, J. (2006) Chronic inflammation and oxidative stress in the genesis and perpetuation of cancer: role of lipid peroxidation, DNA damage, and repair. *Langenbecks Arch Surg* 391, 499-510
2. Coussens, L. M., and Werb, Z. (2002) Inflammation and cancer. *Nature* 420, 860-867
3. Ohshima, H., Tatemichi, M., and Sawa, T. (2003) Chemical basis of inflammation-induced carcinogenesis. *Arch Biochem Biophys* 417, 3-11
4. Steenken, S., Jovanovic, S.V. (1997) How easily oxidized is DNA? One-electron reduction potentials of adenosine and guanosine radicals in aqueous solution. *J Am Chem Soc* 119, 617-618

5. Neeley, W. L., and Essigmann, J. M. (2006) Mechanisms of formation, genotoxicity, and mutation of guanine oxidation products. *Chem Res Toxicol* 19, 491-505
6. Hall, D. B., Holmlin, R. E., and Barton, J. K. (1996) Oxidative DNA damage through long-range electron transfer. *Nature* 382, 731-735
7. Saito, I., Nakamura T., Nakatani K., Yoshioka Y., Yamaguchi K., Sugiyama H. (1998) Mapping of the hot spots for DNA damage by one-electron oxidation: Efficacy of GG doublets and GGG triplets as a trap in long-range hole migration. *J Am Chem Soc* 120, 12686-12687
8. Henderson, P. T., Jones, D., Hampikian, G., Kan, Y., and Schuster, G. B. (1999) Long-distance charge transport in duplex DNA: the phonon-assisted polaron-like hopping mechanism. *Proc Natl Acad Sci U S A* 96, 8353-8358
9. Huie, R. E., and Padmaja, S. (1993) The reaction of no with superoxide. *Free Radic Res Commun* 18, 195-199
10. Kissner, R., Nauser, T., Bugnon, P., Lye, P. G., and Koppenol, W. H. (1997) Formation and properties of peroxynitrite as studied by laser flash photolysis, high-pressure stopped-flow technique, and pulse radiolysis. *Chem Res Toxicol* 10, 1285-1292
11. Lymar, S. V., Hurst, J.K. (1995) Rapid reaction between peroxynitrite ion and carbon dioxide: implications for biological activity. *J Am Chem Soc* 117, 8867-8868
12. Lymar, S. V., Jiang, Q., and Hurst, J. K. (1996) Mechanism of carbon dioxide-catalyzed oxidation of tyrosine by peroxynitrite. *Biochemistry* 35, 7855-7861
13. Squadrito, G. L., Pryor, W. A. (2002) Mapping the reaction of peroxynitrite with CO_2: energetics, reactive species and biological implications. *Chem Res Toxicol* 15, 885-895
14. Shafirovich, V., Dourandin, A., Huang, W., and Geacintov, N. E. (2001) The carbonate radical is a site-selective oxidizing agent of guanine in double-stranded oligonucleotides. *J Biol Chem* 276, 24621-24626
15. Margolin, Y., Cloutier, J. F., Shafirovich, V., Geacintov, N. E., and Dedon, P. C. (2006) Paradoxical hotspots for guanine oxidation by a chemical mediator of inflammation. *Nat Chem Biol* 2, 365-366
16. Gu, F., Stillwell, W. G., Wishnok, J. S., Shallop, A. J., Jones, R. A., and Tannenbaum, S. R. (2002) Peroxynitrite-induced reactions of synthetic oligo 2'-deoxynucleotides and DNA containing guanine: formation and stability of a 5-guanidino-4-nitroimidazole lesion. *Biochemistry* 41, 7508-7518
17. Lee, Y. A., Yun, B. H., Kim, S. K., Margolin, Y., Dedon, P. C., Geacintov, N. E., and Shafirovich, V. (2007) Mechanisms of oxidation of guanine in DNA by carbonate radical anion, a decomposition product of nitrosoperoxycarbonate. *Chemistry* 13, 4571-4581
18. Gueron, M., and Leroy, J. L. (1995) Studies of base pair kinetics by NMR measurement of proton exchange. *Methods Enzymol* 261, 383-413

19. Pardi, A., Morden, K. M., Patel, D. J., and Tinoco, I., Jr. (1982) Kinetics for exchange of imino protons in the d(C-G-C-G-A-A-T-T-C-G-C-G) double helix and in two similar helices that contain a G . T base pair, d(C-G-T-G-A-A-T-T-C-G-C-G), and an extra adenine, d(C-G-C-A-G-A-A-T-T-C-G-C-G). *Biochemistry* 21, 6567-6574
20. Dornberger, U., Leijon, M., and Fritzsche, H. (1999) High base pair opening rates in tracts of GC base pairs. *J Biol Chem* 274, 6957-6962
21. Bhattacharya, P. K., Cha, J., and Barton, J. K. (2002) 1H NMR determination of base-pair lifetimes in oligonucleotides containing single base mismatches. *Nucleic Acids Res* 30, 4740-4750
22. Patel, D. J., Ikuta, S., Kozlowski, S., and Itakura, K. (1983) Sequence dependence of hydrogen exchange kinetics in DNA duplexes at the individual base pair level in solution. *Proc Natl Acad Sci U S A* 80, 2184-2188
23. Johnston, D. H., Glasgow, K. C., and Thorp, H. H. (1995) Electrochemical measurement of the solvent accessibility of nucleobases using electron transfer between DNA and metal complexes. *J Am Chem Soc* 117, 8933-8938
24. Pryor, W. A., Cueto, R., Jin, X., Koppenol, W. H., Ngu-Schwemlein, M., Squadrito, G. L., Uppu, P. L., and Uppu, R. M. (1995) A practical method for preparing peroxynitrite solutions of low ionic strength and free of hydrogen peroxide. *Free Radic Biol Med* 18, 75-83
25. Peyret, N., Seneviratne, P. A., Allawi, H. T., and SantaLucia, J., Jr. (1999) Nearest-neighbor thermodynamics and NMR of DNA sequences with internal A.A, C.C, G.G, and T.T mismatches. *Biochemistry* 38, 3468-3477
26. Allawi, H. T., and SantaLucia, J., Jr. (1998) Nearest-neighbor thermodynamics of internal A.C mismatches in DNA: sequence dependence and pH effects. *Biochemistry* 37, 9435-9444
27. Allawi, H. T., and SantaLucia, J., Jr. (1998) Thermodynamics of internal C.T mismatches in DNA. *Nucleic Acids Res* 26, 2694-2701
28. Allawi, H. T., and SantaLucia, J., Jr. (1998) Nearest neighbor thermodynamic parameters for internal G.A mismatches in DNA. *Biochemistry* 37, 2170-2179
29. Allawi, H. T., and SantaLucia, J., Jr. (1997) Thermodynamics and NMR of internal G.T mismatches in DNA. *Biochemistry* 36, 10581-10594
30. Patel, D. J., Kozlowski, S. A., Ikuta, S., and Itakura, K. (1984) Deoxyguanosine-deoxyadenosine pairing in the d(C-G-A-G-A-A-T-T-C-G-C-G) duplex: conformation and dynamics at and adjacent to the dG X dA mismatch site. *Biochemistry* 23, 3207-3217
31. Hare, D., Shapiro, L., and Patel, D. J. (1986) Wobble dG X dT pairing in right-handed DNA: solution conformation of the d(C-G-T-G-A-A-T-T-C-G-C-G) duplex deduced from distance geometry analysis of nuclear Overhauser effect spectra. *Biochemistry* 25, 7445-7456
32. Patel, D. J., Kozlowski, S. A., Marky, L. A., Rice, J. A., Broka, C., Dallas, J., Itakura, K., and Breslauer, K. J. (1982) Structure, dynamics, and energetics of deoxyguanosine . thymidine wobble base pair formation in

the self-complementary d(CGTGAATTCGCG) duplex in solution. *Biochemistry* 21, 437-444
33. Borden, K. L., Jenkins, T. C., Skelly, J. V., Brown, T., and Lane, A. N. (1992) Conformational properties of the G.G mismatch in d(CGCGAATTGGCG)2 determined by NMR. *Biochemistry* 31, 5411-5422
34. Li, Y., and Agrawal, S. (1995) Oligonucleotides containing G.A pairs: effect of flanking sequences on structure and stability. *Biochemistry* 34, 10056-10062
35. Nikonowicz, E. P., and Gorenstein, D. G. (1990) Two-dimensional 1H and 31P NMR spectra and restrained molecular dynamics structure of a mismatched GA decamer oligodeoxyribonucleotide duplex. *Biochemistry* 29, 8845-8858
36. Kan, L. S., Chandrasegaran, S., Pulford, S. M., and Miller, P. S. (1983) Detection of a guanine X adenine base pair in a decadeoxyribonucleotide by proton magnetic resonance spectroscopy. *Proc Natl Acad Sci U S A* 80, 4263-4265
37. Nikonowicz, E. P., Meadows, R. P., Fagan, P., and Gorenstein, D. G. (1991) NMR structural refinement of a tandem G.A mismatched decamer d(CCAAGATTGG)2 via the hybrid matrix procedure. *Biochemistry* 30, 1323-1334
38. Lane, A., Ebel, S., and Brown, T. (1994) Properties of multiple G.A mismatches in stable oligonucleotide duplexes. *Eur J Biochem* 220, 717-727
39. Mooers, B. H., Eichman, B. F., and Ho, P. S. (1997) The structures and relative stabilities of d(G x G) reverse Hoogsteen, d(G x T) reverse wobble, and d(G x C) reverse Watson-Crick base-pairs in DNA crystals. *J Mol Biol* 269, 796-810
40. Skelly, J. V., Edwards, K. J., Jenkins, T. C., and Neidle, S. (1993) Crystal structure of an oligonucleotide duplex containing G.G base pairs: influence of mispairing on DNA backbone conformation. *Proc Natl Acad Sci U S A* 90, 804-808
41. Lane, A. N., and Peck, B. (1995) Conformational flexibility in DNA duplexes containing single G.G mismatches. *Eur J Biochem* 230, 1073-1087
42. Cognet, J. A., Gabarro-Arpa, J., Le Bret, M., van der Marel, G. A., van Boom, J. H., and Fazakerley, G. V. (1991) Solution conformation of an oligonucleotide containing a G.G mismatch determined by nuclear magnetic resonance and molecular mechanics. *Nucleic Acids Res* 19, 6771-6779
43. Brown, J., Brown, T., Fox, K. R. (2003) Cleavage of fragments containing DNA mismatches by enzymic and chemical probes. *Biochem. J.* 371, 697-708
44. Wurdeman, R. L., Douskey, M. C., and Gold, B. (1993) DNA methylation by N-methyl-N-nitrosourea: methylation pattern changes in single- and double-stranded DNA, and in DNA with mismatched or bulged guanines. *Nucleic Acids Res* 21, 4975-4980

45. Chen, X., Rokita, S. E., and Burrows, C. J. (1991) DNA modification: intrinsic selectivity of nickel(II) complexes. *J Am Chem Soc* 113, 5884-5886
46. Chen, X., Burrows, C. J., and Rokita, S. E. (1992) Conformation-specific detection of guanine in DNA: ends, mismatches, bulges, and loops. *J Am Chem Soc* 114, 322-325

Chapter 4

Development of a general method to quantify sequence-specific nucleobase damage in the presence of strand breaks

ABSTRACT

In order to study sequence-selective nucleobase damage by reagents that cause high levels of deoxyribose oxidation, a method was developed to remove the background of direct strand breaks in sequencing gel-based assays. Exonuclease III (Exo III) activity was used to degrade labeled strands of phosphorothioate-modified duplex oligonucleotides containing unprotected 3' termini formed as a result of deoxyribose damage. The utility of this approach was successfully verified in the case of DNA damage produced by Fe^{+2}-EDTA complex. Exo III activity was shown to generate no artifacts capable of affecting measurements of relative guanine damage produced by both photoactivated riboflavin and peroxynitrite in bicarbonate buffer. A complete inactivation of Exo III activity was accomplished by a combination of EDTA chelation and filtration.

INTRODUCTION

Knowledge of mechanisms associated with sequence-specific target selection by DNA oxidants may provide ways to predict the locations and relative amounts of mutagenic nucleobase lesions in the genome. Studies of such mechanisms may involve determinations of oxidative damage hotspots produced by various reagents in duplex DNA, as has been described in Chapter 2 for two guanine-specific oxidants, photoactivated riboflavin and nitsoroperoxycarbonate ($ONOOCO_2^-$). These studies made use of ^{32}P labeled, double-stranded oligonucleotides in oxidation reactions conducted under "single-hit conditions" that produced a maximum of an average single damage event per oligonucleotide molecule. The damage is subsequently revealed as direct strand breaks by hot alkali or *E. Coli* Fpg glycosylase treatment, generating unique, quantifiable bands on an autoradiography image after sequencing gel electrophoresis (1, 2). This experimental approach, however, cannot be used for analyses of sequence-specific nucleobase damage caused by reagents that also produce substantial amounts of deoxyribose oxidation, such as Fe^{+2}-EDTA, γ-radiation, or $ONOO^-$, as the resulting direct strand breaks greatly complicate sequencing gel-based studies (3).

We have, therefore, developed a method to remove the high background of direct strand breaks and to unmask nucleobase oxidation. This method exploits the activity of exonuclease III (Exo III), a 3' → 5' duplex-specific DNA exonuclease that also possesses 3'-phosphatase and AP endonuclease activities

(4-6). The exonuclease activity of Exo III is inhibited by phosphorothioate linkages in DNA (7) (Figure 4-1).

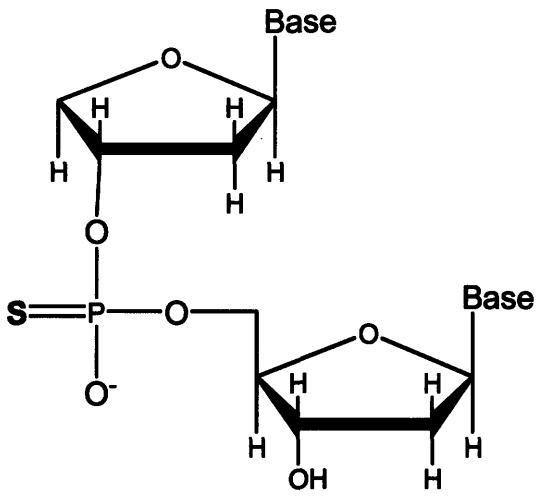

Figure 4-1. Structure of a phosphorothioate linkage.

Figure 4-2 outlines a general strategy for the strand break removal method. The procedure utilizes short double-stranded oligonucleotides that, in addition to containing guanines within all possible three-base sequence contexts, also include three consecutive phosphorothioate linkages at the 3' ends of each strand. These linkages confer a complete resistance of a full-length oligonuleotide to digestion by Exo III, as determined by control experiments (not shown). Deoxyribose damage leading to strand breaks, but not nucleobase damage, produces unprotected 3' ends that are recognized as substrates by Exo III, leading to degradation of a labeled strand in a 3' to 5' direction. This reaction will generate very short, 5'-^{32}P-labeled fragments as products that can be easily

separated from the rest of oligonucleotides during electrophoresis, and will not interfere with subsequent nucleobase damage quantification. Undigested, full-length 5'-^{32}P-labeled oligonucleotides remaining in the solution after reaction with Exo III will contain only nucleobase damage that can be revealed by treatment with *E.Coli* Fpg glycosylase or hot piperidine and quantified by gel electrophoresis in the usual manner (See Materials and Methods, Chapter 2). We have validated our method of strand break removal using Fe^{+2}-EDTA complex that produces both direct strand breaks and nucleobase lesions.

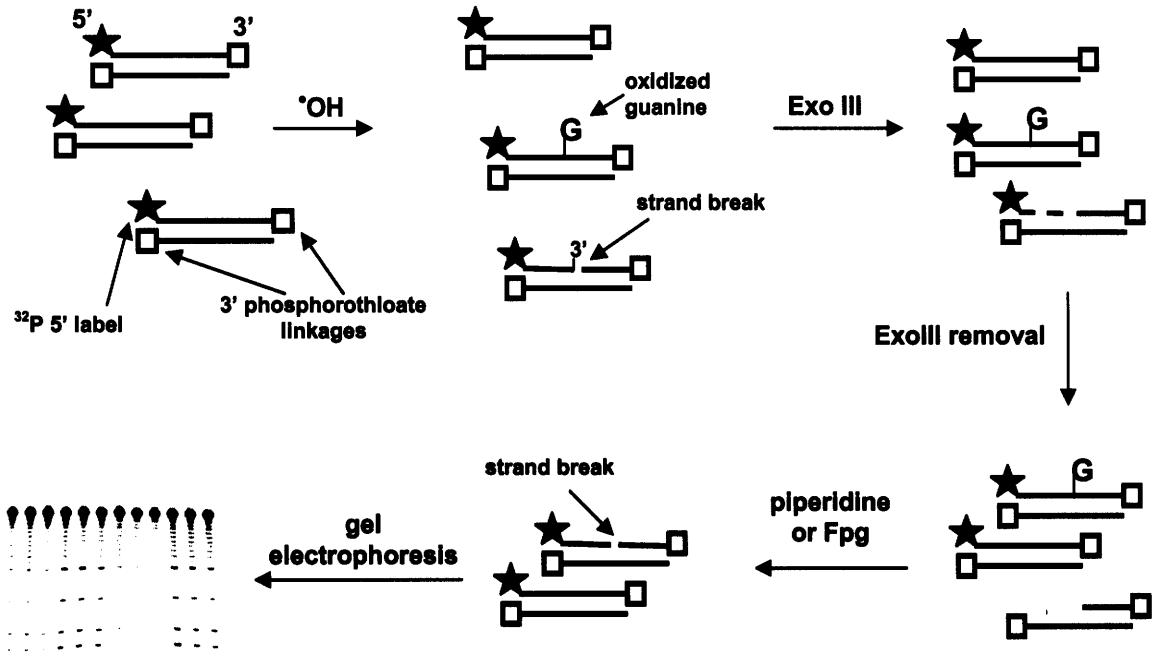

Figure 4-2. General approach for removing background of direct strand breaks for sequencing gel analysis of base lesions. The hydroxyl radical (•OH) is shown as an example of an oxidant that produces both deoxyribose and nucleobase damage.

MATERIALS AND METHODS

Materials. Synthetic, phosphorothioate-modified oligonucleotides were purchased from Integrated DNA Technologies (Coralville, IA). $ONOO^-$ was purchased from Cayman Chemical (Ann Arbor, MI). Riboflavin, piperidine and TEMED (N,N,N',N'-Tetramethylethylenediamine) were purchased from Sigma-Aldrich. Urea, boric acid, tris base, ammonium persulfate and 40% solution of acrylamide:bis (19:1) were obtained from American Bioanalytical (Natick, MA). K_2HPO_4, KH_2PO_4, $NaHCO_3$ and EDTA (ethylenediaminetetraacetic acid, sodium salt) were purchased from Mallinckrodt Baker (Phillipsburg, NJ). All chemicals were used without further purification. Chelex-100 was purchased from Bio-Rad (Hercules, CA), Sephadex G-25 mini-spin columns were purchased from Roche Diagnostics, and Micropure-EZ spin filters were obtained from Millipore (Bedford, MA). *E. Coli* Fpg (formamidopyrimidine [fapy]-DNA glycosylase) was purchased from Trevigen (Gaithersburg, MD), and T4 PNK (polynucleotide kinase) and Exonuclease III (Exo III) were purchased from New England Biolabs (Ipswich, MA). [γ-^{32}P]-ATP with activity of 6000 Ci/mmol was obtained from Perkin Elmer (Waltham, MA). Distilled and deionized water (ddH_2O) was purified using a Milli-Q system from Millipore (Bedford, MA) and was used for all experiments.

Preparation of buffers. A buffer containing 175 mM potassium phosphate at pH 7.4 was prepared and treated with Chelex-100 resin overnight

at 4 ^{0}C to remove adventitious metals. Following treatment, the buffer was passed through a 0.2 micron filter and stored at 4 ^{0}C.

Purification of synthetic oligonucleotides. The oligonucleotides were dissolved in TE buffer, pH 8.0 with 20% glycerol, and loaded on a 20% acrylamide:bis, 8M urea preparative gel electrophoresis. The gel was run in 1x TBE at a constant power of 70 watts for 6 hrs. Oligonucleotides were visualized by UV shadowing, cut out from the gel, eluted by overnight shaking in 0.5 M ammounium acetate and 10 mM magnesium acetate, filtered and ethanol precipitated. All oligonucleotides were desalted by Sephadex G-25 spin columns and transferred to 175 mM potassium phosphate buffer before use.

Labelling and annealing of oligonucleotides. Oligonucleotides were 5'-end labeled with ^{32}P in a reaction containing approximately 100 pmol of 5' ends, 20 units of T4 polynucleotide kinase and 50 μCi of γ-^{32}P-ATP in 1x PNK buffer (New England Biolabs, Ipswich, MA) in a total volume of 50 μl. After incubation at 37 ^{0}C for 1 hr, unreacted γ-^{32}P-ATP was removed by a G-25 Sephadex column that has been washed with 2x300 μl of 175 mM potassium phosphate buffer. For annealing, approximately 200 pmol of unlabeled complement was added to the labeled oligonucleotide, and the mixture was allowed to cool down to room temperature over a course of approximately 90 min, after a 5-min incubation at 95 ^{0}C.

Damage of labeled oligonucleotides with Fe^{+2}-EDTA, $ONOOCO_2^-$ and riboflavin. All damage analyses and controls were carried out three times, in triplicates. Each Fe^{+2}-EDTA reaction contained 20 pmol of labeled, double-stranded oligonucleotide and 2 mM of $FeSO_4$-EDTA (in the ratio of 1:1.1, freshly prepared before each experiment), in 175 mM chelexed photassium phosphate buffer and a total volume of 50 µl. The DNA was always added last, and the controls contained potassium phosphate buffer instead of $FeSO_4$-EDTA solution. The reactions were incubated at 37 ^{0}C for 2 hours, after which Fe^{+2}-EDTA was removed by filtration through Sephadex G-25 columns. Damage reactions with 3 mM $ONOO^-$ and 30 µM riboflavin were carried out as described in previously (See Materials and Methods, Chapter 2).

Exonuclease III and hot piperidine treatment of damaged oligonucleotides. Damaged and de-salted oligonuleotides were treated with 5 units of Exonuclease III in 1 x NEbuffer 1, (New England Biolabs, Ipswich, MA) at 37 ^{0}C for 1 hr in a total volume of 60 µl. (One unit is defined as the amount of enzyme required to produce 1 nmol of acid-soluble total nucleotides in a total reaction volume of 50 µl in 30 min at 37 ^{0}C in 1 x NEbuffer 1 with 0.15 mM sonicated duplex [^{3}H]-DNA.) These conditions were sufficient to remove all direct strand breaks generated during damage reactions, as determined by control experiments (results not shown). For hot piperidine treatment, oligonucleotides were de-salted by gel filtration, incubated with 1M piperidine at 90 ^{0}C for 20 min in a total volume of 120 µl and dried by lyophilization.

Gel electrophoresis and damage quantification. Lyophilized samples were dissolved in a total of 5 μl of formamide gel loading buffer, and 2 μl from each sample was resolved on a 20% polyacrylamide gel (8M urea) that was run in 1 x TBE at the constant power of 70 watts for 3 hrs, and then subjected to phosphorimager analysis (ImageQuant, Molecular Dynamics). For $ONOOO_2^-$ and riboflavin experiments, phosphorimager data for guanine cleavage was normalized to total radioactivity in the gel lane, with damage values corrected for background, and relative reactivity was determined in relation to the 5'-TGG-3' sequence in each oligonucleotide.

RESULTS

Using Exo III to unmask nucleobase oxidation: proof of concept. We validated our method of background removal using a single oligonucleotide of the sequence 5'-CGTACTCTTTGGTTGATGGGTTCTTTC*T*A*T-3', where * represents a phosphorothioate linkage. A 2-hr incubation of this oligonucleotide with a 2mM Fe^{+2}-EDTA complex in an air-saturated 175 mM chelexed potassium phosphate buffer at pH of 7.4 for 2 hrs at 37 ^{0}C produces considerable amounts of both direct strand breaks and piperidine-labile nucleobase damage, as demonstrated in Figure 4-3. This damage is characterized by formation of double bands as a result of 3'-phosphate and 3'-phosphoglycolate termini being generated at every nucleotide position (8). Incubation of damaged oligonucleotide with 0.1 units of Exo III at 37 ^{0}C for 1 hr results in complete

removal of direct strand breaks and leads to formation of lower-molecular weight bands at the bottom of the gel. The intensities of these bands correspond to the relative amounts of unprotected 3' ends present in each oligonucleotide before and after damage reaction. Since short, ^{32}P-labeled products of Exo III reaction run substantially faster than other oligonucleotide fragments produced after hot piperidine treatment, they do not interfere with quantification of relative nucleobase damage levels.

Treatment of damaged oligonucleotides with Exo III does not produce artifacts. We wished to determine if Exo III activity can introduce yet uncharacterized artifacts, such as adventitious removal of base damage, which would alter measurements of relative reactivities of DNA bases. We have, therefore, measured relative damage induced within four defined guanine sequence contexts by two guanine-specific oxidants – photooxidized riboflavin and peroxynitrite and $ONOOCO_2^-$ in bicarbonate buffer, in the absence and presence of Exo III. Two oligonucleotides of the sequences 5'-GTACTCTT***TGG***T<u>CG</u>G<u>TGC</u>TTCTTTCTAT-3' and 5'-CGTACTCTT***TGG***T<u>GGC</u>T<u>CGT</u>TTCTTTCTAT-3' were treated with either 30 mM photooxidized riboflavin for 20 min or with 3 mM $ONOO^-$ in 150 mM sodium phosphate, 25 mM sodium bicarbonate buffer at pH 7.4 (Materials and Methods, Chapter 2), and then with either 0 or 5 units of Exo III at 37 ^{0}C for 1 hr in 1xNEbuffer 1 (New England Biolabs, Ipswich, MA). Relative reactivities of central guanines (bold) within four representative sequence contexts (underlined)

were determined as previously described (See Materials and Methods, Chapter 2), and expressed relative to the reactivity of the central guanine within the invariant TGG sequence context (italicized). Figure 4-4 shows that Exo III activity has no effect on the relative amounts of piperidine-sensitive guanine oxidation products measured in the case of damage produced by either reagent in four representative sequence contexts.

Removal of Exo III activity prior to base damage analysis. In a typical assay of sequence-selective DNA damage, oxidized nucleobases are expressed as direct strand breaks by hot piperidine or *E. Coli* Fpg treatments (9). Unprotected 3' ends that result from these treatments can become substrates for Exo III, leading to degradation of products of interest. A complete removal of Exo III activity prior to either hot piperidine or Fpg treatment is, therefore, required. This condition is particularly crucial in the case of Fpg treatment that, unlike hot piperidine-mediated cleavage, is performed at mild conditions. Figure 4-5 shows that removal of Exo III activity can be accomplished by combining EDTA addition to chelate Mg^{2+} ions required for exonuclease activity (18), and subsequent removal of the enzyme by filtration through protein-binding Micropure-EZ filters (Millipore, Bedford, MA). As Figure 4-5 further demonstrates, neither of these methods alone is sufficient to protect a 5' labeled duplex oligonucleotide of the sequence 5'-GTACTCTTTGGTAGCTGGTTTCTTTCTAT-3' from degradation by Exo III.

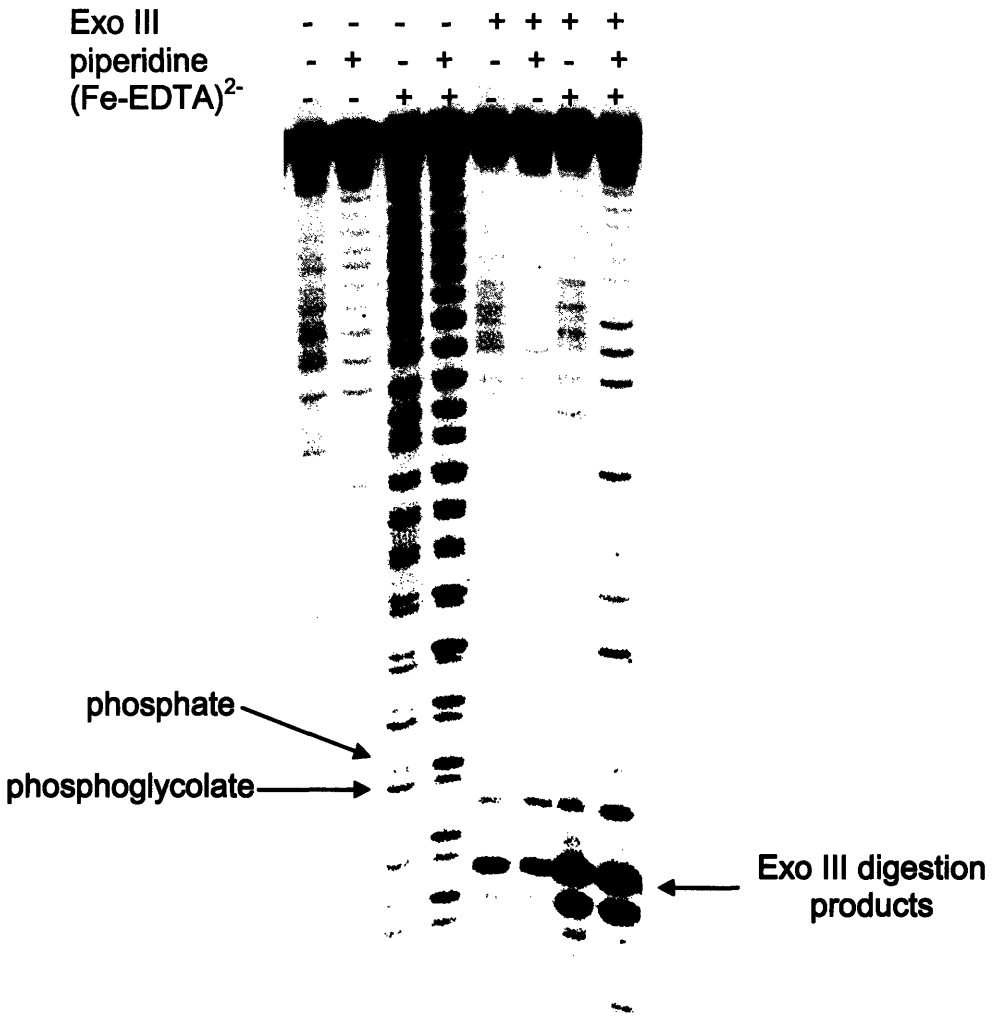

Figure 4-3. Use of Exonuclease III to unmask guanine oxidation. A phosphorothioate-protected double-stranded oligonucleotide was incubated with 0 or 2 mM Fe^{+2}-$EDTA^{2-}$ at 37 ^{0}C for 2 hours, then with 0 or 0.1 units of Exo III, and 0 or 1M piperidine, as described in Materials and Methods.

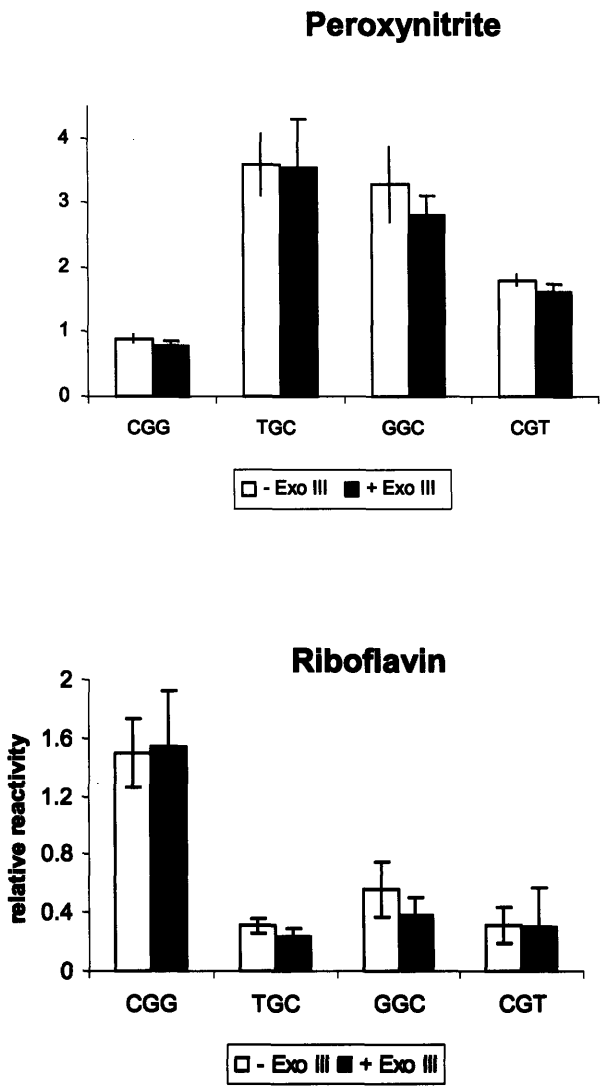

Figure 4-4. Relative reactivities of guanines with $ONOOCO_2^-$ and photoactivated riboflavin measured in the absence or presence of Exo III. Relative reactivities of guanines within four representative sequence contexts with 3 mM $ONOO^-$ in 150 mM potassium phosphate, 25 mM sodium bicarbonate buffer, pH 7.4, and with 30 mM photoactivated riboflavin in 175 mM potassium phosphate buffer, pH 7.4, were measured before and after treatment with 5 units of Exo III (See Materials and Methods).

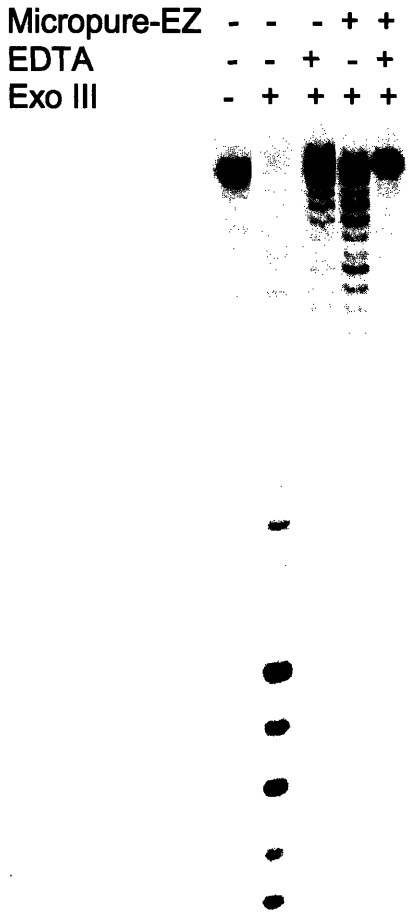

Figure 4-5. Addition of EDTA combined with filtration through Micropure-EZ filter is sufficient to completely remove ExoIII activity. A 5'-labeled, double-stranded oligonucleotide was mixed with 5 units of Exo III, and incubated at 37 ^{0}C for 1 hr after addition of 0 or 20 mM EDTA and/or filtration through Micropure-EZ filters.

DISCUSSION

A high background of direct strand breaks presents a formidable challenge to gel-based analyses of sequence-selective nucleobase damage. In previous

studies in which DNA damage produced by Cu (II), Fe(III) and Cr (VI) in the presence of hydrogen peroxide has been analyzed by ligation-mediated PCR (LMPCR), the problem of direct strand breaks has been addressed by addition of sucrose to the damage reactions suppress deoxyribose oxidation (10). While only partially effective, this method can also introduce yet uncharacterized artifacts as a result of sucrose modification by the resulting hydroxyl radicals, and can potentially change guanine oxidation chemistry. This can happen through generation of DNA-damaging alkyl and alkoxyl radicals that have been shown to form during incubation of sucrose with the Fenton reagent (11).

Our method of direct strand break removal is based on introducing phosphorothioate linkages at the 3' ends of substrate oligonucleotides and using Exo III to degrade only those oligonucleotides that contain unprotected 3' ends and contribute to the strand break background. Control experiments demonstrated that Exo III activity has no influence on the relative amounts of oxidative guanine lesions detected after oligonucleotide damage by photoactivated riboflavin and peroxynitrite in bicarbonate buffer. In addition, Exo III activity was easily removed from the reaction mixture by a combination of EDTA addition and filtration, and, therefore, did not interfere with subsequent Fpg treatment. Because Exo III is inactivated at the conditions of hot piperidine cleavage, no prior removal of Exo III activity is required (12).

For many oxidants, deoxyribose damage often leads to structurally heterogeneous strand breaks; for example, irradiation of DNA with ionizing γ-rays has been shown to produce 3'-phosphate and 3'-phosphoglycolate-containing

termini (8, 13). Wide applicability of our method of strand break removal is based on the remarkable ability of Exo III to recognize both these 3' strand break products as substrates (14). In addition, the AP endonuclease activity of Exo III allows for conversion of oxidatively generated abasic sites to free, unprotected 3' ends that are subsequently degraded by the exonuclease activity, resulting in the removal of the abasic site background (6). Our method of background strand break removal can be used to probe sequence selectivity of nucleobase oxidation induced by a variety of oxidants that generate substantial amounts of direct strand breaks, such as peroxynitrite $ONOO^-$, Fe^{+2}-EDTA, γ-radiation, or peroxyl radicals (3, 15-17).

REFERENCES

1. Margolin, Y., Cloutier, J. F., Shafirovich, V., Geacintov, N. E., and Dedon, P. C. (2006) Paradoxical hotspots for guanine oxidation by a chemical mediator of inflammation. *Nat Chem Biol* 2, 365-366
2. Saito, I., Nakamura T., Nakatani K., Yoshioka Y., Yamaguchi K., Sugiyama H. (1998) Mapping of the hot spots for DNA damage by one-electron oxidation: Efficacy of GG doublets and GGG triplets as a trap in long-range hole migration. *J Am Chem Soc* 120, 12686-12687
3. Kennedy, L. J., Moore, K., Jr., Caulfield, J. L., Tannenbaum, S. R., and Dedon, P. C. (1997) Quantitation of 8-oxoguanine and strand breaks produced by four oxidizing agents. *Chem Res Toxicol* 10, 386-392
4. Richardson, C. C., Lehman, I. R., and Kornberg, A. (1964) A Deoxyribonucleic Acid Phosphatase-Exonuclease from Escherichia Coli. Ii. Characterization of the Exonuclease Activity. *J Biol Chem* 239, 251-258
5. Richardson, C. C., and Kornberg, A. (1964) A Deoxyribonucleic Acid Phosphatase-Exonuclease from Escherichia Coli. I. Purification of the Enzyme and Characterization of the Phosphatase Activity. *J Biol Chem* 239, 242-250
6. Rogers, S. G., and Weiss, B. (1980) Exonuclease III of Escherichia coli K-12, an AP endonuclease. *Methods Enzymol* 65, 201-211

7. Putney, S. D., Benkovic, S. J., and Schimmel, P. R. (1981) A DNA fragment with an alpha-phosphorothioate nucleotide at one end is asymmetrically blocked from digestion by exonuclease III and can be replicated in vivo. *Proc Natl Acad Sci U S A* 78, 7350-7354
8. Henner, W. D., Rodriguez, L. O., Hecht, S. M., and Haseltine, W. A. (1983) gamma Ray induced deoxyribonucleic acid strand breaks. 3' Glycolate termini. *J Biol Chem* 258, 711-713
9. Burrows, C. J., and Muller, J. G. (1998) Oxidative Nucleobase Modifications Leading to Strand Scission. *Chem Rev* 98, 1109-1152
10. Rodriguez, H., Holmquist, G. P., D'Agostino, R., Jr., Keller, J., and Akman, S. A. (1997) Metal ion-dependent hydrogen peroxide-induced DNA damage is more sequence specific than metal specific. *Cancer Res* 57, 2394-2403
11. Luo, G. M., Qi, D. H., Zheng, Y. G., Mu, Y., Yan, G. L., Yang, T. S., and Shen, J. C. (2001) ESR studies on reaction of saccharide with the free radicals generated from the xanthine oxidase/hypoxanthine system containing iron. *FEBS Lett* 492, 29-32
12. Kow, Y. W. (1989) Mechanism of action of Escherichia coli exonuclease III. *Biochemistry* 28, 3280-3287
13. Henner, W. D., Grunberg, S. M., and Haseltine, W. A. (1982) Sites and structure of gamma radiation-induced DNA strand breaks. *J Biol Chem* 257, 11750-11754
14. Henner, W. D., Grunberg, S. M., and Haseltine, W. A. (1983) Enzyme action at 3' termini of ionizing radiation-induced DNA strand breaks. *J Biol Chem* 258, 15198-15205
15. Tretyakova, N. Y., Burney, S., Pamir, B., Wishnok, J. S., Dedon, P. C., Wogan, G. N., and Tannenbaum, S. R. (2000) Peroxynitrite-induced DNA damage in the supF gene: correlation with the mutational spectrum. *Mutat Res* 447, 287-303
16. Paul, T., Young, M. J., Hill, I. E., and Ingold, K. U. (2000) Strand cleavage of supercoiled DNA by water-soluble peroxyl radicals. The overlooked importance of peroxyl radical charge. *Biochemistry* 39, 4129-4135
17. Sanchez, C., Shane, R. A., Paul, T., and Ingold, K. U. (2003) Oxidative damage to a supercoiled DNA by water soluble peroxyl radicals characterized with DNA repair enzymes. *Chem Res Toxicol* 16, 1118-1123

Chapter 5

Role of electrostatic interactions in sequence-selective oxidation of guanines in DNA

ABSTRACT

To test the hypothesis that the charge of an oxidant influences its reactivity with guanine in DNA, sequence-specific patterns of guanine oxidation produced by the negatively charged Fe^{+2}-EDTA complex in the absence and presence of H_2O_2 were compared to guanine oxidation produced by γ-radiation, a neutral oxidant. This was accomplished with the use of double-stranded oligonucleotides containing guanines within all possible three-base sequence contexts (XGY) and a previously developed method for quantifying sequence-specific nucleobase damage in the presence of strand breaks. We observed that both Fe^{+2}-EDTA and γ-radiation produced identical guanine oxidation patterns, demonstrating that negative charge of Fe^{+2}-EDTA played no role in selection of targets by this agent. Both reagents were equally reactive with all guanines, irrespective of their ionization potential (IP) or sequence context, consistent with the expected chemistry of guanine oxidation by the hydroxyl radicals (•OH).

Guanines located within 5'-GT-3' motifs were characterized by lower yields of Fpg-sensitive lesions, implying a role of local DNA structure and steric hindrance by the thymine methyl group in 8-oxoguanine formation.

INTRODUCTION

Our previous studies demonstrated that nitrosoperoxycarbonate ($ONOOCO_2^-$), a chemical mediator of inflammation and a one-electron oxidant, caused selective oxidation of guanines located within 5'-GC-3' sequence contexts that were characterized by the highest sequence-specific ionization potentials (IPs) (Chapter 2). This reactivity stood in violation of the rules of oxidative charge transfer and was mediated by solvent exposure of the target guanines, as was evidenced by the increased reactivities of guanines within single-stranded oligonucleotides or mismatches with $ONOOCO_2^-$ (Chapters 2 and 3). We hypothesized that negative charge of $ONOOCO_2^-$ was an important determinant of its preference for solvent-exposed guanines; unfavorable interactions of $ONOOCO_2^-$ with the negatively charged DNA backbone limited accessibility of $ONOOCO_2^-$ to the guanines buried inside helix and favored its reactivity with the more accessible bases. The effect of electrostatic forces in mediating interactions of various reactive agents with DNA is well-documented. For example, the ability of thiols to protect calf thymus DNA from damage by ionizing radiation was found to correlate with their net charge, with the highest levels of protection exhibited by the positively charged species (1); a similar

pattern of radioprotection ability was also observed for polyamines (2). The role of electrostatic interactions in affecting oxidative DNA damage is exemplified by the reactions of charged peroxyl radicals (3, 4) and naphthalimide derivatives substituted with cationic and anionic side chains (5) with the DNA.

To find out if electrostatic interactions were indeed major determinants of sequence-selective guanine damage by $ONOOCO_2^-$, we tested if guanine oxidation by another negatively charged reagent, Fe^{+2}-EDTA complex, was affected by its negative charge. Oxidizing properties of Fe^{+2}-EDTA arise through the Fenton reaction-dependent production of highly reactive hydroxyl radicals ($^{\bullet}OH$), generated in the presence of molecular oxygen (O_2) or hydrogen peroxide (H_2O_2) according to the following reactions (6, 7):

$$Fe^{+2}\text{-EDTA} + O_2 \rightarrow Fe^{+3}\text{-EDTA} + O_2^{\bullet -} \quad [1]$$

$$Fe^{+2}\text{-EDTA} + O_2^{\bullet -} + 2H^+ \rightarrow Fe^{+3}\text{-EDTA} + H_2O_2 \quad [2]$$

$$Fe^{+2}\text{-EDTA} + H_2O_2 \rightarrow Fe^{+3}\text{-EDTA} + {}^{\bullet}OH + {}^{-}OH \quad [3]$$

The hydroxyl radicals generated in these reactions are extremely short-lived, reacting at the site of their generation with all known biomolecules at diffusion-controlled rates ($10^7 - 10^{10}$ M^{-1} s^{-1}) (8). Meanwhile, irradiation of an aqueous solution with γ-rays causes radiolysis of H_2O and generation of diffusible $^{\bullet}OH$ that are not associated with a negative charge (9). Therefore, comparison of sequence-selective guanine oxidation produced by Fe^{+2}-EDTA and γ-radiation

provides a direct way to assess the effect of negative charge of an oxidant on its reactivity with guanines in DNA.

In conducting experiments with Fe^{+2}-EDTA we were also mindful of a long-standing debate that surrounds the question of the efficiency of $^{\bullet}OH$ production by the Fe^{+2}-EDTA complex. Formation of alternative oxidizing species was proposed by several groups on the basis of kinetic considerations and the observed reactivities with various organic substrates that displayed inconsistencies with the chemical properties of $^{\bullet}OH$ (10-12). Although structural characterization of these species has not yet been achieved, it is believed that they consist of perferryl and ferryl ions, also termed "iron-oxo complexes". The perferryl ion can be formed by either Fe^{+2}-/O_2 or Fe^{+3}-/$O_2^{\bullet-}$ in the absence or presence of EDTA (7):

$$Fe^{+2} + O_2 \leftrightarrow [Fe^{+2}\text{-}O_2 \leftrightarrow Fe^{+3}\text{-}O_2^{\bullet-}] \leftrightarrow Fe^{+3} + O_2^{\bullet-} \quad [4]$$

perferryl ion

Its subsequent reaction with Fe^{+2} results in the production of ferryl species (7):

$$Fe^{+2} + [Fe^{+2}\text{-}O_2 \leftrightarrow Fe^{+3}\text{-}O_2^{\bullet-}] \rightarrow Fe^{+2}\text{-}O_2\text{-}Fe^{+2} \quad [5]$$

$$Fe^{+2}\text{-}O_2\text{-}Fe^{+2} \rightarrow 2Fe^{+4}{=}O \quad [6]$$

ferryl ion

Alternatively, ferryl species can also be generated through a separate mechanism involving recombination of Fe^{+2} with H_2O_2 (7, 13):

$$Fe^{+2} + O_2 \rightarrow Fe^{+4}=O \qquad [7]$$

Although ferryl and perferryl ions are very strong oxidants that readily react with a variety of organic compounds (10, 12, 14, 15), they are less reactive than $^{\bullet}OH$ with chemicals such as benzoate, tert-butyl alcohol, acetate ion, arginine and serine (10, 11). This decreased reactivity follows from an approximate 1.3 V difference in the reduction potentials between ($^{\bullet}OH_{aq}/H_2O_1$) and (FeO^{2+}-/Fe^{3+}-chelate) ion pairs (estimated to be E^0 = 2.18 V and 0.9 V, respectively) (13).

Numerous studies found that relative yields of $^{\bullet}OH$ and iron-oxo complexes generated in the course of Fenton reaction were strongly dependent on the reaction conditions, such as pH, solvent polarity, buffer components, nature of the chelator, or relative stoichiometry (7, 12, 14, 16, 17). In particular, the concentration of H_2O_2 in the reaction mixture was shown to have a profound effect on the efficiency of $^{\bullet}OH$ generation. For example, Qian and Buettner determined that the formation of putative ferryl and perferryl ions at the expense of $^{\bullet}OH$ was highest when the concentration of O_2 exceeded the concentration of H_2O_2, such that $[O_2]/[H_2O_2] \geq 100$ (7). These findings were corroborated by the experiments of Welch and co-workers who showed that the species formed during auto-oxidation of 50 μM Fe^{+2}-EDTA complex in air-saturated aqueous

solution were not scavenged by Tris, in contrast to the oxidant formed by 50 μM Fe^{II} in the presence of equimolar amounts of H_2O_2 that displayed properties of $^{\bullet}OH$ (17). Similarly, Reinke *et al.* found that the product of $FeSO_4$ auto-oxidation in air-saturated phosphate buffer exhibited chemical reactivity of ferryl species, and the hydroxyl radical adducts of 5,5-dimethyl-1-pyrroline N-oxide (DMPO), α-phenyl-N-t-butylnitrone (PBN) or azide could only be detected in the solution after addition of H_2O_2 (14). Thus, oxidizing species formed by the Fenton reagent at very low H_2O_2 concentrations are characterized by a high proportion of putative ferryl and perferryl species.

Taking into account the complicated chemistry of Fe^{+2}-EDTA, we conducted Fe^{+2}-EDTA-mediated DNA oxidation reactions in the absence and presence of 2 mM H_2O_2. The former condition (subsequently referred to as "Fe^{+2}-EDTA") was expected to favor production of iron-oxo complexes, while the latter condition (subsequently referred to as "Fe^{+2}-EDTA/H_2O_2") was expected to favor generation of $^{\bullet}OH$.

In the present studies we measured relative levels of oxidative guanine lesions produced by Fe^{+2}-EDTA, Fe^{+2}-EDTA/H_2O_2 and γ-radiation within all possible three-base sequence contexts (XGY) located in double-stranded oligonucleotides. Because Fe^{+2}-EDTA, Fe^{+2}-EDTA/H_2O_2 and γ-radiation cause high levels of deoxyribose oxidation, a previously developed method to quantify sequence-dependent nucleobase oxidation in the presence of strand breaks was employed (Chapter 4). We determined that the three oxidants caused approximately equal levels of guanine damage in all sequence contexts,

suggesting that negative charge plays no role in selection of oxidation targets by Fe^{+2}-EDTA.

MATERIALS AND METHODS

Materials. A total of 16 phosphorothioate-modified oligonucleotides (8 oligonucleotides with unique sequences and their complements) were purchased from Integrated DNA Technologies (Coralville, IA) and gel-purified as described previously (See Chapter 4). The sequences of the oligonucleotides are shown in Table 5-1.

Piperidine, TEMED (N,N,N',N'-Tetramethylethylenediamine) and 30% w/w) solution of H_2O_2 were purchased from Sigma-Aldrich. Urea, boric acid, tris base, ammonium persulfate and 40% solution of acrylamide:bis (19:1) were obtained from American Bioanalytical (Natick, MA). K_2HPO_4, KH_2PO_4, $NaHCO_3$ and EDTA (ethylenediaminetetraacetic acid, sodium salt) were purchased from Mallinckrodt Baker (Phillipsburg, NJ). All chemicals were used without further purification. Chelex-100 was purchased from Bio-Rad (Hercules, CA), Sephadex G-25 mini-spin columns were purchased from Roche Diagnostics, and Micropure-EZ spin filters were obtained from Millipore (Bedford, MA). *E. Coli* Fpg (formamidopyrimidine [fapy]-DNA glycosylase) was purchased from Trevigen (Gaithersburg, MD), and T4 PNK (polynucleotide kinase) and Exonuclease III (Exo III) were purchased from New England Biolabs (Ipswich, MA). [γ-^{32}P]-ATP with activity of 6000 Ci/mmol was obtained from Perkin Elmer (Waltham, MA).

Distilled and deionized water (ddH_2O) was purified using a Milli-Q system from Millipore (Bedford, MA) and was used for all experiments.

Oligonucleotide name	Oligonucleotide sequence (5' to 3')
S1-S	CGTACTCTT***TGG***TT**G**AT**GG**TTCTTTC*T*A*T
S2-S	CGTACTCTT***TGG***TC**G**GTT**G**CTTCTTTC*T*A*T
S3-S	CGTACTCTT***TGG***TA**G**TT**GG**ATTCTTTC*T*A*T
S4-S	CGTACTCTT***TGG***TA**GG**TT**G**TTTCTTTC*T*A*T
S5-S	CGTACTCTT***TGG***TC**G**CTC**G**ATTCTTTC*T*A*T
S6-S	CGTACTCTT***TGG***TA**G**CTA**G**ATTCTTTC*T*A*T
S8-S	CGTACTCTT***TGG***TG**G**CTC**G**TTTCTTTC*T*A*T
S9-S	CGTACTCTT***TGG***TA**G**CT**GG**TTTCTTTC*T*A*T

Table 5-1. Sequences of oligonucleotides used for analysis of guanine damage induced by Fe^{+2}-EDTA, Fe^{+2}-EDTA/H_2O_2 and γ-radiation. Relative reactivities of guanines shown in bold within underlined sequence contexts were quantified. The invariant TGG sequence used for normalizing damage is italicized, and * represents a phosphorothioate linkage.

Labeling and annealing of oligonucleotides. Purified single-stranded oligonucleotides were 5'-end labeled with ^{32}P by incubation at 37 ^0C for 1 hr in a reaction that contained 0.2 nmol of 5' ends, 0.1 mCi of [γ-^{32}P]-ATP and 40 units of T4 PNK in 1xPNK buffer (New England Biolabs, Ipswich, MA), in a total volume of 100 μl. Excess label was removed by gel filtration using Sephadex G-

25 columns (Roche Diagnostics, Indianapolis, IN) that were washed with a total of 4x300 µl of chelexed 175 mM potassium phosphate buffer (prepared as described in Chapter 4, Materials and Methods). For the annealing reaction, a total of 0.4 nmol of unlabeled complement was added to each labeled oligonucleotide, the mixture was heated at 95 ^{0}C for 5 min and was then allowed to slowly cool to room temperature over the course of 2 hr.

Analysis of damage in double-stranded oligonucleotides. All damage analyses and controls were performed three separate times, in triplicates. Each Fenton reaction contained 0.1 mM $FeSO_4$-EDTA (in the ratio of 1:1.1, freshly prepared before each experiment) and 2 mM H_2O_2 (concentration determined by using extinction coefficient value of 39.4 M^{-1} cm^{-1}), or 2 mM $FeSO_4$-EDTA. The rest of the reaction components included 20 pmol of labeled, double-stranded oligonucleotide in 175 mM chelexed potassium phosphate buffer and total volume of 50 µl. The DNA was always added last, and the controls contained potassium phosphate buffer instead of $FeSO_4$-EDTA solution. The reactions were incubated at 37 ^{0}C for 2 hr, after which the $FeSO_4$-EDTA complex was removed by filtration through Sephadex G-25 columns that were washed with 2x300 µl of ddH_2O. For γ-irradiation experiments, samples containing a total of 20 pmol of labeled, double-stranded oligonucleotide in a total of 50 µl of chelexed potassium phosphate buffer were irradiated in a ^{60}Co source for a total dose of 50 Gray. Following treatment, the samples were normally incubated at ambient

temperature for 20 min before purification by filtration using Sephadex G-25 columns.

Damaged and purified oligonuleotides were treated with 5 units of Exonuclease III in 1xNEbuffer 1 (New England Biolabs, Ipswich, MA) at 37 ^{0}C for 1 h in a total volume of 60 µl. These conditions were sufficient to remove all direct strand breaks generated during damage reactions, as determined by control experiments (results not shown). For hot piperidine treatment, oligonucleotides were de-salted by gel filtration, incubated with 1M piperidine at 90 ^{0}C for 20 min in a total volume of 120 µl, lyophilized, and dissolved in a total of 5 µl of formamide gel loading buffer. To remove Exo III activity prior to Fpg reactions, oligonucleotides were incubated with 20 mM EDTA to chelate Mg^{2+} present in NEbuffer 1, and passed through protein-binding Micropure-EZ filters. The oligonucleotides were subsequently treated with 8 units of Fpg at 37 ^{0}C for 1 h, precipitated with ethanol, and dissolved in a total of 5 µl of formamide gel loading buffer.

A total of 2 µl of DNA from each sample was resolved on a 20% polyacrylamide, 8 M urea gel, and was subjected to phosphorimager analysis (ImageQuant, Molecular Dynamics). Relative reactivities of guanines in each oligonucleotide sequence were determined as previously described (See Chapter 2).

RESULTS

Fe^{+2}-EDTA/H_2O_2, Fe^{+2}-EDTA, and γ-radiation produce similar levels of piperidine-sensitive guanine lesions in all sequence contexts. We measured relative amounts of oxidative guanine lesions produced by Fe^{+2}-EDTA/H_2O_2, Fe^{+2}-EDTA, and γ-radiation within different sequence contexts. For our studies, we used oligonucleotides of the general sequence 5'-CGTACTCTTTGGTX$_1$G$_1$Y$_1$TX$_2$G$_2$Y$_2$TTCTTTC*T*A*T-3' containing three consecutive phosphorothioate linkages (designated by *), two variable guanine contexts ($X_iG_iY_i$) and an invariant TGG sequence for normalizing damage (underlined). The same oligonucleotide sequences were previously used for similar analyses of sequence-specific guanine oxidation produced by photoactivated riboflavin and $ONOOCO_2^-$ in bicarbonate buffer (18, 19) (Chapter 2). To remove the background of direct strand breaks that are generated in relatively high amounts by Fe^{+2}-EDTA/H_2O_2, Fe^{+2}-EDTA and γ-radiation, we used a previously developed method, described in Chapter 4.

Damage reactions with Fe^{+2}-EDTA/H_2O_2 were accomplished by incubating ^{32}P-labeled double-stranded oligonucleotides with freshly prepared 0.1 mM Fe^{2+}-EDTA and 2 mM H_2O_2 in 175 mM chelexed phosphate buffer at pH 7.4. At these conditions the efficiency of $^{\bullet}OH$ production in the air-saturated solution was maximized, according to a recent study (7). Damage with Fe^{2+}-EDTA was accomplished by incubating the same oligonucleotides with freshly prepared 2 mM Fe^{2+}-EDTA, while for γ-irradiation experiments the oligonucleotides were

exposed to a total dose of 50 Gray of γ-rays at the rate of 1.1 Gray/min. The reaction conditions utilized in all experiments were chosen to produce strong damage signals needed for efficient quantification and, according to Poisson distribution, resulted in a maximum of a single detectable base oxidation event per an oligonucleotide molecule. This was evidenced by more than 70% of the parent duplex unaffected by hot piperidine or *E.Coli* Fpg treatments after Exo III reaction. After damage, all oligonucleotides were treated with Exo III to remove strand break background, and then with hot piperidine to create strand breaks at the sites of guanine oxidation. The resulting cleavage products were separated on a sequencing gel, and damage induced within central guanine of each XGY sequence context was quantified relative to the damage at the central guanine within the invariant TGG normalization sequence.

Relative amounts of piperidine-labile guanine lesions produced by all three oxidants were graphed versus guanine's sequence-specific IPs. The data for Fe^{+2}-EDTA/H_2O_2 and γ-radiation is graphed in Figure 5-2, while data for Fe^{+2}-EDTA is graphed in Figure 5-3. Representative gels used for damage quantification are shown in Figure 5-1. Relative piperidine-sensitive guanine damage produced by all agents varies only modestly with sequence contexts and ranges from 0.71 to 0.96 for Fe^{2+}-EDTA/H_2O_2 and from 0.60 to 1.0 for γ-radiation. Relative piperidine-sensitive guanine oxidation produced by Fe^{+2}-EDTA displays a greater variability from 0.60 to 1.0, reflective of somewhat lower relative damage induced within 5'-GT-3' motifs. For comparison, relative reactivities of guanines with riboflavin and $ONOOCO_2^-$, determined previously within the same

oligonucleotides and under similar experimental conditions, ranged from 0.2 to 1.4 and from 0.6 to 3.3, respectively (Chapter 2).

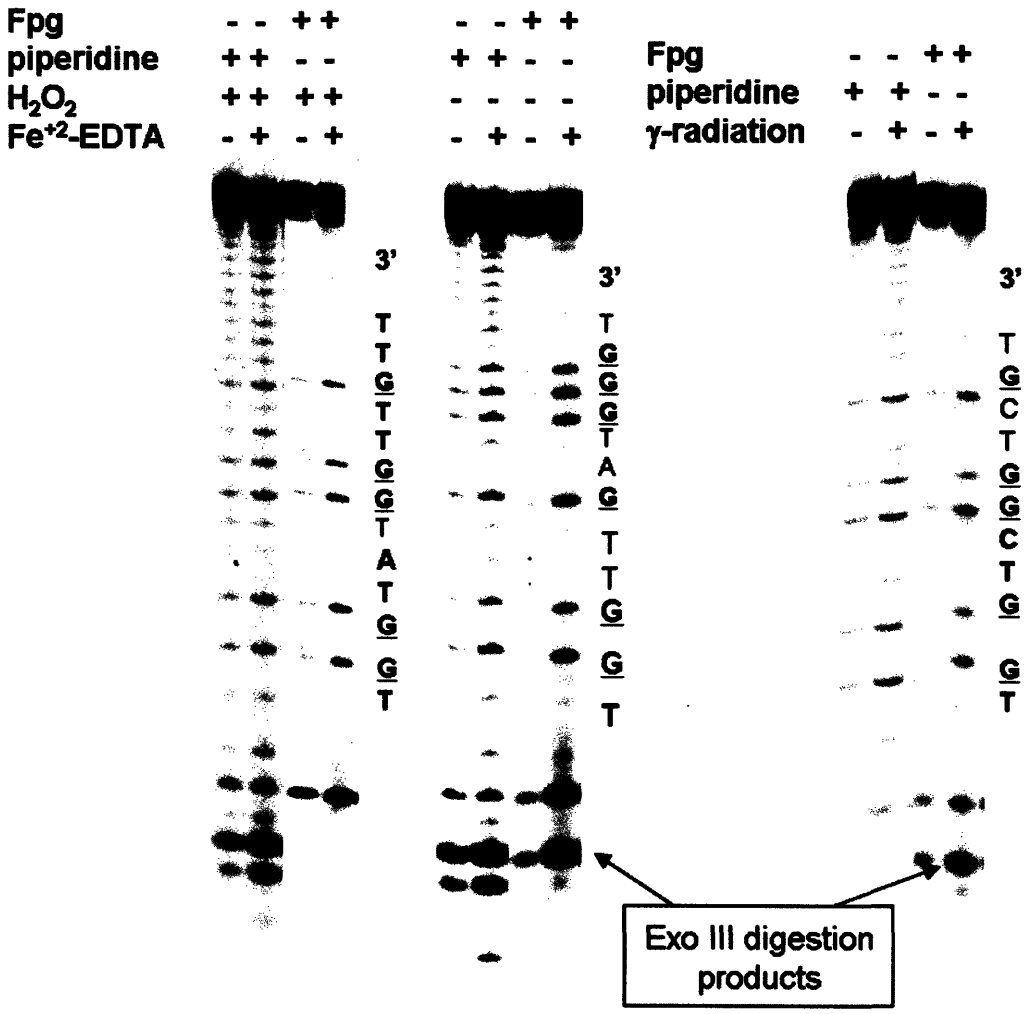

Figure 5-1. Representative lanes of the sequencing gels used for quantitative analysis of guanine damage induced by Fe^{+2}-EDTA/H_2O_2, Fe^{+2}-EDTA, and γ-radiation (See Materials and Methods).

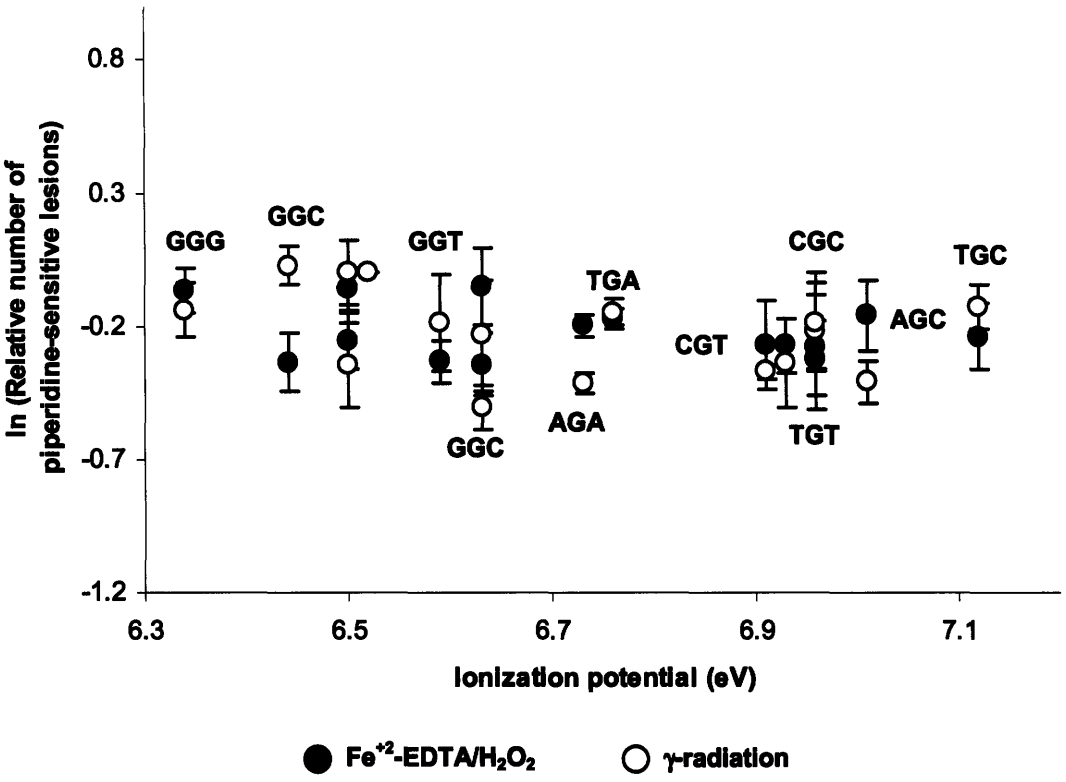

Figure 5-2. Relative reactivities of guanines within all possible three-base sequence contexts (XGY) with Fe^{+2}-EDTA/ H_2O_2 and γ-radiation, hot piperidine treatment. Relative amounts of piperidine-sensitive guanine lesions produced by 0.1 mM Fe^{+2}-EDTA in the presence of 2 mM H_2O_2 (closed circles) and by a total of 50 Gray of γ-radiation (open circles) are graphed vs. guanines' sequence-specific IPs. Damage reactions and the subsequent analysis of relative reactivities were performed as described in Materials and Methods.

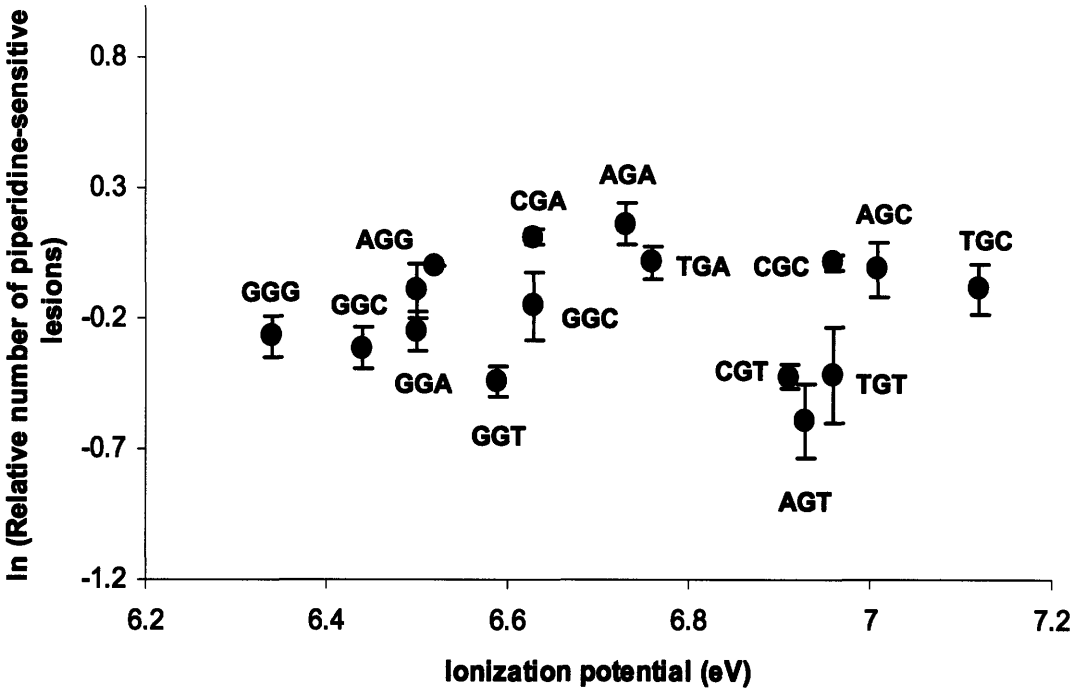

Figure 5-3. Relative reactivities of guanines within all possible three-base sequence contexts (XGY) with Fe^{+2}-EDTA, hot piperidine treatment. Relative numbers of piperidine-sensitive guanine lesions produced by 2 mM Fe^{+2}-EDTA complex within different sequence contexts are graphed vs. guanines' sequence-specific IPs. Damage reactions and the subsequent analysis of relative reactivities were performed as described in Materials and Methods.

5'-GT-3' sequence contexts are characterized by lower relative amounts of Fpg-labile guanine lesions. We also measured relative amounts of Fpg-sensitive guanine lesions produced by Fe^{+2}-EDTA/H_2O_2, Fe^{+2}-EDTA and γ-radiation in all possible sequence contexts. All damage reactions and

subsequent treatment with Exo III to remove the background of direct strand breaks were carried out in a manner analogous to the one already described for the analysis of piperidine-sensitive products. Prior to Fpg treatment, Exo III activity was removed by a combination of addition of EDTA and filtration through Micropure-EZ filters, as described in Materials and Methods and in Chapter 4. After Exo III treatment, damaged oligonucleotides were incubated with Fpg, and resulting fragments were separated on a sequencing gel. Amounts of Fpg-sensitive lesions induced within central guanine of each XGY sequence context were quantified relative to the damage at the central guanine within the invariant TGG normalization sequence and graphed versus guanine's sequence-specific IPs.

The data for Fe^{+2}-EDTA/H_2O_2 and γ-radiation is shown in Figures 5-2 and 5-4, while data for Fe^{+2}-EDTA is shown in Figures 5-3 and 5-5. Similar to the case of piperidine-sensitive damage, relative numbers of Fpg-sensitive products produced by all three oxidants display only a modest variation with sequence contexts. However, lower relative amounts of Fpg-sensitive damage was induced within 5'-CGT-3', 5'-AGT-3', 5'-TGT-3' and 5'-GGT-3' motifs. This was especially evident for the damage produced by Fe^{+2}-EDTA, where relative reactivity values ranged from 0.47 to 0.50 and differed in a statistically significant manner ($p < 0.001$) from the rest of the values ranging from 0.78 to 1.1.

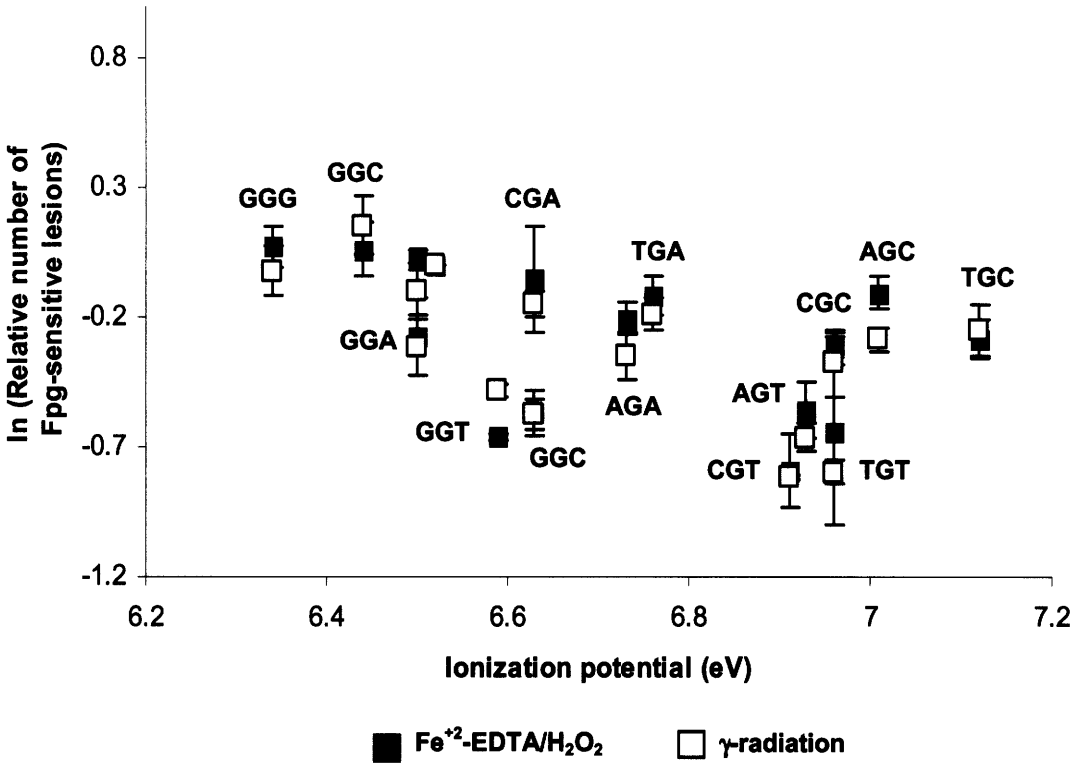

Figure 5-4. Relative reactivities of guanines within all possible three-base sequence contexts (XGY) with Fe^{+2}-EDTA/ H_2O_2 and γ-radiation, Fpg treatment. Relative amounts of Fpg-sensitive guanine lesions produced by 0.1 mM Fe^{+2}-EDTA in the presence of 2 mM H_2O_2 (closed squares) and by a total of 50 Gray of γ-radiation (open squares) are graphed vs. guanines' sequence-specific ionization potentials. Damage reactions and the subsequent analysis of relative reactivities were performed as described in Materials and Methods.

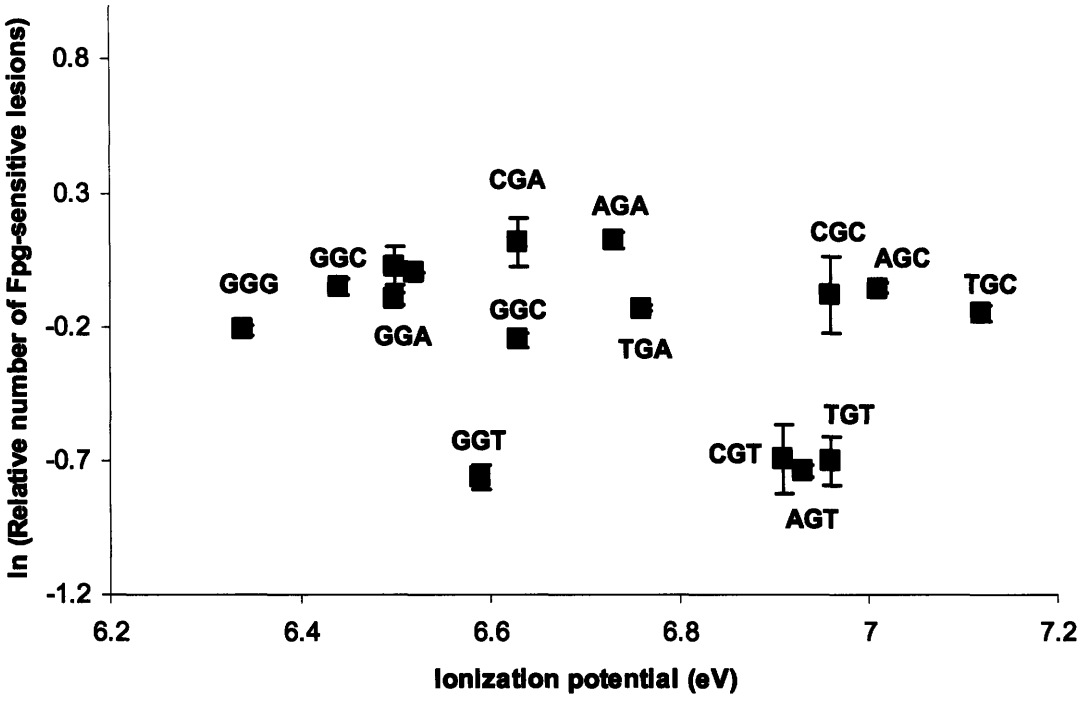

Figure 5-5. Relative reactivities of guanines within all possible three-base sequence contexts (XGY) with Fe^{+2}-EDTA, Fpg treatment. Relative numbers of Fpg-sensitive guanine lesions produced by a 2 mM Fe^{+2}-EDTA complex within different sequence contexts graphed as a function of guanines' sequence-specific IPs. Damage reactions and the subsequent analysis of relative reactivities were performed as described in Materials and Methods.

Ratios of Fpg- to piperidine-sensitive lesions produced by all three oxidants display moderate variability as a function of sequence context. Because 8-oxoG, the most common guanine lesion, displays differential sensitivities toward hot piperidine and Fpg treatments, comparison of the relative

ratios of Fpg- to piperidine-sensitive lesions across all sequence contexts provides a measure of sequence-specific guanine oxidation chemistry. Ratios of Fpg to piperidine sensitive lesions produced by Fe^{+2}-EDTA/H_2O_2, Fe^{+2}-EDTA and γ-radiation in all sequence contexts are graphed in Figure 5-6 and display an approximate two-fold variability. This is contrasted with similar ratios of Fpg to piperidine-sensitive lesions induced by $ONOOCO_2^-$ within the same oligonucleotides that display an approximate 5.4-fold variability (Chapter 2). As was previously indicated, guanines located within 5'-GT-3' motifs (5'-CGT-3', 5'-AGT-3', 5'-GGT-3' and 5'-TGT-3') are characterized by lower Fpg/piperidine ratios.

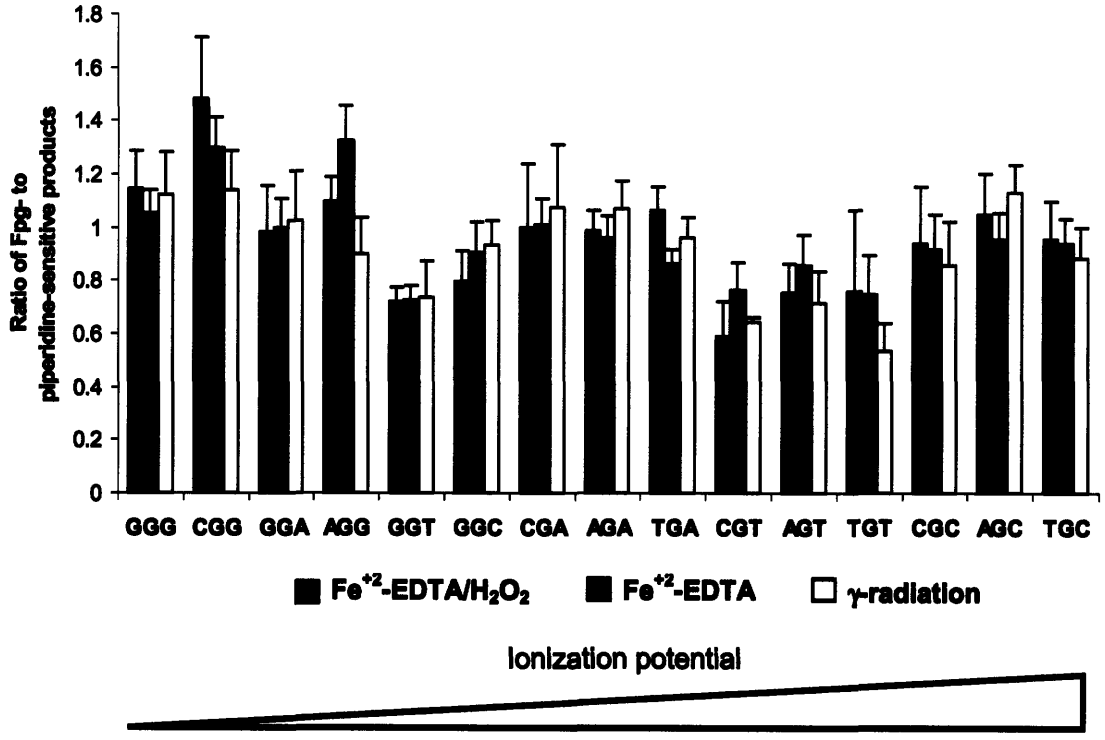

Figure 5-6. Ratios of relative amounts of Fpg to piperidine-sensitive guanine lesions produced by Fe^{+2}-EDTA/H_2O_2 (closed bars), Fe^{+2}-EDTA (grey bars), and γ-radiation (open bars) within different sequence contexts.

DISCUSSION

Electrostatic forces are known to modulate interactions of DNA with small reagents, such as thiols (1), polyamines (2), peroxyl radicals (3, 4), or naphthalimide derivatives (5). We proposed that negative charge was also a determinant of guanine oxidation by $ONOOCO_2^-$, a chemical mediator of inflammation that is selective for guanines of highest IPs and displays enhanced reactivity toward solvent-exposed bases (Chapters 2 and 3). To test the hypothesis that electrostatic repulsion between the negatively charged reagent and polyanionic DNA backbone restricted its reactivity to the more solvent accessible targets, we investigated sequence-selective guanine oxidation pattern produced by another negatively charged species, Fe^{+2}-EDTA and compared it to guanine oxidation produced by γ-radiation, a neutral oxidant. A study by Li *et al.* demonstrated that electrostatic interactions played a significant role in determining diffusion distances of Fe^{+2}-EDTA species and the associated oxidants that caused direct strand breaks in isolated and nuclear DNA (20). Additionally, Balasubramanian *et al.* showed that generation of direct strand breaks within a double-stranded DNA fragment by Fe^{+2}-EDTA in the presence of H_2O_2 was governed by solvent accessibility of hydrogen atoms of the deoxyribose moiety (21). These studies provided preliminary evidence for the influence of both solvent exposure and negative charge on the reactivity of DNA with Fe^{+2}-EDTA.

Reactions of oligonucleotides with Fe^{+2}-EDTA were conducted in oxygenated aqueous solutions in the presence and absence of H_2O_2. Multiple studies provided evidence that the nature of the predominant oxidizing species formed at each condition may be different; the former condition was shown to promote generation of $^{\bullet}OH$, while the latter condition favored formation of the putative Fe^{+2}-EDTA-oxo complexes (6, 7, 10, 14). We observed small differences in the patterns of guanine reactivity produced by Fe^{+2}-EDTA/H_2O_2 and Fe^{+2}-EDTA, consistent with similar reactivity of $^{\bullet}OH$ and Fe^{+2}-EDTA-oxo complexes. Consistently lower levels of both piperidine-sensitive and Fpg-sensitive guanine damage produced within 5'-GT-3' sequence context was a pronounced feature Fe^{+2}-EDTA-mediated damage (Figures 5-3 and 5-5). Meanwhile, both piperidine- and Fpg-sensitive damage produced by Fe^{+2}-EDTA/H_2O_2 and γ-radiation was identical. This is consistent with $^{\bullet}OH$ mediating guanine oxidation in the cases of Fe^{+2}-EDTA/H_2O_2 and γ-radiation, and a different species, possibly Fe^{+2}-EDTA-oxo complex, mediating guanine oxidation in the case of Fe^{+2}-EDTA.

The effect of negative charge on guanine oxidation. Sequence-selective guanine oxidation produced by Fe^{+2}-EDTA/H_2O_2 and Fe^{+2}-EDTA within double-stranded oligonucleotides was compared to the guanine oxidation mediated by γ-radiation, a neutral oxidant and an independent source of diffusible $^{\bullet}OH$. Figures 5-2 and 5-3 demonstrate that Fe^{+2}-EDTA/H_2O_2 and γ-radiation produced identical guanine oxidation patterns. This indicates that negative

charge of Fe^{+2}-EDTA failed to affect its reactivity with guanines in different sequence contexts. Consistent with our results, Pogozelski *et al.* also observed identical DNA strand cleavage patterns produced by γ-radiolysis and Fe^{+2}-$EDTA^{2-}$ in a variety of buffers (22).

Oligonucleotide damage reactions with Fe^{+2}-EDTA/H_2O_2, Fe^{+2}-EDTA and γ-radiation were carried out in 175 mM potassium phosphate buffer to mimic the conditions of earlier experiments with $ONOOCO_2^-$ (Chapter 2); presence of counterions was anticipated to result in a partial screening of the negative charge of the DNA backbone. However, we did not expect these buffer conditions to eliminate unfavorable electrostatic interactions between DNA and Fe^{+2}-EDTA, given that Ingold and co-workers observed a minimal effect of addition of 140 mM NaCl or 140 mM KCl on the extent of DNA damage mediated by the charged peroxyl radicals (3, 4).

Nearly equal reactivity of guanines in all sequence contexts with Fe^{+2}-EDTA/ H_2O_2, Fe^{+2}-EDTA and γ-radiation. We observed a virtual lack of variation in the relative numbers of guanine lesions produced within all possible three-base sequence contexts by Fe^{+2}-EDTA/H_2O_2 and by γ-radiation, while minimal variations were evident in the case of Fe^{+2}-EDTA (Figures 5-2 and 5-3). Equal distribution of guanine damage across all sequence contexts is consistent with chemistry of guanine oxidation by the •OH. Candeias and Steenken demonstrated that the initial steps in this process consist of addition of •OH to the double bonds of guanine heterocycle, resulting in generation of G-8•OH and G-

4•OH radicals (23) (See Figure 5-5). Subsequent transformations of G-8•OH yield 7,8-dihydro-8-oxoguanine (8-oxoG) or 2,6-diamino-5-formamido-4-hydroxypyrimidine(FAPy-G) as final oxidation products, while loss of a water molecule by G-4•OH at physiological pH results in formation a neutral guanine radical (G•) (23). The same radical can also arise from deprotonation of the guanine radical cation ($G^{\bullet+}$) and is, therefore, a common intermediate to both electron transfer and hydroxyl radical-mediated oxidative processes that is consumed by a diffusion-controlled recombination with superoxide to be converted into imidazolone (Iz) (24), (25) (Figure 5-7). No electron hole migration is expected to result from hydroxyl radical-mediated guanine oxidation at physiological pH, due to lack of $G^{\bullet+}$ formation. Therefore, distribution of guanine damage along a double-stranded sequence will be primarily determined by the initial, sequence-independent rates of hydroxyl radical addition to the guanine, in good agreement with our present results.

Sequence-independent distribution of guanine damage induced by γ-radiation is also consistent with the results of mutational studies involving MBL50 bacterial cells, which demonstrated that γ-radiation-specific mutational hotspots are equally distributed along all guanines within a *supF* gene, and lack a common sequence motif (27). This stands in contrast with the results of similar mutagenesis studies involving $ONOOCO_2^-$, which showed that the majority of mutational hotspots induced in the supF gene within the same bacterial cells are characterized by a common 5'-GC-3' sequence motif (28), consistent with previously identified damage hotspots (29) (Chapter 2).

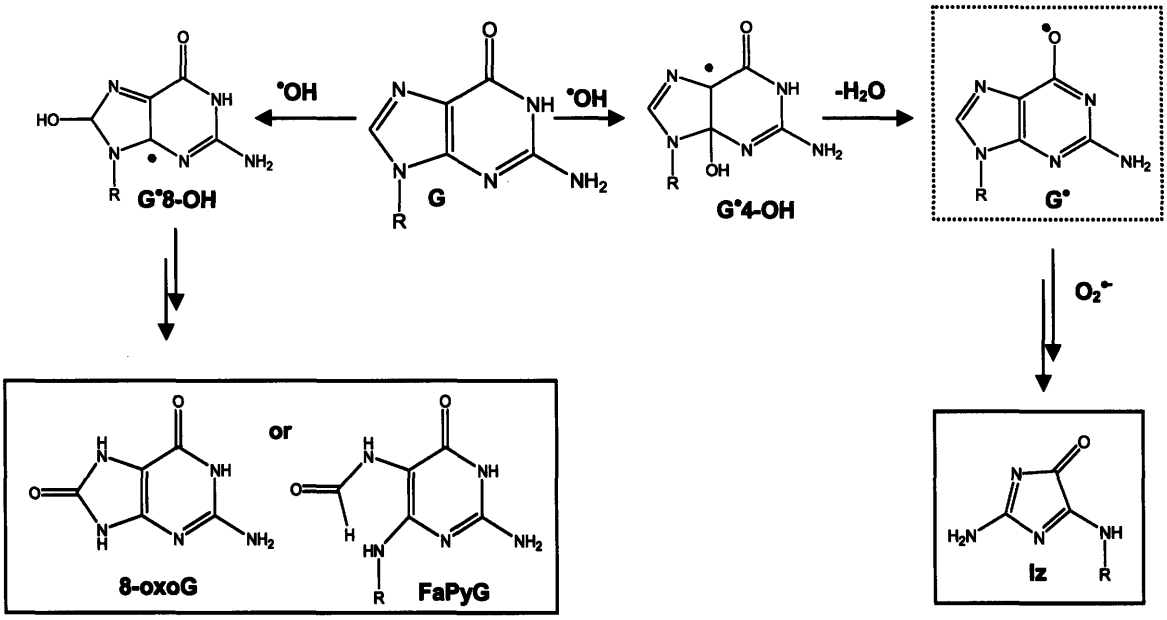

Figure 5-7. Hydroxyl radical-mediated guanine oxidation (23, 26).

Sequence-independent distribution of guanine damage induced by γ-radiation is also consistent with the results of mutational studies involving MBL50 bacterial cells, which demonstrated that γ-radiation-specific mutational hotspots are equally distributed along all guanines within a *supF* gene, and lack a common sequence motif (27). This stands in contrast with the results of similar mutagenesis studies involving $ONOOCO_2^-$, which showed that the majority of mutational hotspots induced in the supF gene within the same bacterial cells are characterized by a common 5'-GC-3' sequence motif (28), consistent with previously identified damage hotspots (29) (Chapter 2).

Moderate variations in the ratios of Fpg- to piperidine-sensitive products produced by Fe^{+2}-EDTA/ H_2O_2, Fe^{+2}-EDTA and γ-radiation. Earlier studies identified 8-oxoG and Im as the two major products of •OH-mediated guanine oxidation (26), of which only 8-oxoG has differential sensitivities toward hot piperidine and Fpg treatments (30-32). Therefore, differences in the relative ratios of Fpg- to piperidine-sensitive products are indicative of differential sequence-dependent distribution of 8-oxoG. We note moderate, ~2-fold variations in the ratios of Fpg- to piperidine-sensitive guanine lesions produced by Fe^{+2}-EDTA/H_2O_2, Fe^{+2}-EDTA and γ-radiation in different sequence contexts (Figure 5-5). We previously observed a much greater variability in the ratios of Fpg- to piperidine-sensitive products produced by $ONOOCO_2^-$ (Chapter 2) that may be partially reflective of a more complicated chemistry of $ONOOCO_2^-$ that results in a rich spectrum of oxidation and nitration final products (23, 33).

Guanines located within 5'-GT-3' motifs are consistently characterized lower Fpg- to piperidine-sensitive ratios not only in the cases of guanine oxidation mediated by Fe^{+2}-EDTA/H_2O_2, Fe^{+2}-EDTA and γ-radiation, but also for $ONOOCO_2^-$ and photoactivated riboflavin (Chapter 2). This observation points to an unfavorable effect of the 3' neighboring thymine on 8-oxoG formation that may be dependent on several factors. Intrinsic flexibility of a DNA sequence consisting of alternating purine and pyrimidine bases (34) may cause a DNA backbone to adapt a conformation that hinders reaction at its C8 position. Additionally, steric environment of the guanine within a double-stranded sequence may also influence its reactivity. Indeed, using molecular dynamic

simulations, Cleveland *et al.* have recently observed that steric blocking by a thymine methyl group prevented a molecule of H_2O from interacting with the C8 of 5' guanine within 5'-TGGT-3' motif. The authors claimed that this steric blocking provided the basis for this guanine's decreased reactivity toward one-electron oxidation, as compared to a guanine in the same position within 5'-AGGA-3' and 5'-UGGU-3' sequences (35).

In conclusion, we have determined that negative charge plays no role in the selection of oxidation targets by Fe^{+2}-EDTA/H_2O_2, and that guanine damage by this reagent is mediated by $^{\bullet}OH$. Sequence-independent oxidation of guanines by Fe^{+2}-EDTA/H_2O_2 and γ-radiation is consistent with the chemistry of $^{\bullet}OH$ and with the lack of $G^{\bullet+}$ generation. In addition, steric and structural factors may be responsible for the decreased formation of Fpg-sensitive lesions within 5'-GT-3' sequence contexts.

REFERENCES

1. Zheng, S., Newton, G. L., Gonick, G., Fahey, R. C., and Ward, J. F. (1988) Radioprotection of DNA by thiols: relationship between the net charge on a thiol and its ability to protect DNA. *Radiat Res* 114, 11-27
2. Spotheim-Maurizot, M., Ruiz, S., Sabattier, R., and Charlier, M. (1995) Radioprotection of DNA by polyamines. *Int J Radiat Biol* 68, 571-577
3. Paul, T., Young, M. J., Hill, I. E., and Ingold, K. U. (2000) Strand cleavage of supercoiled DNA by water-soluble peroxyl radicals. The overlooked importance of peroxyl radical charge. *Biochemistry* 39, 4129-4135
4. Sanchez, C., Shane, R. A., Paul, T., and Ingold, K. U. (2003) Oxidative damage to a supercoiled DNA by water soluble peroxyl radicals characterized with DNA repair enzymes. *Chem Res Toxicol* 16, 1118-1123
5. Takada, T., Kawai, K., Tojo, S., and Majima, T. (2004) Effects of interaction of photosensitizer with DNA and stacked G bases on

photosensitized one-electron oxidation of DNA. *Journal of Physical Chemistry B* 108, 761-766

6. Cheng, Z. Y., and Li, Y. Z. (2007) What is responsible for the initiating chemistry of iron-mediated lipid peroxidation: An update (vol 107, pg 748, 2007). *Chemical Reviews* 107, 2165-2165
7. Qian, S. Y., and Buettner, G. R. (1999) Iron and dioxygen chemistry is an important route to initiation of biological free radical oxidations: an electron paramagnetic resonance spin trapping study. *Free Radic Biol Med* 26, 1447-1456
8. Davies, M. J. (2005) The oxidative environment and protein damage. *Biochim Biophys Acta* 1703, 93-109
9. Becker, D., Sevilla, M.D. (1993) The chemical consequences of radiation damage to DNA. *Adv. Radiat. Biol.* 17, 121-180
10. Rush, J. D., and Koppenol, W. H. (1986) Oxidizing intermediates in the reaction of ferrous EDTA with hydrogen peroxide. Reactions with organic molecules and ferrocytochrome c. *J Biol Chem* 261, 6730-6733
11. Wink, D. A., Nims, R. W., Saavedra, J. E., Utermahlen, W. E., Jr., and Ford, P. C. (1994) The Fenton oxidation mechanism: reactivities of biologically relevant substrates with two oxidizing intermediates differ from those predicted for the hydroxyl radical. *Proc Natl Acad Sci U S A* 91, 6604-6608
12. Sawyer, D. T., Kang, C., Llobet, A., and Redman, C. (1993) Fenton reagents (1:1 $Fe^{II}L_x$/HOOH) react via [$L_xFe^{II}OOH(BH^+)$] (1) as hydroxylases (RH -> ROH), not as generators of free hydroxyl radicals ($HO^{\cdot}$). *J Am Chem Soc* 115, 5817-5818
13. Koppenol, W. H., and Liebman, J. F. (1984) The oxidizing nature of the hydroxyl radical. A comparison with ferryl ion (FeO^{2+}). *J Phys Chem* 88, 99-101
14. Reinke, L. A., Rau, J. M., and Mccay, P. B. (1994) Characteristics of an Oxidant Formed During Iron(Ii) Autoxidation. *Free Radical Biology and Medicine* 16, 485-492
15. Saran, M., Michel, C., Stettmaier, K., and Bors, W. (2000) Arguments against the significance of the Fenton reaction contributing to signal pathways under in vivo conditions. *Free Radic Res* 33, 567-579
16. Seibig, S., and vanEldik, R. (1997) Kinetics of [Fe-II(edta)] oxidation by molecular oxygen revisited. New evidence for a multistep mechanism. *Inorganic Chemistry* 36, 4115-4120
17. Welch, K. D., Davis, T. Z., and Aust, S. D. (2002) Iron autoxidation and free radical generation: Effects of buffers, ligands, and chelators. *Archives of Biochemistry and Biophysics* 397, 360-369
18. Saito, I., Nakamura T., Nakatani K., Yoshioka Y., Yamaguchi K., Sugiyama H. (1998) Mapping of the hot spots for DNA damage by one-electron oxidation: Efficacy of GG doublets and GGG triplets as a trap in long-range hole migration. *J Am Chem Soc* 120, 12686-12687

19. Margolin, Y., Cloutier, J. F., Shafirovich, V., Geacintov, N. E., and Dedon, P. C. (2006) Paradoxical hotspots for guanine oxidation by a chemical mediator of inflammation. *Nat Chem Biol* 2, 365-366
20. Li, H., Jacque, A., Wang, F., and Byrnes, R. W. (1999) Diffusion distances of known iron complexes in model systems. *Free Radic Biol Med* 26, 61-72
21. Balasubramanian, B., Pogozelski, W. K., and Tullius, T. D. (1998) DNA strand breaking by the hydroxyl radical is governed by the accessible surface areas of the hydrogen atoms of the DNA backbone. *Proc Natl Acad Sci U S A* 95, 9738-9743
22. Pogozelski, W. K., McNeese, T.J., Tullius, T.D. (1995) What species is responsible for strand scission in the reaction of $[Fe^{II}EDTA]^{2-}$ and H_2O_2 with DNA? *J Am Chem Soc* 117, 6428-6433
23. Candeias, L. P., and Steenken, S. (2000) Reaction of HO* with guanine derivatives in aqueous solution: formation of two different redox-active OH-adduct radicals and their unimolecular transformation reactions. Properties of G(-H)*. *Chemistry* 6, 475-484
24. Giese, B., and Wessely, S. (2001) The significance of proton migration during hole hopping through DNA. *Chem Commun (Camb)*, 2108-2109
25. Misiaszek, R., Crean, C., Joffe, A., Geacintov, N. E., and Shafirovich, V. (2004) Oxidative DNA damage associated with combination of guanine and superoxide radicals and repair mechanisms via radical trapping. *J Biol Chem* 279, 32106-32115
26. Cadet, J., Delatour, T., Douki, T., Gasparutto, D., Pouget, J. P., Ravanat, J. L., and Sauvaigo, S. (1999) Hydroxyl radicals and DNA base damage. *Mutat Res* 424, 9-21
27. Jeong, J. K., Juedes, M. J., and Wogan, G. N. (1998) Mutations induced in the supF gene of pSP189 by hydroxyl radical and singlet oxygen: relevance to peroxynitrite mutagenesis. *Chem Res Toxicol* 11, 550-556
28. Kim, M. Y., Dong, M., Dedon, P. C., and Wogan, G. N. (2005) Effects of peroxynitrite dose and dose rate on DNA damage and mutation in the supF shuttle vector. *Chem Res Toxicol* 18, 76-86
29. Tretyakova, N. Y., Burney, S., Pamir, B., Wishnok, J. S., Dedon, P. C., Wogan, G. N., and Tannenbaum, S. R. (2000) Peroxynitrite-induced DNA damage in the supF gene: correlation with the mutational spectrum. *Mutat Res* 447, 287-303
30. Gasparutto, D., Ravanat, J.-L., Gerot, O., Cadet, J. (1998) Characterization and Chemical Stability of Photooxidized Oligonucleotides that Contain 2,2-Diamino-4-[(2-deoxy--D-erythro-pentofuranosyl)amino]-5(2H)-oxazolone. *J Am Chem Soc* 120, 10283-10286
31. Tchou, J., Kasai, H., Shibutani, S., Chung, M. H., Laval, J., Grollman, A. P., and Nishimura, S. (1991) 8-oxoguanine (8-hydroxyguanine) DNA glycosylase and its substrate specificity. *Proc Natl Acad Sci U S A* 88, 4690-4694
32. Tretyakova, N. Y., Wishnok, J. S., and Tannenbaum, S. R. (2000) Peroxynitrite-induced secondary oxidative lesions at guanine

nucleobases: chemical stability and recognition by the Fpg DNA repair enzyme. *Chem Res Toxicol* 13, 658-664

33. Lee, Y. A., Yun, B. H., Kim, S. K., Margolin, Y., Dedon, P. C., Geacintov, N. E., and Shafirovich, V. (2007) Mechanisms of oxidation of guanine in DNA by carbonate radical anion, a decomposition product of nitrosoperoxycarbonate. *Chemistry* 13, 4571-4581
34. Packer, M. J., Dauncey, M. P., and Hunter, C. A. (2000) Sequence-dependent DNA structure: tetranucleotide conformational maps. *J Mol Biol* 295, 85-103
35. Cleveland, C. L., Barnett, R. N., Bongiorno, A., Joseph, J., Liu, C., Schuster, G. B., Landman, U. (2007) Steric effects on water accessibility control sequence-selectivity of radical cation reactions in DNA. *J Am Chem Soc* 129, 8408-8409

Chapter 6

Guanine is not the primary target of nucleobase oxidation mediated by unchelated Fe^{+2} ions

ABSTRACT

Iron, an essential component of all living systems, can lead to tissue damage through generation of reactive oxygen species (ROS) by Fenton reaction. In its unchelexed form, Fe^{+2} and Fe^{+3} ions were previously shown to coordinate to the DNA and to cause production of strand breaks in a sequence-specific manner in the presence of hydrogen peroxide (H_2O_2). In this study we investigated sequence-selectivity of nucleobase oxidation caused by DNA-bound Fe^{+2} ions, using a previously developed method for quantifying sequence-specific nucleobase damage in the presence of strand breaks. We demonstrated that binding of Fe^{+2} ions to DNA shifts the spectrum of nucleobase oxidation from guanines to thymines located within 5'-TGG-3' motif. This suggests that the two adjacent guanines constitute the preferred site of Fe^{+2} complexation to double-stranded DNA, and that this coordination prevents the guanines from reacting with the reactive oxygen species produced by the redox cycling of Fe^{+2}. In

addition, possible structural distortions of the helix caused by Fe^{+2} binding may be responsible for the increased reactivity of thymine.

INTRODUCTION

Iron is a key component of enzymes involved in electron transfer and oxygen management and is, therefore, an essential element for the majority of living organisms. In humans, iron deficiency is the most widespread form of malnutrition worldwide and a major cause of anemia that affects approximately 400-500 million people in third-world countries (1, 2). However, iron can also stimulate production of reactive oxygen species (ROS) through redox cycling, and iron overloads can lead to tissue damage in conditions such as primary and secondary hemochromatosis, as well as in the course of cerebrovascular or cardiovascular diseases (3). This potentially deleterious property of iron necessitates a complex mechanism of iron homeostasis control that is operative *in vivo* and includes systems regulating iron absorption, transport and storage within a cell. A small percentage of cellular iron (estimated to be about 3-5% at concentrations of approximately 50-100 μM), constitutes an intracellular labile iron pool (LIP) composed of weakly chelated redox-active Fe^{+2} and Fe^{+3} ions (4, 5). It has been suggested that LIP components are primarily responsible for the adverse effects for iron *in vivo*, and several studies have demonstrated significant correlations between increased LIP levels and greater yields of DNA and protein damage products (5-7). Iron toxicity is mediated through the Fenton

reaction-dependent production of highly reactive hydroxyl radicals ($^{\bullet}OH$) or iron-oxo complexes in the presence of molecular oxygen (O_2) or hydrogen peroxide (H_2O_2) (8). Generation of $^{\bullet}OH$ proceeds according to the following reactions (8, 9):

$$Fe^{+2} + O_2 \rightarrow Fe^{+3} + O_2^{\bullet-} \quad [1]$$

$$Fe^{+2} + O_2^{\bullet-} + 2H^{+} \rightarrow Fe^{+3} + H_2O_2 \quad [2]$$

$$Fe^{+2} + H_2O_2 \rightarrow Fe^{+3} + {}^{\bullet}OH + {}^{-}OH \quad [3]$$

Binding of unchelexed Fe^{+2} ions to DNA may result in generation of reactive forms of oxygen directly adjacent to the DNA, contributing to oxidative DNA damage. In fact, it has been previously demonstrated that both Fe^{+2} and Fe^{+3} ions can bind to DNA components, exhibiting particularly strong affinities to guanines and the sugar-phosphate backbone (10). Additionally, S. Linn and co-workers showed in a series of studies that preferential nicking of a DNA backbone at consensus sequences of 5'-purine-GGG-3' and 5'-purine-TG-purine-3' can be explained by the selective binding of Fe^{+2} ions at these sites (11-13). This sequence-specific nicking pattern sharply contrasts with previously observed sequence-independent generation of strand breaks by a negatively charged Fe^{+2}-EDTA complex (14). We previously determined that EDTA-chelexed Fe^{+2} ions produced sequence-independent oxidation of guanines in double-stranded oligonucleotides (Chapter 5). We now extended our studies to include sequence-specific nucleobase oxidation produced by DNA-bound Fe^{+2} ions, using a previously developed method to analyze sequence-specific

nucleobase oxidation in the presence of high levels of direct strand breaks (Chapter 4). Here we show that thymines, and not guanines, located within a 5'-TGG-3' sequence motif, are the primary targets of oxidative damage mediated by DNA-bound Fe^{+2}.

MATERIALS AND METHODS

Materials. Phosphorothioate-modified oligonucleotides were purchased from Integrated DNA Technologies (Coralville, IA) and gel-purified as described previously (See Chapter 4). The sequences of the oligonucleotides are shown in the Table 6-1.

Oligonucleotide name	Oligonucleotide sequence (5' to 3')
S10-S	CGTACTCTT***TGG***TGGCTTGATTCTTTC*T*A*T
S11-S	CGTACTCTT***TGG***TGGGTCGTTTCTTTC*T*A*T
S12-S	CGTACTCTT***TGG***TAGCTGGTTTCTTTC*T*A*T

Table 6-1. Sequences of oligonucleotides used Fe^{+2}-mediated nucleobase damage analysis. Relative reactivities of guanines shown in bold within underlined sequence contexts were quantified. The invariant TGG sequence used for normalizing damage is italicized, and * represents a phosphorothioate linkage.

Piperidine, TEMED (N,N,N',N'-Tetramethylethylenediamine) and 30% w/w) solution of H_2O_2 were purchased from Sigma-Aldrich. Urea, boric acid, tris base, ammonium persulfate and 40% solution of acrylamide:bis (19:1) were obtained from American Bioanalytical (Natick, MA). K_2HPO_4, KH_2PO_4, $NaHCO_3$, EDTA (ethylenediaminetetraacetic acid, sodium salt) and NaCl were purchased from Mallinckrodt Baker (Phillipsburg, NJ). All chemicals were used without further purification. Chelex-100 was purchased from Bio-Rad (Hercules, CA), Sephadex G-25 mini-spin columns were purchased from Roche Diagnostics, and Micropure-EZ spin filters were obtained from Millipore (Bedford, MA). T4 PNK (polynucleotide kinase) and Exonuclease III (Exo III) were purchased from New England Biolabs (Ipswich, MA). [γ-^{32}P]-ATP with activity of 6000 Ci/mmol was obtained from Perkin Elmer (Waltham, MA). Distilled and deionized water (ddH_2O) was purified using Milli-Q system from Millipore (Bedford, MA) and was used for all experiments.

Labeling and annealing of oligonucleotides. Purified single-stranded oligonucleotides were 5'-end labeled with ^{32}P by incubation at 37 ^{0}C for 1 hr in a reaction that contained 0.2 nmol of 5' ends, 0.1 mCi of [γ-^{32}P]-ATP and 40 units of T4 PNK in 1xPNK buffer (New England Biolabs, Ipswich, MA), in a total volume of 100 µl. Excess label was removed by gel filtration using Sephadex G-25 columns (Roche Diagnostics, Indianapolis, IN). The oligonucleotide annealing reactions were carried out in 20 mM NaCl. A total of 0.4 nmol unlabeled complement was added to each ^{32}P-labeled oligonucleotide, the mixture was

heated at 95 ^{0}C for 5 min, and then was allowed to cool to room temperature over the course of 2 hrs.

Analysis of Fe^{+2}-mediated nucleobase damage. All control and damage reactions were performed in duplicates and contained either 0 or 5 μM of $FeSO_4$ (freshly prepared), 2.2 nmol of labeled, double-stranded oligonucleotide, 50 mM H_2O_2, and 50 mM NaCl in a total volume of 50 μl. The oligonucleotides were incubated with $FeSO_4$ for 5 minutes before the addition of H_2O_2, and were allowed to incubate at 37 ^{0}C for 30 min. Damage reactions were stopped by addition of 0.5 mM desferoxamine mesylate to chelate Fe^{+2}, and subsequent filtration through Sephadex G-25 columns that were washed with 2x300 μl of ddH_2O. Reactions with Exonuclease III were followed by hot piperidine treatment, and the analysis of resulting fragments by gel electrophoresis was accomplished as described in Chapter 5. Damage of the same oligonucleotides with $ONOOCO_2^-$ was accomplished as described in Chapter 2.

RESULTS

Binding of Fe^{+2} to DNA changes sequence selectivity of nucleobase oxidation. In our previous studies we have investigated guanine oxidation produced by a negatively Fe^{+2}-EDTA complex that is prevented from complexation to DNA by unfavorable electrostatic interactions with the negatively charged backbone (Chapter 5). To investigate influence of Fe^{+2} binding on

sequence selectivity of guanine oxidation, we incubated unchelexed Fe^{+2} ions with ^{32}P-labeled double-stranded oligonucleotides in 60 mM NaCl, in the presence of 50 mM H_2O_2. These conditions were previously used for studies of Fe^{II}-mediated DNA nicking (11), and produced direct strand breaks at each nucleotide position, irrespective of sequence context (results not shown). After treatment with Exo III to remove the strand break background according to the method described in Chapter 4, nucleobase modifications were expressed as strand breaks by hot piperidine treatment, and the resulting fragments were separated by sequencing gel electrophoresis. A typical gel picture, shown in Figure 6-1, demonstrated a striking shift in the patterns of nucleobase modifications, as compared to Fe^{+2}-EDTA/H_2O_2 and Fe^{+2}-EDTA data (Chapter 5), with thymine becoming a primary target of Fe^{+2}-mediated oxidative damage. All damaged thymines were located within 5'-TGGX-3' sequences, and the identity of X modulated the extent of thymine modification in the following manner: 5'-TGGG-3' = 5'-TGGC-3' > 5'-TGGT-3' > 5'-TGGA-3'. Guanine oxidation was only observed in 5'-TGGG-3' sequence context, with the extent of damage decreasing in the 5' to 3' direction.

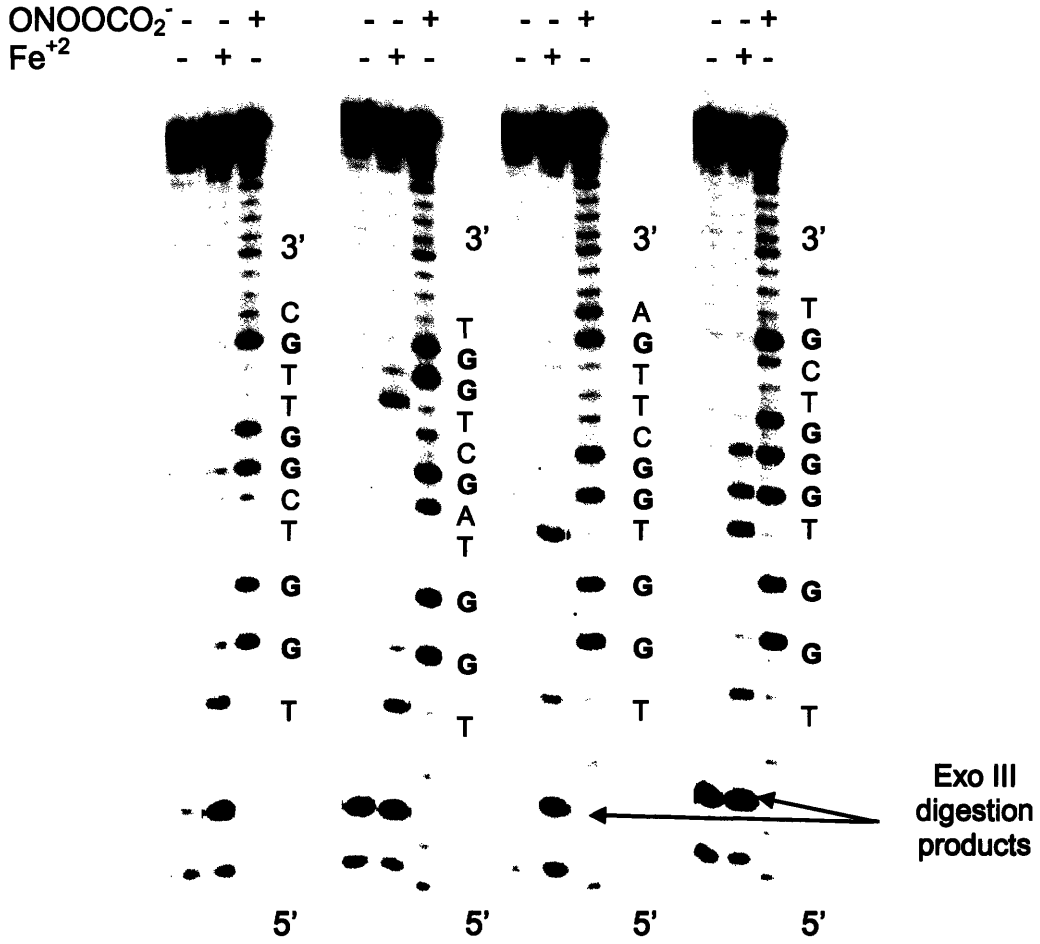

Figure 6-1. Oxidative nucleobase damage induced in double-stranded oligonucleotides by Fe^{+2}. ^{32}P-labeled, double-stranded oligonucleotides with sequences listed in Table 6-1 were incubated with 5 μM $FeSO_4$ and 50 mM H_2O_2 in 60 mM NaCl for 30 minutes. Damaged oligonucleotides were subsequently treated with Exo III to remove the strand break background, oxidized lesions were converted to strand breaks by hot piperidine, and the resulting fragments were separated by gel electrophoresis, as described in Materials and Methods. Oxidative damage induced by $ONOOCO_2^-$ was used to map guanine locations, and was carried out as described in Materials and Methods, Chapter 2.

DISCUSSION

Numerous experiments provided evidence for binding of Fe^{+2} and Fe^{+3} ions to DNA components (10, 15, 16). We investigated sequence-specific nucleobase oxidation, induced by DNA-bound Fe^{+2} ions in the presence of 50 mM H_2O_2, constituting conditions directly analogous to previous nicking studies (11). We determined that, unlike oxidants that were demonstrated to cause mainly guanine oxidation, such as Fe^{+2}-EDTA/H_2O_2, Fe^{+2}-EDTA and γ-radiation, DNA-bound Fe^{+2} ions induced damage only in thymines located within a 5'-TGG-3' motif. We also showed that guanine damage occurred only within a 5'-TGGG-3' sequence context, where yields of nucleobase oxidation decreased in a 5' to 3' direction. These observations are in a general agreement with the results of S. Linn and co-workers, who demonstrated in a series of experiments that binding of Fe^{+2} ions to the DNA occurs in a sequence-specific manner, and correlates with the sites of preferential nicking observed after incubation of Fe^{+2}-DNA complexes with different concentrations of H_2O_2 (11-13). Specifically, they showed that at 50 mM H_2O_2, consensus motifs containing guanine runs, such as 5'-GGGG-3' or 5'-AGGG-3' sequences, sustained the highest levels of nicking, with the yields of strand breaks decreasing in the 5' to 3' direction (11, 13).

Our results indicate that 5'-TGG-3' sequence context is both a necessary and a sufficient element for nucleobase oxidation by DNA-bound Fe^{+2} ions, with two adjacent guanines being the major sites of Fe^{+2} coordination. This agrees well with the recent study of Ouameur *et al.*, who used capillary electrophoresis

and Fourier transform infrared (FTIR) difference spectroscopy to show that the major sites of Fe^{+2} binding to double-stranded DNA include N-7 positions of guanines, as well as phosphates, characterized by the binding constants of K_G = 5.40 x 10^4 M^{-1} and K_P = 2.4 x 10^4 M^{-1}, respectively (10). In our studies, the identity of the base located immediately 3' to the 5'-TGG-3' consensus sequence can modulate the extent of thymine damage by possibly providing additional coordination sites for the Fe^{+2} ion. Guanine oxidation is observed only within a 5'-TGGG-3' sequence context, and can be explained by a possible tandem coordination of two Fe^{+2} ions at this site, resulting in the increased local production of reactive oxygen species.

Henle *et al.* used both molecular modeling and NMR to investigate Fe^{+2} interactions with a duplex sequence 5'-ATGA-3', and concluded that Fe^{+2} associates with the thymine flipped out from the helix to allow octahedrally-oriented coordination of the Fe^{+2} ion with purine residues (11). It is likely that Fe^{+2} associates with a 5'-TGG-3' sequence in a similar manner, and that increased solvent exposure of thymine in this complex makes it more vulnerable to the oxidants generated by Fe^{+2} and H_2O_2, resulting in preferential damage. It is also evident that the structure of Fe^{+2} coordination complex with the DNA prevents guanines from reacting with the oxidants produced by Fe^{+2} and H_2O_2. Participation of the 3' adenine of 5'-ATGA-3' sequence studied by Henle *et al.* in the coordination complex with the Fe^{+2} ion is consistent with our results that display an influence of the base located 3' to the 5'-TGG-3' consensus sequence on the extent of thymine oxidation.

Our experiments show that electron hole migration does not play a role in sequence-selective nucleobase oxidation by DNA-bound Fe^{+2} ions, in agreement with our previous studies of guanine oxidation mediated by Fe^{+2}-EDTA/H_2O_2 and Fe^{+2}-EDTA. Therefore, guanine radical cation ($G^{\bullet+}$) is not an intermediate in Fe^{II}/H_2O_2-induced nucleobase damage.

REFERENCES

1. Crichton, R. R., Wilmet, S., Legssyer, R., and Ward, R. J. (2002) Molecular and cellular mechanisms of iron homeostasis and toxicity in mammalian cells. *J Inorg Biochem* 91, 9-18
2. Moy, R. J. (2006) Prevalence, consequences and prevention of childhood nutritional iron deficiency: a child public health perspective. *Clin Lab Haematol* 28, 291-298
3. Nairz, M., and Weiss, G. (2006) Molecular and clinical aspects of iron homeostasis: From anemia to hemochromatosis. *Wien Klin Wochenschr* 118, 442-462
4. Kakhlon, O., and Cabantchik, Z. I. (2002) The labile iron pool: characterization, measurement, and participation in cellular processes(1). *Free Radic Biol Med* 33, 1037-1046
5. Kruszewski, M. (2003) Labile iron pool: the main determinant of cellular response to oxidative stress. *Mutat Res* 531, 81-92
6. Gackowski, D., Kruszewski, M., Bartlomiejczyk, T., Jawien, A., Ciecierski, M., and Olinski, R. (2002) The level of 8-oxo-7,8-dihydro-2'-deoxyguanosine is positively correlated with the size of the labile iron pool in human lymphocytes. *J Biol Inorg Chem* 7, 548-550
7. Kakhlon, O., Gruenbaum, Y., and Cabantchik, Z. I. (2001) Repression of ferritin expression increases the labile iron pool, oxidative stress, and short-term growth of human erythroleukemia cells. *Blood* 97, 2863-2871
8. Cheng, Z. Y., and Li, Y. Z. (2007) What is responsible for the initiating chemistry of iron-mediated lipid peroxidation: An update (vol 107, pg 748, 2007). *Chemical Reviews* 107, 2165-2165
9. Qian, S. Y., and Buettner, G. R. (1999) Iron and dioxygen chemistry is an important route to initiation of biological free radical oxidations: an electron paramagnetic resonance spin trapping study. *Free Radic Biol Med* 26, 1447-1456
10. Ouameur, A. A., Arakawa, H., Ahmad, R., Naoui, M., and Tajmir-Riahi, H. A. (2005) A comparative study of Fe(II) and Fe(III) interactions with DNA

duplex: Major and minor grooves bindings. *DNA and Cell Biology* 24, 394-401
11. Henle, E. S., Han, Z., Tang, N., Rai, P., Luo, Y., and Linn, S. (1999) Sequence-specific DNA cleavage by Fe2+-mediated fenton reactions has possible biological implications. *J Biol Chem* 274, 962-971
12. Rai, P., Cole, T. D., Wemmer, D. E., and Linn, S. (2001) Localization of Fe(2+) at an RTGR sequence within a DNA duplex explains preferential cleavage by Fe(2+) and H2O2. *J Mol Biol* 312, 1089-1101
13. Rai, P., Wemmer, D. E., and Linn, S. (2005) Preferential binding and structural distortion by Fe2+ at RGGG-containing DNA sequences correlates with enhanced oxidative cleavage at such sequences. *Nucleic Acids Res* 33, 497-510
14. Pogozelski, W. K., McNeese, T.J., Tullius, T.D. (1995) What species is responsible for strand scission in the reaction of $[Fe^{II}EDTA]^{2-}$ and H_2O_2 with DNA? *J Am Chem Soc* 117, 6428-6433
15. Ambroz, H. B., Kemp, T. J., Rodger, A., and Przybytniak, G. (2004) Ferric and ferrous ions: binding to DNA and influence on radiation-induced processes. *Radiation Physics and Chemistry* 71, 1023-1030
16. Colwell, B. A., and Morris, D. L. (2003) Formation of the oxidative damage marker 8-hydroxy-2 '-deoxyguanosine from the nucleoside 2 '-deoxyguanosine: parameter studies and evidence of Fe(II) binding. *Journal of Inorganic Biochemistry* 94, 100-105

Chapter 7

Conclusions and future directions

The purpose of studies described in this thesis was to investigate the basis for the unusual sequence-selective oxidation of guanines by nitrosoperoxycarbonate ($ONOOCO_2^-$), a chemical mediator of inflammation and a one-electron oxidant. Previous results indicated that $ONOCOO_2^-$ preferentially oxidized guanines located within 5'-TGC-3' and 5'-AGC-3' motifs that were characterized by the highest sequence-specific ionization potentials (1, 2). These preliminary observations contradicted the model of oxidative charge transfer that predicted that the reactivity of a guanine toward one-electron oxidation was determined by its sequence-specific ionization potential (IP) (2).

Sequence-selective guanine oxidation by $ONOOCO_2^-$. As the first step in exploring sequence-selective guanine oxidation by $ONOOCO_2^-$, we undertook a comprehensive and systematic study to define relative reactivities of guanines in all possible three-base sequence contexts (XGY) with $ONOOCO_2^-$ and photooxidized riboflavin (Chapter 2). With respect to riboflavin-mediated photooxidation, we were able to reproduce the results of earlier studies that found a strong inverse correlation between reactivities of guanines and their

calculated sequence-specific IPs (2). We also demonstrated that $ONOOCO_2^-$ exhibited enhanced reactivity with guanines in 5'-GC-3' sequences; of these, 5'-TGC-3', 5'-AGC-3' and 5'-CGC-3' were characterized by the highest calculated sequence-specific IPs, and 5'-GGC-3' sequence context exhibited the highest IP of all GG-containing motifs (2). This selectivity of $ONOOCO_2^-$ was also confirmed in genomic DNA isolated from human lymphoblastoid cells, where 5'-AGC-3' and 5'-TGC-3' motifs were observed as the major oxidative damage hotspots. These experiments demonstrated that sequence-specific IPs were not the determinants of guanine oxidation by $ONOOCO_2^-$. The guanine reactivity patterns for both riboflavin and $ONOOCO_2^-$ were double strand-specific and, therefore, dependent on the secondary structure of the DNA.

Solvent exposure as a determinant of guanine reactivity with $ONOOCO_2^-$. Solvent-exposed guanines displayed greater reactivity with $ONOOCO_2^-$, as was evidenced by approximately 5- to 9 times greater levels of damage sustained by single-stranded oligonucleotides, as compared to double-stranded sequences. In contrast, no differences in reactivity between single-stranded and duplex oligonucleotides were observed for riboflavin-mediated photooxidation. Additionally, solvent-exposed guanines located within mismatches also displayed enhanced reactivity with $ONOOCO_2^-$. A crucial aspect of solvent exposure model that remains to be tested is whether guanines within 5'-GC-3' sequences that were identified as hotspots of $ONOOCO_2^-$-mediated guanine damage are indeed characterized by higher average levels of

solvent exposure in the context of duplex oligonucleotides. This can be accomplished by NMR-based measurements of the rates of guanine's imino proton exchange in different sequence contexts (3). These rates are reflective of "base-pair lifetime", a length of time that a G-C pair spends in a fully hydrogen-bonded state. A number of previous studies indicated that this quantity may be sequence context-dependent, but a systematic and consistent comparison of the lifetimes of G-C base-pairs in different sequence motifs is currently lacking (4, 5).

Negative charge as a determinant of oxidant's reactivity with guanine in DNA. We proposed that electrostatic repulsion between negatively charged $ONOOCO_2^-$ and the polyanionic DNA backbone limited accessibility of $ONOOCO_2^-$ to the guanines buried in the helix and restricted its reactivity to more accessible targets. To test the hypothesis that negative charge of an oxidant drives its reactivity with the solvent exposed bases, we determined sequence-specific patterns of guanine oxidation produced by Fe^{+2}-EDTA, a negatively charged complex and compared them to the guanine oxidation produced by γ-radiation, a neutral oxidant. Both are sources of hydroxyl radicals ($^{\bullet}OH$), highly oxidizing species that react at the site of their generation (6, 7).

DNA oxidation by Fe^{+2}-EDTA and γ-radiation is characterized by high levels of deoxyribose damage that results in production of direct strand breaks (8). To extend our studies of sequence-selective guanine oxidation to Fe^{+2}-EDTA and γ-radiation, we developed a general method for quantifying nucleobase oxidation in the presence of direct strand breaks. This method

exploited activity of Exonuclease III (Exo III), a 3' to 5' exonuclease, and utilized phosphorothioate-modified synthetic oligonucleotides that were resistant to Exo III activity. Control experiments demonstrated that treatment with Exo III generated no artifacts capable of affecting guanine reactivity measurements. This method was successfully applied to the study of sequence-selective guanine oxidation by Fe^{+2}-EDTA/H_2O_2, Fe^{+2}-EDTA and γ-radiation, and can be utilized in the future studies to assess sequence-selective nucleobase damage by other oxidants that produce high levels of direct strand breaks, such as $ONOO^-$ and peroxyl radicals.

We determined that negative charge of Fe^{+2}-EDTA/H_2O_2 was not a factor in modulating its reactivity with guanines in DNA and that both Fe^{+2}-EDTA/H_2O_2 and γ-radiation produced identical patterns of sequence-selective guanine damage. All guanines were equally reactive with Fe^{+2}-EDTA/H_2O_2 and γ-radiation, irrespective of their sequence contexts or IPs. This reactivity was consistent with the chemistry of $^{\bullet}OH$-mediated guanine oxidation that does not involve the intermediacy of $G^{\bullet+}$ capable of supporting oxidative charge transfer. Our results provide preliminary evidence that the nature of the oxidant and the mechanism of its reaction with guanine are better predictors of its sequence selectivity than the negative charge. However, to further define the role of negative charge in sequence-selective guanine oxidation, studies of other negatively charged species, such as $ONOO^-$, $(SCN)_2^{\bullet-}$, and negatively charged peroxyl radicals, will be needed.

Sequence-selective nucleobase oxidation by DNA-bound Fe^{+2} ions. We applied our method to quantify nucleobase damage in the presence of direct strand breaks to study guanine oxidation by DNA-bound Fe^{+2} ions. We observed that this damage was produced in a sequence-specific manner at 5'-TGG-3' motifs, consistent with previous nicking studies (9). Surprisingly, thymine, and not guanine was found to be the main oxidation target, demonstrating that binding of Fe^{+2} can affect sequence selectivity of nucleobase damage in a profound manner. Similar studies with other redox-active and biologically relevant ions, such as Cu^{+2}, Ni^{+2} and Cr^{+6}, can be used to map sequence-specific DNA binding sites for these metals and reveal patterns of oxidative damage.

Sequence-specific chemistry of guanine oxidation. We observed that the ratios of Fpg- to piperidine-sensitive products varied as a function of sequence context, indicating that the chemical yields of different guanine lesions were sequence context-dependent. This was especially evident in the case of guanine oxidation produced by $ONOOCO_2^-$ that displayed an approximate 5.4-fold variability in the ratios of Fpg- to piperidine-sensitive lesions; 4.5-fold variability was observed for photoactivated riboflavin, and a 2-fold variability for Fe^{+2}-EDTA/H_2O_2, Fe^{+2}-EDTA and γ-radiation across different sequence contexts. Interestingly, in all cases 5'-GT-3' motifs were characterized by the lowest Fpg- to piperidine-sensitive ratios (with some variations). This demonstrates an effect of a neighboring 3' thymine on the reactivity of an intermediate common to all agents, the neutral guanine radical ($G^{\bullet}$). To further assess the effect of

sequence context on guanine oxidation chemistry, the identities and chemical yields of guanine lesions produced within different sequence contexts will need to be determined. This can be accomplished by using a combination of stable isotope labeling and HPLC-electrospray ionization tandem mass spectrometry approach that was already utilized to quantify sequence-dependent distribution of acetaldehyde-derived ^{2}N-deoxyguanine adducts (10).

Overall, we demonstrated that a complicated interplay of different factors governs reactivity of a guanine toward one-electron oxidation and that sequence-specific IP is not a determinant of oxidative damage produced by the biological oxidants $ONOOCO_2^-$ and $^{\bullet}OH$. Further studies of the role of sequence context on the reactivity of guanine and its oxidation intermediates will help predict the location and identities of mutagenic guanine lesions in the genome.

REFERENCES

1. Tretyakova, N. Y., Burney, S., Pamir, B., Wishnok, J. S., Dedon, P. C., Wogan, G. N., and Tannenbaum, S. R. (2000) Peroxynitrite-induced DNA damage in the supF gene: correlation with the mutational spectrum. *Mutat Res* 447, 287-303
2. Saito, I., Nakamura T., Nakatani K., Yoshioka Y., Yamaguchi K., Sugiyama H. (1998) Mapping of the hot spots for DNA damage by one-electron oxidation: Efficacy of GG doublets and GGG triplets as a trap in long-range hole migration. *J Am Chem Soc* 120, 12686-12687
3. Leroy, J. L., Kochoyan, M., Huynh-Dinh, T., and Gueron, M. (1988) Characterization of base-pair opening in deoxynucleotide duplexes using catalyzed exchange of the imino proton. *J Mol Biol* 200, 223-238
4. Folta-Stogniew, E., and Russu, I. M. (1994) Sequence dependence of base-pair opening in a DNA dodecamer containing the CACA/GTGT sequence motif. *Biochemistry* 33, 11016-11024

5. Leijon, M., and Graslund, A. (1992) Effects of sequence and length on imino proton exchange and base pair opening kinetics in DNA oligonucleotide duplexes. *Nucleic Acids Res* 20, 5339-5343
6. Becker, D., Sevilla, M.D. (1993) The chemical consequences of radiation damage to DNA. *Adv. Radiat. Biol.* 17, 121-180
7. Rush, J. D., and Koppenol, W. H. (1986) Oxidizing intermediates in the reaction of ferrous EDTA with hydrogen peroxide. Reactions with organic molecules and ferrocytochrome c. *J Biol Chem* 261, 6730-6733
8. Kennedy, L. J., Moore, K., Jr., Caulfield, J. L., Tannenbaum, S. R., and Dedon, P. C. (1997) Quantitation of 8-oxoguanine and strand breaks produced by four oxidizing agents. *Chem Res Toxicol* 10, 386-392
9. Henle, E. S., Han, Z., Tang, N., Rai, P., Luo, Y., and Linn, S. (1999) Sequence-specific DNA cleavage by Fe2+-mediated fenton reactions has possible biological implications. *J Biol Chem* 274, 962-971
10. Matter, B., Guza, R., Zhao, J., Li, Z. Z., Jones, R., and Tretyakova, N. (2007) Sequence Distribution of Acetaldehyde-Derived N(2)-Ethyl-dG Adducts along Duplex DNA. *Chem Res Toxicol*

Biographical note

Yelena Margolin was born on September 16, 1977 in Moscow Russia, and immigrated to the United States with her family in 1993. Having received a Summer Student Research Fellowship from American Heart Association in 1994, she worked in the laboratory of Prof. Paul M. Epstein in the Department of Pharmacology at the University of Connecticut Health Center studying the genomic structure of phosphodiesterases. She began her undergraduate studies at MIT in 1995. In the summer of 1997 she was awarded Karyn Kupcinet International Science School Fellowship, and worked in the laboratory of Prof. Aviva Lapidot in the Department of Organic Chemistry at the Weizmann Institute of Science in Rehovot, Israel studying PCR fidelity in the presence of tetrahydropyrimidine derivatives. For two years before graduating from MIT with dual S.B. degrees in Chemistry and Biology in the June of 1999, she studied the kinetics of aggregation of the β-amyloid peptide in the laboratory of Prof. Vernon M. Ingram in the Department of Biology at MIT. In the fall of the same year she started her graduate studies in the Division of Toxicology at MIT, and joined the laboratory of Prof. Peter C. Dedon. During her graduate career, she received Scholar-in-Training Award and Brigid G. Leventhal Women in Cancer Research Award from the American Association for Cancer Research.